Geology of the

East-Central San Mateo Mountains,

Socorro County, New Mexico

by

Charles A. Ferguson

New Mexico Bureau of Mines and Mineral Resources
Open-File Report 252

New Mexico Institute of Mining and Technology,

Socorro, New Mexico

September, 1986

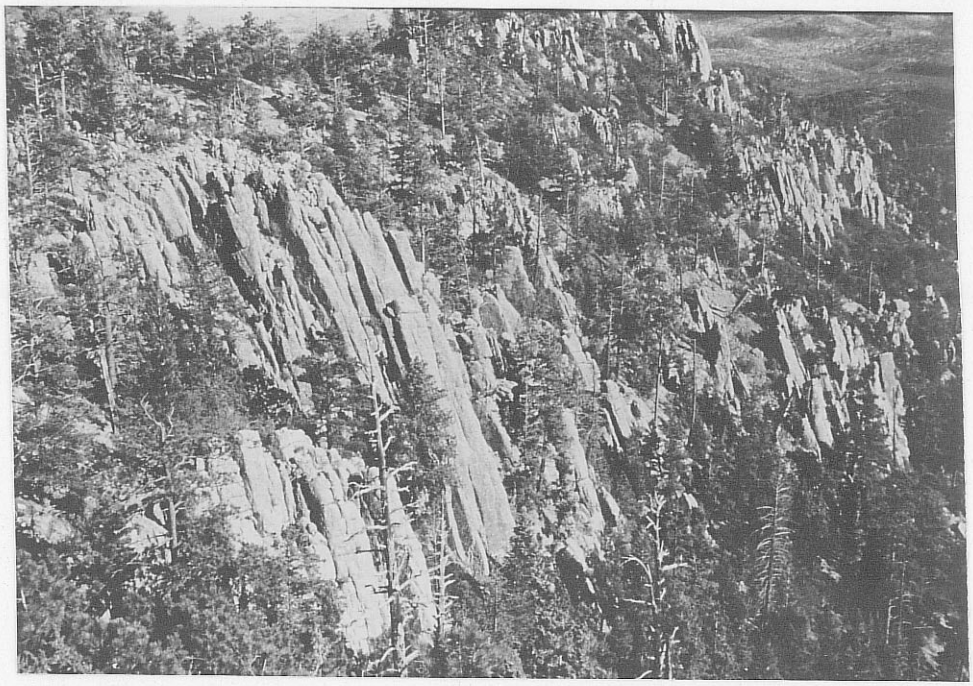

Looking southeast at columnar joints developed in South Canyon Tuff in the upper part of Rosedale Canyon. The southern margin of the Mt. Withington Cauldron, which is the source of the South Canyon, is about 4 miles behind these outctrops.

TABLE OF CONTENTS

CHAPTER 1 INTRODUCTION....1
Location....1
Previous work....3
Purpose....6
Procedures....6
Acknowledgements....7

CHAPTER 2 UNIT DESCRIPTIONS....9
Introduction....9
Basaltic Andesite....9
La Jencia Tuff....11
Distribution....11
Petrography....12
Vicks Peak Tuff....14
Distribution....14
Petrography....18
Lemitar Tuff....24
Distribution....24
Petrography....26
South Canyon Tuff....29
Distribution....29
Members of the South Canyon Tuff....29
Unwelded base member....30
Welded tuff member....30
Lithic-breccia member....32
Crystal-rich member....33
Member of Rosedale Canyon....34
Petrography....35
Hydrothermal alteration....41
Unit of East Red Canyon....43
Distribution....43
Petrography....46
Clast-supported diamictite....46
Matrix-supported diamictite....46
Massive sandstone....50
Clast-supported conglomerate....50
Cross-stratified sandstone....51
Bedded tuff and red mudstone....56
Stratigraphic sections....56
Paleontology....60
Tuff of Turkey Springs....66
Distribution....66
Petrography....68
Rhyolite intrusives and lavas....71
Introduction....71
First generation rhyolites....72
Distribution....72
Petrography....75
Second generation rhyolites....76
Distribution....76

Petrography....76
Third generation rhyolites....76
Distribution....76
Petrography....78
Fourth generation rhyolite....78
Unconstrained rhyolite intrusives....79

CHAPTER 3 CHEMISTRY....80
Introduction....80
Ash-flow tuffs....83
Intrusives....83

CHAPTER 4 PALEOMAGNETISM....85
Introduction....85
Polarity....85
Anisotropy of Susceptibility....88

CHAPTER 5 STRATIGRAPHY....89
Introduction....89
Correlation with previous work....91
Correlation with Deal (1973)....91
Correlation with Atwood (1982)....93
Correlation with Donze (1980)....94
Summary....95
Stratigraphy of this area....95
Introduction....95
Units older than Lemitar Tuff....96
La Jencia Tuff....96
Vicks Peak Tuff....96
First generation rhyolites....96
Lemitar Tuff....97
South Canyon Tuff....98
Unit of East Red Canyon....99
Tuff of Turkey Springs....101
Rhyolites intrusions/lavas....101
Summary....102

CHAPTER 6 STRUCTURE....104
Introduction....104
Volcanic structures....104
Structures related to the Vicks Peak Tuff....104
Mt. Withington Cauldron....105
Basin and Range structures....108
Fault patterns and the least principle stress field.108
Magnitude of tilting and the age
of Basin and Range extension....110
Summary....113

CHAPTER 7 CONCLUSIONS....116

REFERENCES....118

APPENDIX A PETROGRAPHIC PROCEDURES....121

APPENDIX B GEOCHEMICAL PROCEDURES.....122

APPENDIX C PALEOMAGNETIC PROCEDURES.....123

LIST OF FIGURES

Figure 1. Topographic map of Socorro County showing the study area (stippled), and proposed cauldrons in the San Mateo Mountains.....2

Figure 2. Location map of the study area showing forest roads, major drainages,and political boundaries....4

Figure 3. Photograph of basaltic andesite lava.....10

Figure 4. Stratigraphic section of the La Jencia Tuff.....13

Figure 5. Outcrop map of the La Jencia Tuff.....15

Figure 6. Photographs of lineated pumice in the Vicks Peak Tuff.....20

Figure 7. Outcrop map of the Vicks Peak Tuff.....21

Figure 8. Stratigraphic section of the Vicks Peak Tuff....22

Figure 9. Outcrop map of the Lemitar Tuff showing the distribution of paleocanyon walls buried by the unit.....25

Figure 10. Stratigraphic section of the Lemitar Tuff.....27

Figure 11. Outcrop map of the South Canyon Tuff.....31

Figure 12. Photograph of lineated pumice in the South Canyon Tuff.....38

Figure 13. Outcrop map of the South Canyon Tuff.....39

Figure 14. Photomicrograph of glassy pumice in the South Canyon Tuff.....40

Figure 15. Photomicrograph of vapor phase recrystallized pumice in the South Canyon Tuff.....42

Figure 16. Outcrop map of the unit of East Red Canyon.....44

Figure 17(a). Generalized stratigraphic sections of the unit of East Red Canyon.....47

Figure 17(b). Detailed stratigraphic section of eolian sandstone in the unit of East Red Canyon.....48

Figure 18. Photograph of matrix supported diamictite.....49

Figure 19. Photograph of basal portion of a cross-stratified sandstone set.....52

Figure 20. Photograph of cliff of eolian sandstore.....54

Figure 21. Block diagram showing a possible origin of the first order bounding surfaces observed in the unit of East Red Canyon.....55

Figure 22. Photograph of bedded ash-flow tuff.....57

Figure 23. Photograph of desiccation cracks in a mudstone bed.....58

Figure 24. Rose diagram of paleocurrent directions from eolian sandstone in the unit of East Red Canyon.....62

Figure 25. Photograph of arctiodactyl hoof print molds in a slab of bedded tuff.....63

Figure 26. Photograph of inclined burrow.....64

Figure 27. Outcrop map of the tuff of Turkey Springs.....67

Figure 28. Stratigraphic section of the tuff of Turkey Springs.....69

Figure 29. Outcrop map of the rhyolite lava of Drift Fence Canyon.....74

Figure 30. Paleomagnetic pole positions for samples of the La Jencia Tuff, Vicks Peak Tuff, and the Lemitar Tuff.....86

Figure 31. Paleomagnetic pole positions for samples of the South Canyon Tuff, and the tuff of Turkey Springs....87

Figure 32. Stratigraphic sequence from this study compared with the regional sratigraphy of Osburn and Chapin (1983).....90

Figure 33. Stratigraphic sequence from this study compared with the stratigraphic sequences of previous workers in adjacent areas.....92

Figure 34. Four stage model for the formation of the southeast structural margin of the Mt. Withington Cauldron.....107

Figure 35. Structural map of the study area showing the moderately extended domain, and the weakly extended domain.....109

Figure 36. Map showing redefined Mt. Withington Cauldron..115

LIST OF PLATES AND TABLES

Plate 1. Geologic Map.....(in pocket)

Plate 2. East-West Cross Sections.....(in pocket)

Plate 3. North-South Cross Sections.....(in pocket)

Plate 4. Sample Location Map.....(in pocket)

Table 1. Petrographic data from samples of the South Canyon Tuff throughout the study area.....36

Table 2. Percentages of grain types in eolian sandstones from the unit of East Red Canyon.....61

Table 3. Major element chemical data of the South Canyon Tuff, and the Lemitar Tuff.....81

Table 4. Major element chemical data of some rhyolite intrusions in the study area.....82

Table 5. The location and age constraints of dikes in the study area whose trends are thought to have been determined by a regional stress field.....111

ABSTRACT

The San Mateo Mountains are a north-trending Basin and Range uplift on the northeast corner of the mid-Tertiary Datil-Mogollon volcanic field in Socorro County, New Mexico. They are composed dominately of felsic volcanic and volcaniclastic rocks. Detailed mapping was done in the east-central part of the range. The four youngest of five Oligocene regional rhyolite ash-flow tuffs in the Socorro area (oldest to youngest: La Jencia; Vicks Peak; Lemitar; and South Canyon Tuffs) are exposed in the study area.

The eastern part of the study area consists of outflow sheets of the La Jencia, Vicks Peak, and Lemitar Tuffs. Within the study area Vicks Peak Tuff thickens to the southwest (<100m to >300m). Farther south, the Vicks Peak Tuff is buried by a thick sequence of local volcanic units suggesting that a syn-volcanic depression of Vicks Peak age is located in the south-central part of the San Mateo Mountains. Subsequent resurgence of this area is indicated by southwestward thinning of the next youngest unit (Lemitar Tuff). Outflow sheets of the three oldest tuffs regional are truncated to the west by a northeast trending west-side down fault zone which forms a structural basin in the western half of the study area. Stratigraphic relations along this fault zone show that it was activated during the eruption of the South Canyon Tuff. The structural basin is

filled with >600m of the South Canyon Tuff and about 200m of younger volcaniclastic rocks and rhyolite lava. The basin is interpretated to be the southern part of the redefined Mt. Withington cauldron. The sediments and lavas are interpreted as moat-fill. Eolian sandstone in the moat-fill was deposited by prevailing southwest winds.

Except for a basaltic andesite lava, which is the oldest unit exposed, all igneous rocks in the study area are high-SiO_2 (>75%), high-K_2O (5%) rhyolites. Paleomagnetically, all of the ash-flow tuffs in the study area are reversely polarized, except for the Lemitar Tuff.

Basin and Range faulting, the result of a late Oligocene least principle stress field oriented about N63E, was initiated during the waning stages of ash-flow tuff volcanism in the study area. Oligocene strata dip east from 5 to 50 degrees, with the amount of extension (proportional to tilting) increasing from 20% to 100% from south to north in the study area. North-south trending west-side down faults are found throughout the study area. East-west south-side down faults are found only in the southern part. This change in structural style occurs across the margin of the Mt. Withington Cauldron. The change in strain patterns is attributed to the influences of a shallow (3km) pluton beneath the cauldron to the north, and pre-Tertiary basement structures to the south.

CHAPTER 1

INTRODUCTION

Location

The San Mateo Mountains are a north-trending (40 by 15 mile) Basin and Range uplift in the southwest corner of Socorro County, New Mexico. They are composed predominately of Oligocene silicic ash-flow tuffs, lavas, and related volcaniclastic rocks. Paleozoic sedimentary and Precambrian metamorphic rocks are exposed in the extreme southeast corner of the range. Elevations increase from less than 6,000 feet in the southern foot hills to well over 10,000 feet in the north and south ends of the range (Fig. 1). The elevated region to the north has been interpreted as the resurgent dome of the Mt. Withington Caldera (Deal, 1973, Deal and Rhodes, 1976). The elevated region to the south is mostly unmapped, but the proposed Nogal Canyon Caldera (Deal and Rhodes, 1976) overlaps the southeast part of it. The study area, with which this project is concerned, is a 50 square mile block centered on the eastern half of a prominent saddle that seperates these higher areas (Fig. 1).

Total topographic relief in the study area is just under 4,000 feet. Vegetation below 7,000 feet consists of high prairie grasses, with rare juniper and white oak in

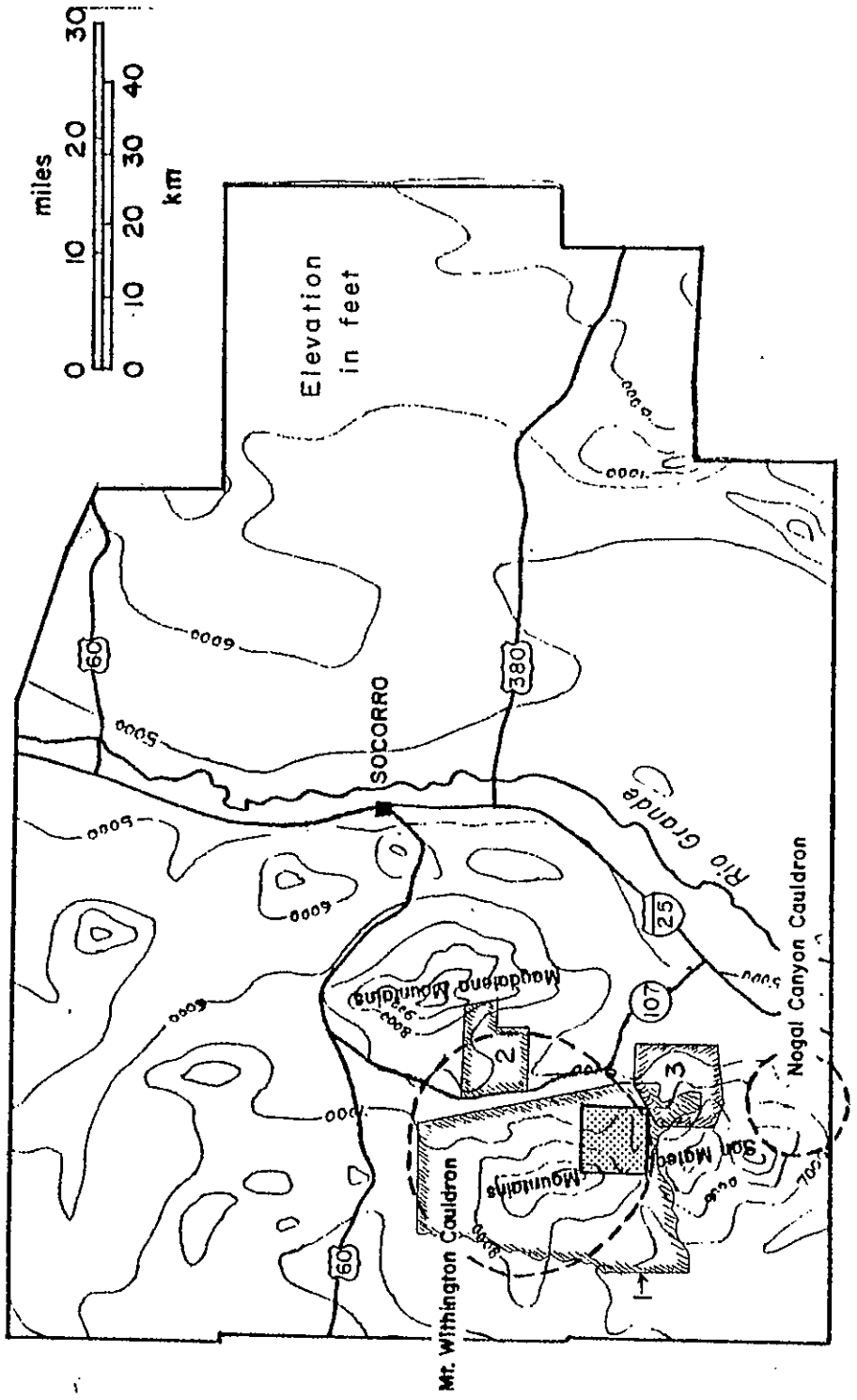

Figure 1. Topographic map of Socorro County showing the study area (stippled), and map areas of adjacent workers: 1) Deal (1973); 2) Donze (1980); and 3) Atwood (1982). The proposed Mt. Withington and Nogal Canyon Cauldrons are from Deal and Rhodes (1976).

sheltered arroyos and canyons. Mixed juniper, pinon pine, oak, and ponderosa pine occupy elevations from 7,000 to 8,000 feet. Above 8,000 feet ponderosa pine is mixed with douglas fir and spruce, and on north-facing slopes groves of aspen are common. No correlation between vegetation and rock type was observed in the study area.

All of the study area is located within Cibola National Forest, except for six sections in the northeast corner. Major access roads include three forest roads (Fig. 2), and in the northeast corner a system of private ranch roads. The forest roads can be negotiated with high clearance two wheel drive vehichles. Travel on the ranch roads requires four-wheel drive, and permission from local ranchers.

The study area is deeply dissected by three major east-flowing drainages; Rosedale Canyon, North Canyon, and East Red Canyon (Fig. 2). These canyons usually contain no running water, but host several springs with drinkable water in the western part of the study area. All major springs are located on the upslope (west) side of north-trending normal faults.

Previous work

Reconnaissance mapping of the northern San Mateo Mountains by Deal (1973) revealed great thicknesses of two major ash-flow tuff units (A-L/ Peak Tuff, and the Potato

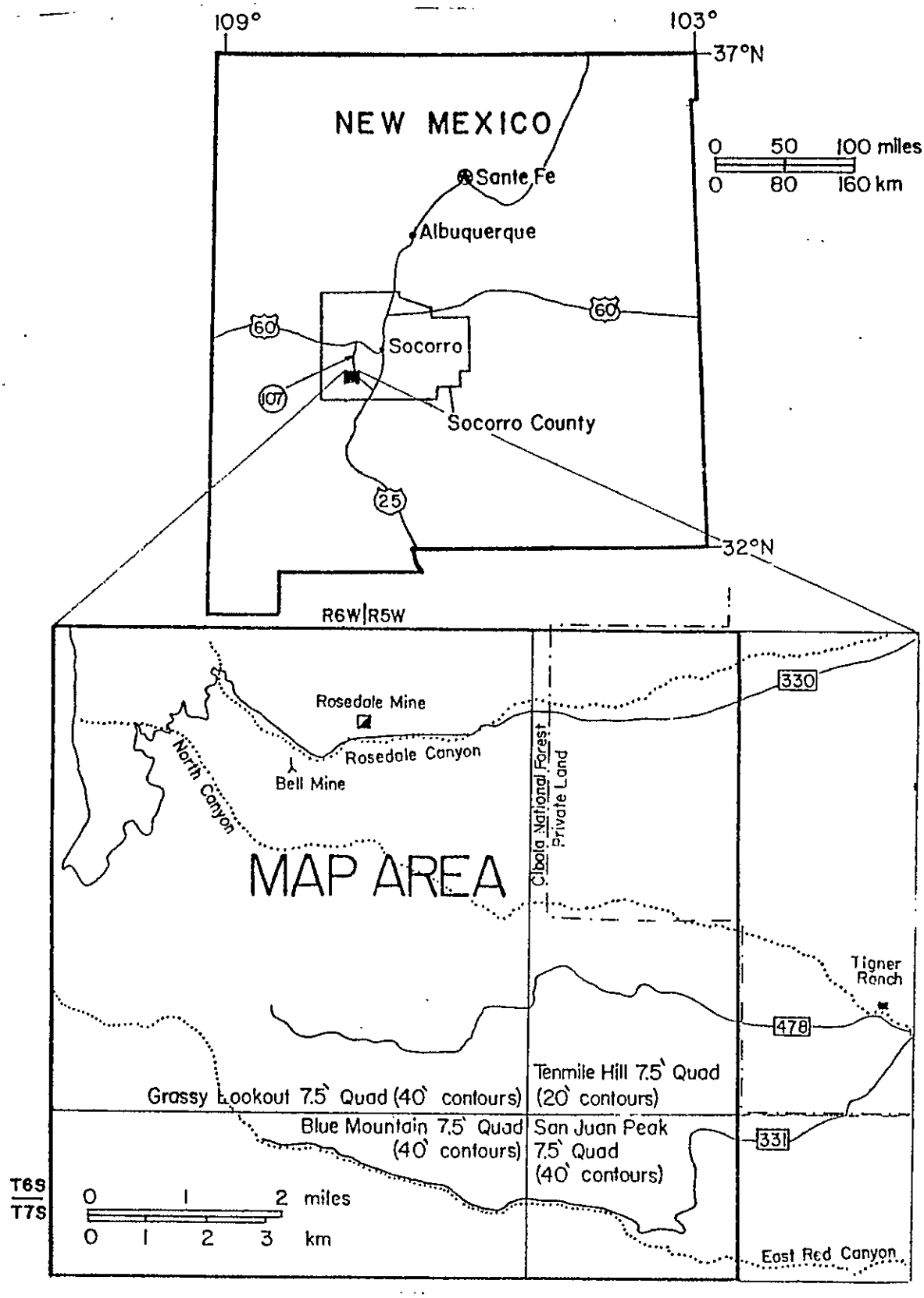

Figure 2. Location map of the study area showing forest roads, major drainages, and political boundaries.

Canyon Tuff). Deal (1973) proposed the Mt. Withington cauldron as the source for these two tuffs. In the central part of the range, Deal mapped a sequence of volcaniclastic sediments, rhyolite lavas, and tuffs overlying the cauldron-filling tuffs. These rocks were grouped into the Beartrap Canyon Formation which was interpreted as a moat sequence for the Mt. Withington cauldron.

Donze (1980) mapped an area about 6km northeast of this study area in a range of hills connecting the Magdalena Range with the north end of the San Mateos (Fig. 1). His map shows at least 670m of Lemitar Tuff with no exposed base. This Lemitar Tuff correlates with the cauldron-filling Potato Canyon Tuff of Deal (1973), and is overlain by 60-300m of volcaniclastic sediment and 50-100m of what Donze (1980) called the South Canyon Tuff. The Lemitar Tuff, as mapped by Donze (1980), has been correlated with the South Canyon Tuff, by Osburn and Chapin (1980). Donze's (1980) South Canyon Tuff is correlated with a local intracaldera tuff informally named the tuff of Turkey Springs in this report.

Mapping by Atwood (1982) in an area adjacent to the southeast corner of this study area revealed great thicknesses of Vicks Peak Tuff (400m). The Vicks Peak Tuff is thought to originate from the Nogal Canyon cauldron (Fig. 1) which is older than the Mt. Withington cauldror.

Atwood's map shows the Vicks Peak Tuff truncated to the southwest (directly south of this study area) by a major west-side down fault. Across this fault, Vicks Peak Tuff is buried by about 300m of ash-flow tuff, volcaniclastic sediment, and rhyolite lava that Atwood (1980) correlated with the Beartrap Canyon Formation of Deal (1973).

Purpose

The purpose of this study is four fold: (1) define stratigraphy for the central San Mateo Mountains and to correlate it with stratigraphy already established to the northeast (Osburn and Chapin, 1983); (2) investigate the margin of the proposed Mt. Withington cauldron, and a possible older volcanic structure, related to the Vicks Peak Tuff, to the southwest; (3) examine lateral changes in style of Basin and Range deformation within the study area; and (4) geochemically characterize the major volcanic units.

Procedures

Detailed geologic mapping was done by the author in the summer-fall of 1983, and the spring of 1984 using 1:24,000 scale, U.S.G.S., 7.5 minute, topographic quadrangles (Fig. 2), supplemented by 1:50,000 scale, 1935 Soil Conservation Survey, aerial photographs 8468-8473, 8486-8490, and 8514-8518. All information on the geologic map (Plate 1)

and cross sections (Plate 2,3) was compiled by the author solely from his field maps and notes.

All petrographic and geochemical samples were collected between the summers of 1983 and 1984. Oriented core samples for paleomagnetic studies of principle units were collected in the spring of 1984, and spring of 1985 by Bill McIntosh and the author. Plate 4 is a location map for all petrographic, geochemical, and paleomagnetic samples for which observations and or data are presented in this paper. The author is responsible for all petrographic observations, and for the preparation of samples for major-element geochemical analyses (X-ray fluorescence) except for samples (84-27,159) which were done by G. R. Osburn of the New Mexico Bureau of Mines and Mineral Resources.

Petrographic, geochemical, and paleomagnetic procedures are described in Appendices A, B, and C, respectively.

Acknowledgments

I would like to thank the New Mexico Bureau of Mines and Mineral Resources for providing field support vehicles, and for funding geochemical analyses, and thin section costs. I would also like to thank Bob Osburn, Bill McIntosh, and Dave Johnson for helpful comments in the field, and Ken Lemley for processing my sedimentary paleocurrent data. Bob Osburn, Dave Johnson, and Phil Kyle

critically reviewed the manuscript, and served on the thesis committee. Fletcher and Lucille Tigner allowed access to their private land, assisted with mechanical problems, and located unmapped springs that saved me a great deal of time and trouble.

CHAPTER 2

UNIT DESCRIPTIONS

Introduction

In this chapter, detailed descriptions of each map unit are presented in ascending stratigraphic order. The description of each unit will include the following observations: (1) stratigraphic position; (2) thickness, and lateral variations in thickness; (3) description of upper and lower contacts; (4) hand specimen and/or field descriptions of macroscopic textures; and (5) micropetrographic descriptions of selected units.

Basaltic Andesite

The oldest exposed unit is a basaltic andesite lava flow, which crops out sporadically over an area of about one square mile in the east-central part of the study area. Lateral extent of the flow is unknown. Its lower contact is not exposed, and only a minimum thickness of 60 meters could be determined.

The best exposure of the lava is in North Canyon where it is nonvesicular and brecciated, and is interpreted as a blocky flow (Fig. 3). South of here, the lava is usually vesicular and non-brecciated. Based on field and hand

Figure 3. Photograph of brecciated basaltic andesite lava (sec. 15, T6S, R5W), which is interpreted to be a blocky flow.

sample examination, the lava contains about 5% plagioclase (1-2mm) and about 3% ferromagnesian phenocrysts (1mm). The ferromagnesian minerals could not be identified, because they were oxidized. The groundmass is grayish-red-purple in color, and is both massive or vesicular.

La Jencia Tuff

Distribution

The La Jencia Tuff (Osburn and Chapin, 1983) is a crystal-poor rhyolite ash-flow tuff, whose source is the composite Sawmill Canyon-Magdalena Cauldron in the central Magdalena Mountains. Formerly the A-L Peak Tuff (Deal, 1973; Deal and Rhodes, 1976), the La Jencia Tuff is the oldest regional unit in the study area. It was originally described by Tonking (1957) as the middle part of the Hells Mesa member of the Datil Formation, and by Brown (1972) as the lower tuff of Bear Springs. Deal (1973) miscorrelated this unit with a younger tuff on A-L Peak (northern San Mateo Mountains) which is now correlatd with the South Canyon Tuff (Osburn and Chapin, 1983).

The La Jencia Tuff is exposed only in the southeast part of the study area, and is conformably overlain by The Vicks Peak Tuff, in most places. In North Canyon, paleocanyons filled with Lemitar Tuff cut through the Vicks

Peak Tuff into it's upper part. The unit's base, exposed only in the North Canyon area, consists of a poorly-welded interval (<3m) which rests on basaltic andesite lava. In North Canyon the unit is divided into a lower massive member (70m) and an upper flow-banded member, whose top is not exposed. In East Red Canyon the massive member is not exposed, but about 200m of the flow-banded member is, making the unit at least 270m thick. Along the walls of East Red Canyon, the flow banded member weathers into distinct ledges separated by 5-15m high cliffs. These cliffs may represent individual flow-units.

Petrography

Three thin sections of the La Jencia Tuff were studied (83-78,83-133,84-19; Fig. 4). Phenocrysts throughout the unit are mostly euhedral blocky or tabular sanidine (2-3mm), with minor amounts of subhedral quartz (1mm), and trace amounts of biotite (0.5mm), sphene (0.5mm), plagioclase (0.2mm), and opaque minerals (0.2mm). The massive member is a pale-red densely welded tuff containing about 7% phenocrysts. It contains about 5% pumice that average 1-3cm in length, and have compaction ratios of about 12:1. The transition from massive to flow-banded members occurs over a 20m interval defined by a rapid increase in pumice content (5 to 25%), and a slight decrease in phenocryst content (7 to 5%).

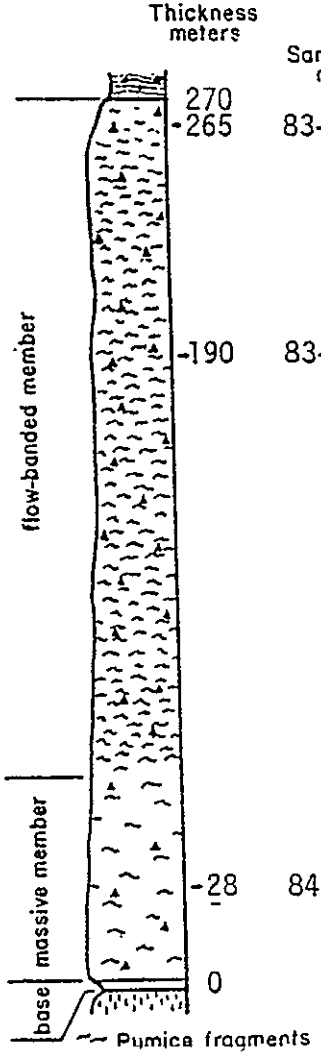

Sample no.	Color unweathered matrix	Lithics	Pumice	Total phen.	San.	Qtz.	Plg.	Biot.	Opaq.	Sphene
83-133	pale-grysh-red 10R 5/2	5-7	2-5	4	4	m	m	t	t	0
83-78	pale-red 5R 6/2	1	20-30	4	4	m	m	t	t	0
84-19	pale-red 10R 6/2	1	4-8	7	7	m	t	t	t	t

m-minor(less than 0.5%) t-trace(less than 0.1%) 0-not observed

Figure 4. Stratigraphic section of the La Jencia Tuff (sec. 15, T6S, R5W, and sec. 32, T6S, R5W). Visual estimates of phenocryst percentages are from thin sections. Lithic and pumice percentages are estimated from hand specimens.

The flow-banded member, also pale-red and densely welded, is characterized by exceptionally flattened and elongated pumice fragments (compaction ratios >50:1). The extreme elongation of pumice fragments (up to 0.5m) defines a pronounced east-west lineation that is consistent throughout the study area (Fig. 5). The azimuth to the source of the La Jencia Tuff (central Magdalena Mountains) is almost perpendicular to flow-lineation azimuths measured in this study. There may have been a regional east-west oriented paleoslope in the study area effecting the direction of flow indicators in the unit.

The top of the La Jencia Tuff, where it is preserved, is grayish-red and moderately welded. Small (<3cm) uncompacted pumice compose only about 4% of this tuff, but it's phenocryst assemblage is similar to the rest of the unit.

Vicks Peak Tuff

Distribution

The Vicks Peak Tuff (Furlow, 1965; Deal and Rhodes, 1976)is a densely welded crystal-poor vertically zoned rhyolite ash-flow tuff. The source of the Vicks Peak Tuff is thought to be in the southeast San Mateo Mountains (Nogal Canyon cauldron) where Deal and Rhodes

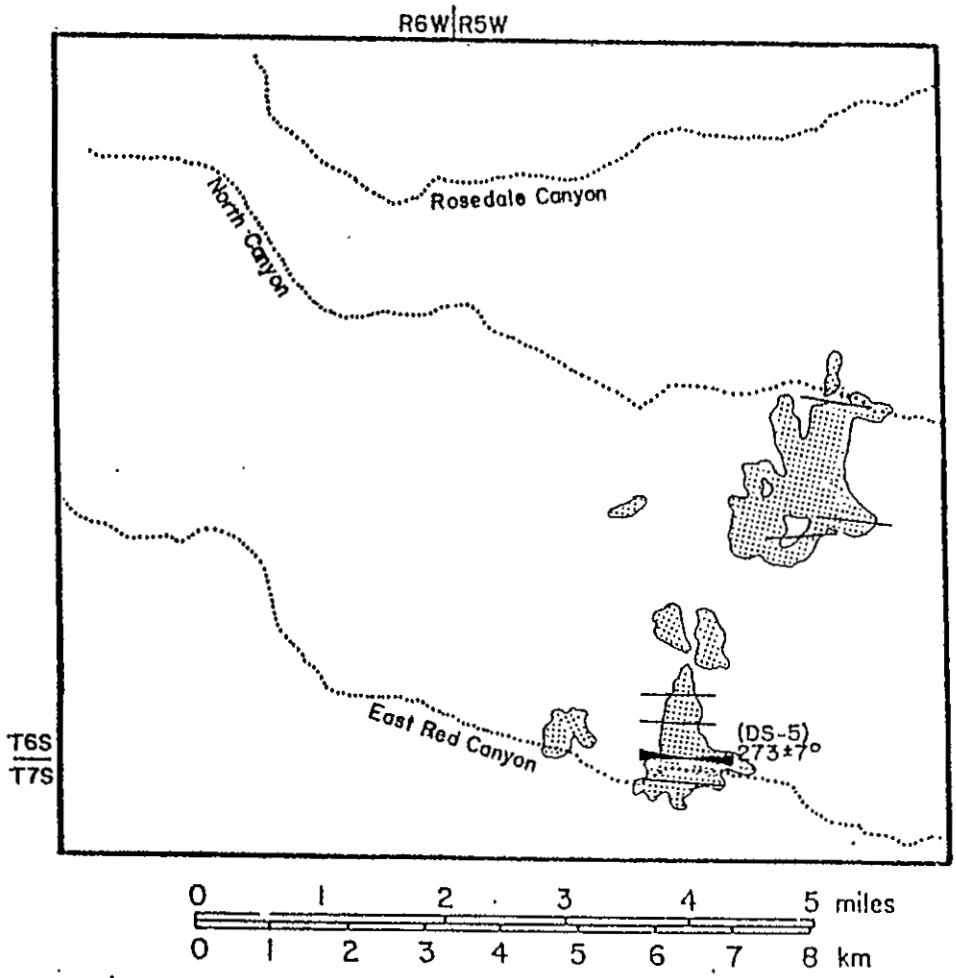

Figure 5. Outcrop map of the La Jencia Tuff showing field measurements of lineated pumice and one magnetic anisotropy of susceptibility azimuth cone of confidence (95% level). The paleomagnetic sample number is shown with the anisotropy azimuth. Paleomagnetic data from McIntosh and others (1986).

(1976) reported thicknesses in excess of 650m. The unit, exposed only in the southeast part of the study area, is best exposed along the walls of East Red Canyon and Drift Fence Canyon. The base is a moderate-orange-pink crystal-poor unwelded bedded tuff 10-20m thick. Abruptly overlying the unwelded interval is a thin (0.5m) pale red vitrophyre which marks the base of the welded Vicks Peak Tuff.

In the southern part of the study area Vicks Peak Tuff is at least 215m thick. To the north, it thins to about 120m just east of Horse Mountain (NW 1/4 sec. 27, T6S, R5W). Farther north, the Vicks Peak Tuff is rarely preserved below a pre-Lemitar Tuff unconformity, and its original thickness is not known.

In the southeast corner of the study area, foliation in the Vicks Peak Tuff steepens, becomes irregular, and is folded along a linear zone that trends about N70E (Plate 1). To the east (sec. 3, T7S, R5W), the zone is 500m wide, and shows a progressive increase in dip from 30 degrees in the north to >70 degrees in the south. The zone ends abruptly to the south and dips return to the regional trend of 10 to 15 degrees east. The structure becomes narrower (200m wide) to the west, where it crosses East Red Canyon. Here the tuff is contorted into a series of north-verging assymetric folds whose axial planes are mostly vertical. From north to

south across the structure, the folds become tighter (nearly isoclinal), and their wavelengths decrease from about 20m to 5m. Farther to the west (sec. 4, T7S, R5W) the structure dies out completely. Apparently the Vicks Peak Tuff slumped over a south-facing scarp such as a south-side down fault, or the buried north wall of a paleocanyon while it was still hot and plastic, perhaps even during deposition. There is evidence 4km to the south, in Cold Spring Canyon, for paleocanyons of similar age (Osburn, 1982). The structure in this study area, however, is not considered to be a buried paleocanyon, because there is no evidence of a paired southern wall. Cross sections (Plate 2,3) through this part of the study area show the Vicks Peak Tuff slumping over a south facing fault scarp.

Along strike to the west of this buried escarpment, where Drift Fence Canyon turns sharply to the west (Plate 1), there is evidence for westward thickening of the Vicks Peak Tuff. The unit thickens from about 200m at the bend in the canyon to at least 300m thick where the canyon first enters the study area (about 1.5km to the west). There is no evidence of folding of the Vicks Peak Tuff in this area.

Petrography

Distinct ledges in the Vicks Peak Tuff, along the steeper walls of East Red and Drift Fence Canyon, are thought to mark the bases of individual flow-units. The ledges, which separate continuous sequences of tuff (2-20m thick), are more deeply eroded intervals (1-50cm thick) which may represent actual cooling breaks. Alternatively, basal shear layers (layer 2a of Sparks, 1976) of flow-units in a simple cooling-unit may also account for the ledges. One of the most distinct ledges, a clast-supported lithic-tuff interval (0.5m thick), occurs about 65m above the base of the unit near the mouth of Drift Fence Canyon. The lithics in this layer, unlike those throughout the unit, are distinctively non-volcanic in origin. Lithologies in the layer (listed in order of abundance) are:
1)medium-grained biotite-rich monzogranite;
2)medium-grained sandstone; 3)limestone; 4)dark colored pieces of a garnet encrusted iron skarn. The granite clasts are similar to those found in nearby lithic breccias of the younger South Canyon Tuff. The skarn fragments are similar to an iron skarn described by Jahns (1944) in the north end of the Sierra Cuchillo (30km to the southeast).
Instrumental neutron activation analysis shows that a skarn fragment (S-37) from this lithic interval contains 89% iron (calculated as FeO), 490ppm cobalt, and about 20ppm chromium, and tungsten.

Pumice content in the Vicks Peak Tuff increases gradually upward (2-15%). The increase, however, is irregular because individual flow-units tend to concentrate pumice in their upper parts. Most pumice fragments throughout the Vicks Peak Tuff have an internal lineation defined by elongate rods (<1mm in diameter) composed of vapor phase minerals. In the lower third of the unit, flattened pumice fragments (compaction ratios of 10:1) are mostly equant in plan view and, although internally lineated, rarely define a preferred orientation (Fig. 6a). The upper two thirds of the unit contains flattened and elongated pumice fragments, up to 30cm long, with compaction ratios commonly >30:1 (Fig. 6b). Field azimuth measurements of elongated pumice in this unit are plotted in Figure 7.

The zonation of phenocrysts, pumice, and lithics in the Vicks Peak Tuff was studied in a vertical series of 8 hand specimens and thin sections (VP-1,3,5 and 85-2,3,4,5,6, Fig. 8). Matrix of the welded tuff, light-brownish-gray to very-light-gray in color, is usually completely devitrified to very fine grained (<0.02mm) K-feldspar. Glass shards (up to 0.5mm long) with compaction ratios of 7:1 were preserved only in the lowermost sample (VP-1), where they compose 40% of the matrix. Phenocryst content in the Vicks Peak Tuff increases from 0.5% at the base to about 2% at 70m above the base. From 70m to 100m above the base, phenocryst content increases from 2% to 10%,

A

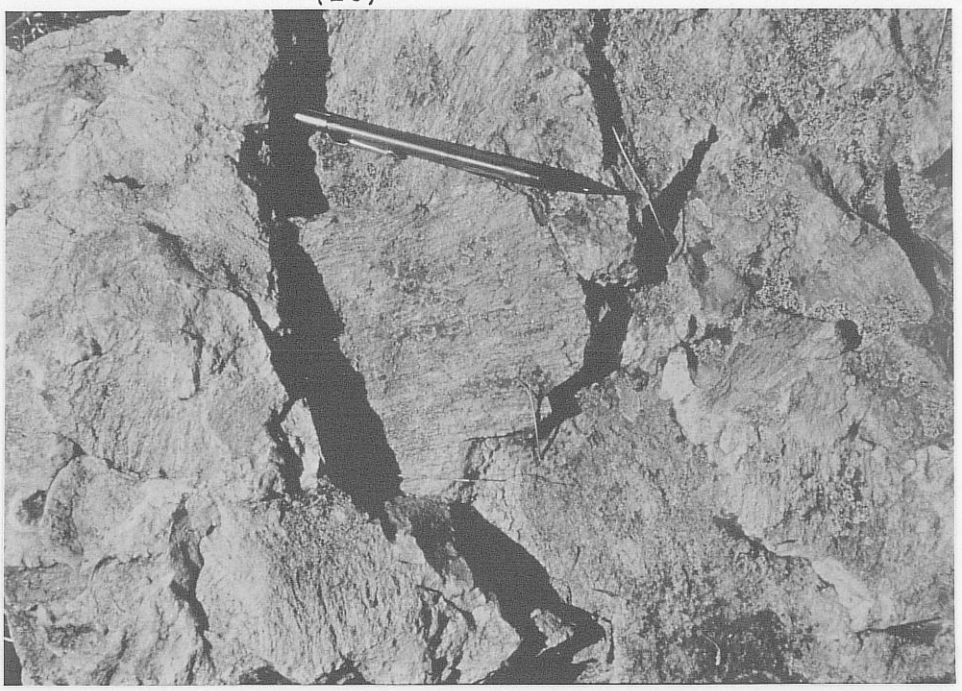

B

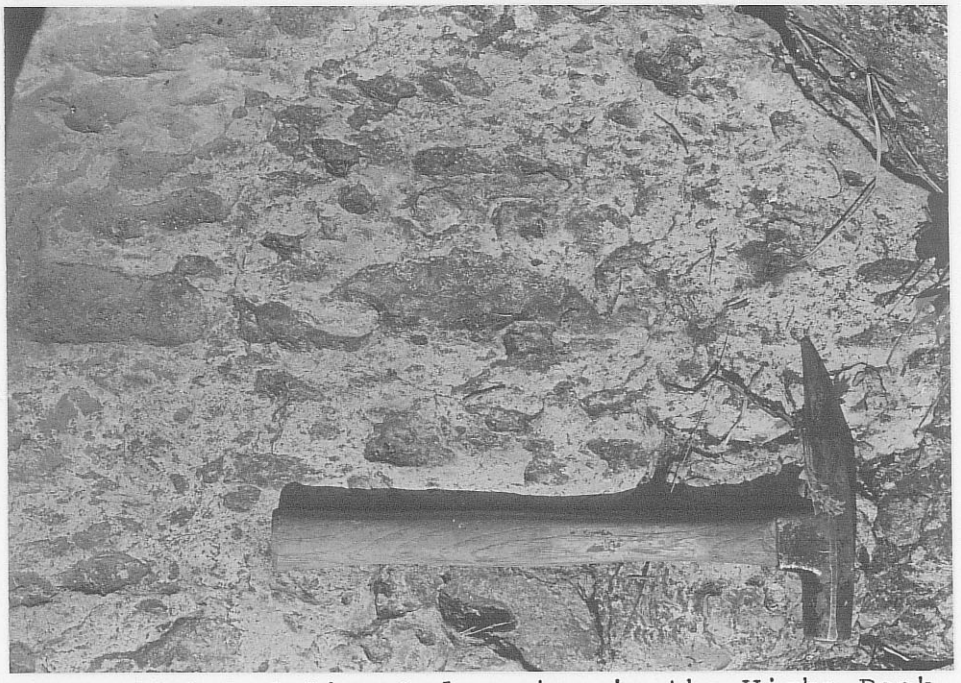

Figure 6. Photographs of lineated pumice in the Vicks Peak Tuff: (a) internally lineated, not preferentially oriented (sec. 6, T7S, R5w); (b) lineated and preferentially oriented (sec. 4, T7S, R5W).

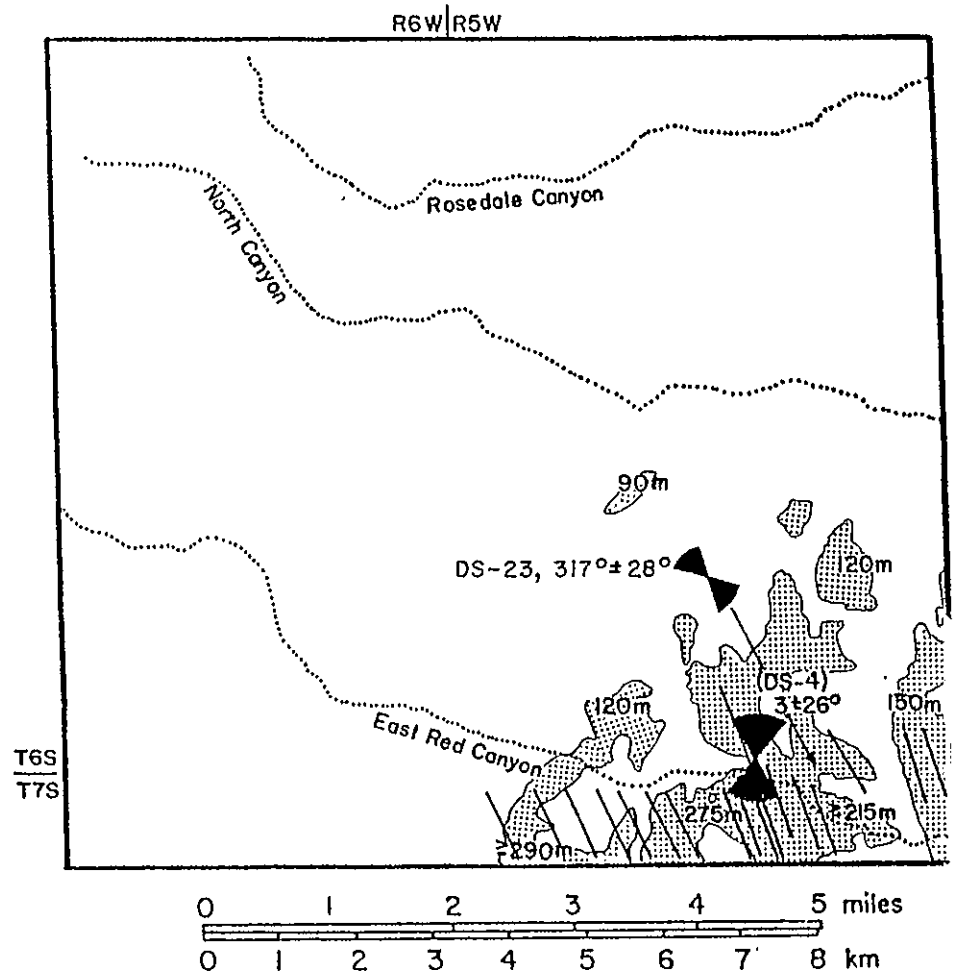

Figure 7. Outcrop map of the Vicks Peak Tuff showing thicknesses of the unit in meters, field measurements of lineated pumice, and two anisotropy of susceptibility azimuth cones of confidence (95% level). Paleomagnetic sample numbers are shown with each anisotropy azimuth. Paleomagnetic data from McIntosh and others (1986).

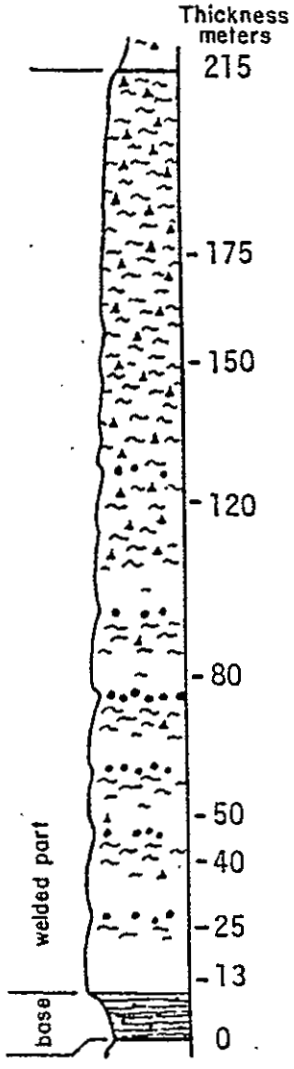

Sample no.	Color unweathered matrix	Lithics	Pumice	Total phen.	San.	Qtz.	Plg.	Biot.	Opaq.	Cpx
85-6	brownish-gray 5YR 4/1	t	12-20	12	12	0	0	0	t	m
85-5	brownish-gray 5YR 5/1	t	8-12	10	10	0	0	0	t	t
85-3	medium-gray N 6	t	4-8	9	9	0	0	t	t	t
85-4	light-brownish-gray 5YR 6/1	t	4-8	2	2	0	0	t	t	t
85-2	light-gray N 7	t	4-8	2	2	t	t	t	t	t
VP-5	light-gray N 7	t	4-8	1.5	1.5	0	t	t	t	t
VP-3	light-gray N 7	t	4-8	1	1	t	t	t	0	0
VP-1	light-brownish-gray 5YR 6/1	1-2	3	0.5	0.5	0	0	t	0	0

m-minor(less than 0.5%) t-trace(less than 0.1%) 0-not observed

Figure 8. Stratigraphic section of the Vicks Peak Tuff (sec. 4, T7S, R5W). Visual estimates of phenocryst percentages are from thin sections. Lithic and pumice percentages are estimated from hand specimens.

and then to about 12% at the top (215m). Phenocrysts throughout the unit are dominately tabular euhedral sanidine (1-4mm). Small phenocrysts (<0.5mm) of quartz, plagioclase, and biotite occur in trace amounts in the lower 100m of the unit. Rounded opaque grains (<0.5mm), and subhedral tabular clinopyroxene (0.2-1.0mm) occur in trace to minor amounts in the middle to upper part of the unit.

Lemitar Tuff

Distribution

The Lemitar Tuff (Osburn, 1978) is a crystal-poor to crystal-rich vertically zoned rhyolite ash-flow tuff. In the western half of the study area, it overlies the rhyolite intusion of Exter Canyon, and is overlain by the South Canyon Tuff. In this part of the study area, the Lemitar Tuff thickens from 5-15m in the south to about 80m in the north. The unit is unexposed in a north-south band across the middle of the study area, except for one exposure (at least 30m thick) underneath the Cave Peak rhyolite dome.

The Lemitar Tuff is intruded by rhyolite lava domes throughout the southeast part of the study area. It is overlain by the unwelded base of the South Canyon Tuff in the North Canyon area, and in the extreme southeast corner of the study area. Lemitar Tuff fills paleocanyons that cut into Vicks Peak Tuff, and in some places into the La Jencia Tuff (Fig. 9). These paleocanyons, which trend north-south or northeast-southwest, attain maximum depths of about 150m, and widths of about 400m. Outside of these paleocanyons, the unit is about 200m thick.

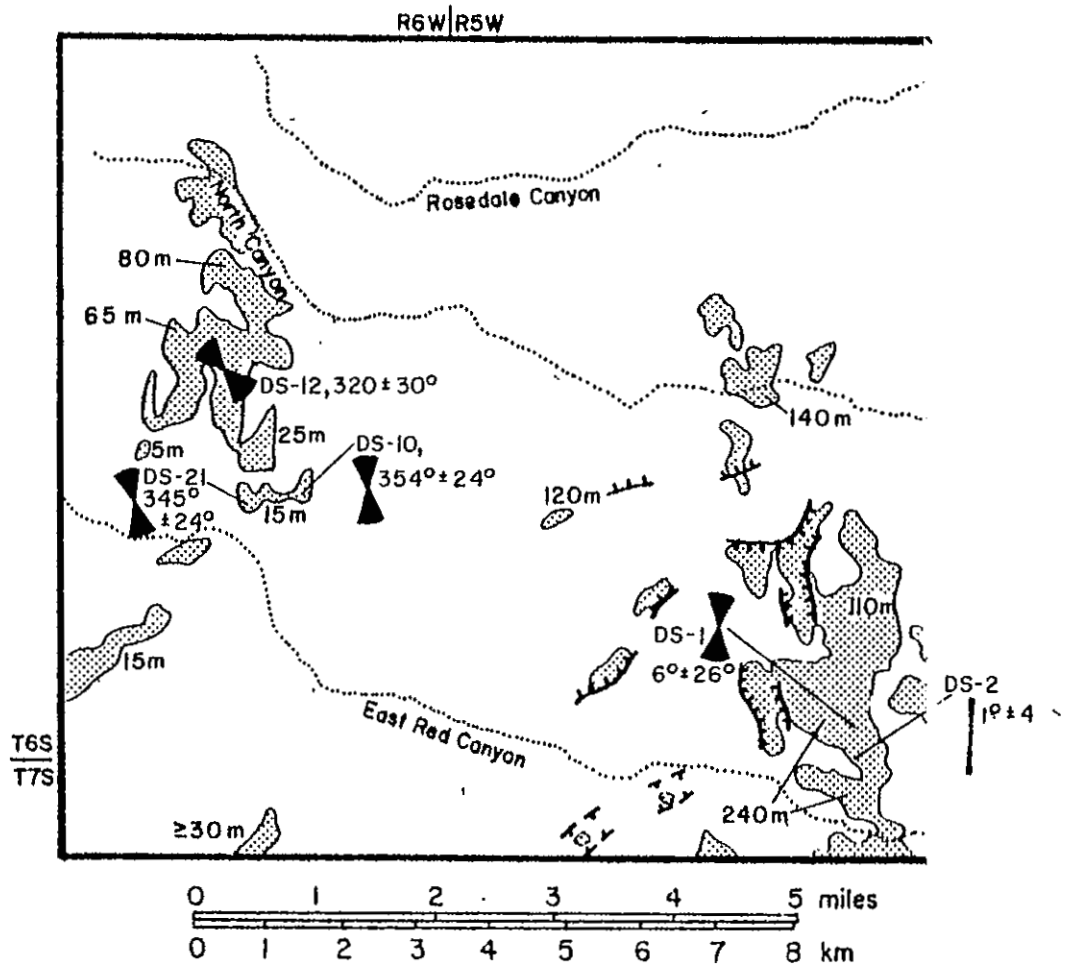

Figure 9. Outcrop map of the Lemitar Tuff showing thicknesses in meters and the distribution of paleocanyon walls buried by the unit. Magnetic anisotropy of susceptibility azimuth cones of confidence (95% level) are also plotted. Paleomagnetic sample numbers are shown with each anisotropy azimuth. Paleomagnetic data from McIntosh and others (1986).

Petrography

The Lemitar Tuff is a pale-red to reddish-brown densely welded tuff except for it's base which is poorly welded and a gray-orange-pink color. Phenocryst content in the unit increases continuously upward from 6-8% at the base to 40% at the top. Pumice content also increases upward from less than 1% at the base to about 10% at the top. Pumice fragments rarely exceed 10 cm in length (average 3-5cm), and compaction ratios are usually <10:1. There is no indication of elongation or lineation of the fragments. Lithic fragments rarely exceed 5% of the tuff, and are usually <2cm in diameter. They are most abundant (5-10%) at the base of a distinctive quartz-poor interval in the lower half of the unit. Lithic fragments in this interval are mostly rhyolitic or andesitic lava, but there are also minor amounts of crystal-rich fragments that are petrographically similar to the upper crystal-rich part of the Lemitar Tuff.

The vertical zonation of phenocrysts in the Lemitar Tuff is it's single most diagnostic feature. A series of 6 samples (83-110, 84-160 to 84-164) was studied from a 80m thick section measured on the west side of North Canyon in the western part of the study area (Plate 4). Petrographic data from this section (Fig. 10) correlates well with a section described by Osburn (1978) of the Lemitar Tuff in the Magdalena Mountains. The base of the unit contains 6-8%

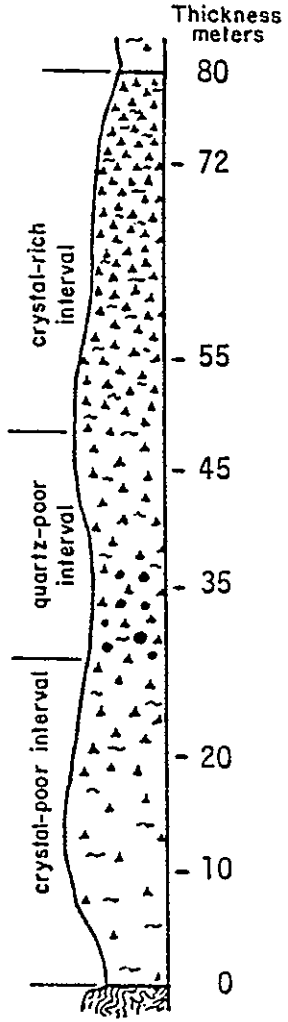

Sample no.	Color unweathered matrix	Lithics	Pumice	Total phen.	San.	Qtz.	Plg.	Biot.	Opaq.	Sphene	Cpx
84-164	pale-red 5R 6/2	1	8-10	40	25	10	5	0.5	t	t	t
84-163	reddish-pink 10R 7/2	1	8-10	35	14	7	14	0.5	t	t	0
84-162	reddish-orange 10R 6/4	1-2	6-8	27	15	2	10	1	t	t	0
84-161	pale-red 10R 6/2	6-8	3-6	17	9	3	5	0.5	t	t	0
84-160	pale-red 10R 6/2	1-2	3-6	12	6	5	1	t	t	t	0
83-110	grayish-orange-pink 10R 8/2	1-2	1-3	5	3	2	t	t	t	0	0

m-minor(less than 0.5%) t-trace(less than 0.1%) 0-not observed

Figure 10. Stratigraphic section of the Lemitar Tuff (sec. 11, T6S, R6W). Visual estimates of phenocryst percentages are from thin sections. Lithic and pumice percentages are estimated from hand specimens.

small (1mm) broken phenocrysts of sanidine, quartz, minor plagioclase, and a trace of biotite. The small size and broken nature of the phenocrysts continues up through the lower third of the unit to where a distinctive quartz-poor interval starts. This interval, about 12 meters thick here, is characterized by low quartz content (1-2%), and an increase in the average size of the feldspar grains (2-4mm). Also in the interval, there is an increase in plagioclase (10%), and biotite (1-2%). Above this interval quartz becomes larger (2-4mm), deeply resorbed, and more abundant (10%). Also above the interval, biotite decreases to <1%, but plagioclase increases to about 15%. At the top of the unit, plagioclase decreases to about 5%, and clinopyroxene (<0.2mm) occurs in trace amounts. Throughout the unit, euhedral sanidine (0.5-4mm) composes at least half of the phenocrysts.

South Canyon Tuff

Distribution

The South Canyon Tuff (Osburn, 1978) is a crystal-poor to moderately crystal-rich vertically zoned rhyolite ash-flow tuff that is exposed over most of the northern half of the study area. In the northern part of the study area, the South Canyon Tuff conformably overlies Lemitar Tuff, and is at least 650m thick. To the southeast South Canyon Tuff thins to a about 100m in the Wildcat Peak area, and rests with angular unconformity on northwest-tilted fault blocks of Lemitar Tuff and rhyolite lava. The fault blocks are part of a northeast trending northwest side down flexure (northwest facing margin of the Mt. Withington Cauldron) that formed during the eruption of the South Canyon Tuff. Along this flexure, South Canyon Tuff is intruded by a chain of rhyolite lava domes, and overlain by at least 200m of volcaniclastic rocks of the unit of East Red Canyon. Southeast of this flexure, South Canyon Tuff is eroded except in one area, and it's original thickness is unknown.

Members of the South Canyon Tuff

Within the study area, five members of the South Canyon Tuff are recognized (Plate 1). Listed in ascending stratigraphic order these are: 1) unwelded basal member;

2,3) welded tuff member and clast-supported lithic breccia member (both same age); 4) crystal-rich member; and 5) member of Rosedale Canyon. All of these are informal names.

UNWELDED BASE MEMBER

The base of the South Canyon Tuff is an unwelded crystal-poor tuff which was mapped as a seperate member only adjacent to Wildcat Peak and in the extreme southeast corner of the study area (Plate 1). The member consists of lithic rich tuff beds 0.1-2.0m thick, and minor volcaniclastic sandstones (<0.5m). Lithic fragments, mostly of rhyolite lava or Lemitar Tuff, rarely exceed 20cm and compcse about 10-20% of these tuffs.

WELDED TUFF MEMBER

Welded tuff is volumetrically the most important member of the South Canyon Tuff. It consists of all welded tuff including a basal vitrophyre, and all matrix-suppcrted lithic tuff above the unwelded base. West of Wildcat Peak, the unwelded basal member abruptly thins to less than 0.5m and is overlain by a brown or black vitrophyre 5-15m thick. The vitrophyre thickens and darkens in color with increasing distance from the southeast margin of the Mt. Withington Cauldron (Fig. 11). The degree of welding (defined by increasingly more elongated and flattened pumice fragments)

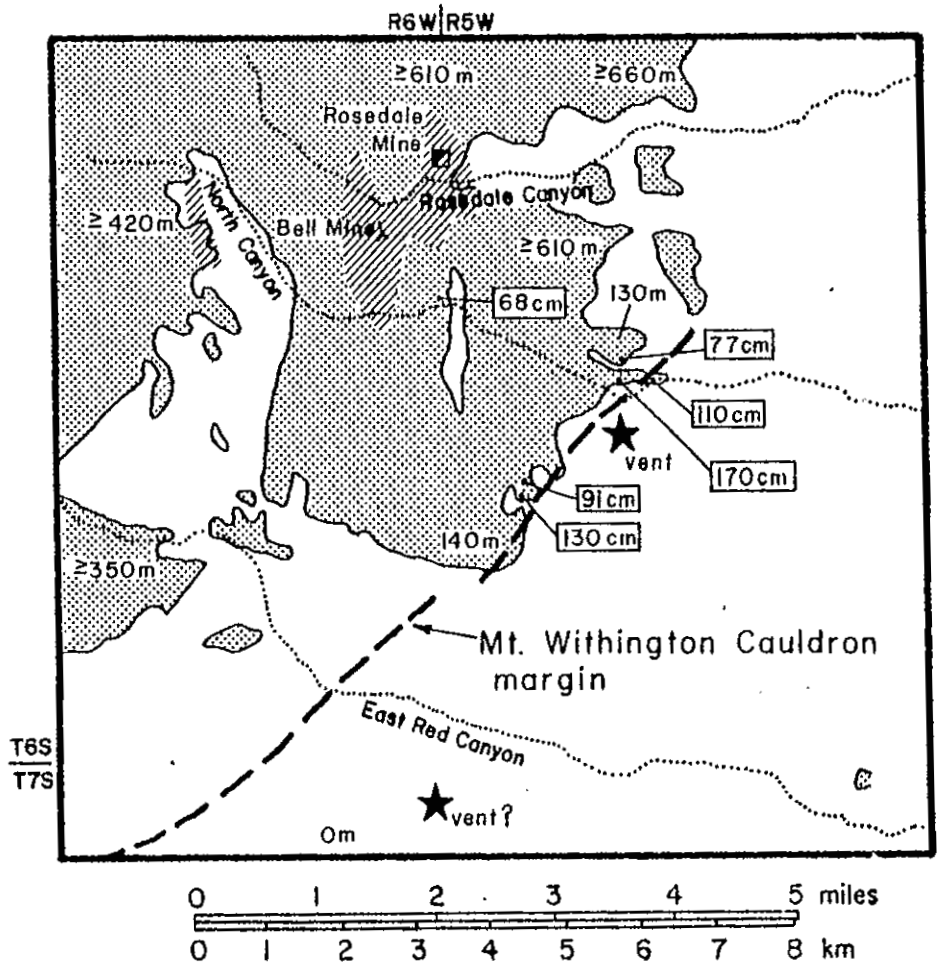

Figure 11. Outcrop map of the South Canyon Tuff showing the average size of the five largest lithic fragments (in centimeters) in exposures of the lithic-breccia member. Also shown are thicknesses of the unit (meters), zones of hydrothermal argillic alteration (lined pattern), and possible vents for the South Canyon Tuff.

similarly increases to the northwest.

LITHIC BRECCIA MEMBER

Intervals of moderately lithic-rich (10-30%) matrix-supported tuff are mapped with the welded tuff member. These intervals occur throughout the welded tuff member from Wildcat Peak southwest to The Park, and northwest to the Rosedale Mine area. They are interpreted to be distal equivelents of the clast-supported lithic breccia member. They contain lithic fragments mostly of rhyolite lava, Lemitar Tuff, and basaltic andesite lava which rarely exceed 20cm in diameter. Clasts of medium to fine-grained biotite rich monzogranite (IUGS classification) are minor but significant contributors to the population of lithic fragments in the uppermost part of the South Canyon Tuff.

The clast-supported lithic breccia member occurs within the welded tuff member, and is restricted to an area described by a 2km radius semicircle centered on and extending to the northwest of Wildcat Peak (Plate 1). It consists of four stratigraphically distinct lenses (10-100m thick) of clast-supported lithic breccia, with poorly welded tuff matrix. Lithic fragments in this member range in size from <1cm to >300cm, and are composed mostly of rhyolite lava or Lemitar Tuff. The average size of the largest 5

lithic fragments at each exposure of this member is plotted in Figure 11. One breccia occurs at the base and the others near the top of the welded tuff member. The basal breccia (60m thick) is crudely stratified dipping northwest, and contains minor matrix-supported intervals. It conformably overlies northwest tilted bedded tuff of the unwelded basal member northeast of Wildcat Peak (S1/2 sec. 17, T6S, R5W). Poorly welded tuff matrix in this breccia grades upward into welded tuff above with no indication of a cooling break. Eutaxitic foliation in the overlying welded tuff conforms with the regional 10-30 degrees east dips. Two breccia lenses southwest of Wildcat Peak (sec. 19, T6S, R5W) are both <10m thick (the north one is stratigraphically higher). Both lenses are unstratified, and occur just below the top of the welded tuff member. Northwest of Wildcat Peak (sec. 13, T6S, R6W, unsurveyed) an unstratified breccia lense (40m thick) occurs at the top of the welded tuff member. This lense pinches out into poorly welded tuff with <5% lithics from north to south across North Canyon.

CRYSTAL-RICH MEMBER

The crystal-rich member of the South Canyon Tuff is recognized only in the northern part of the study area. It is a 20-30m thick interval at the top of the welded tuff member that contains 30-35% phenocrysts. Crystal-rich tuff is common at the top of the South Canyon Tuff in the

Rosedale Canyon area. It was separated as a mappable member only where Bell Canyon enters North Canyon, because crystal-rich tuff here abruptly overlies a clast-supported lithic breccia member lense.

MEMBER OF ROSEDALE CANYON

The member of Rosedale Canyon of the South Canyon Tuff is recognized only in the extreme northeast corner of the study area. It is a moderately crystal-rich rhyolite ash-flow tuff that overlies crystal-rich (30-40% phenocrysts) South Canyon Tuff. It is interpreted as a seperate cooling unit of the South Canyon Tuff, younger than the crystal-rich member. One sample of the member was studied in thin section (84-167). It contains about 15% phenocrysts of euhedral blocky sanidine (0.5-2.0mm), and blocky euhedral resorbed quartz (0.5-2.0mm) in an approximate 2:1 ratio. Blocky subhedral plagioclase (0.5mm) occurs in minor amounts. Biotite (0.5mm), euhedral sphene (0.5mm), and opaque minerals (0.3mm) occur in trace amounts. The matrix of the tuff is completely devitrified (no evidence of shards), and contains spherical lithophysae (2mm) filled with vapor phase sanidine and quartz. Pumice fragments (about 1cm long), replaced by vapor phase quartz and sanidine, compose about 3% of the tuff. Pumice are compacted with flattening ratios of about 10:1), but there is no apparent elongation or preferred orientation of the

fragments. Lithic fragments of South Canyon Tuff and basaltic andesite (2mm-2cm) compose about 3-5% of the tuff.

Petrography

No vertical section of the South Canyon Tuff was described in the study area. Instead, 19 samples (thin sections and hand specimens) were described from locations laterally and vertically throughout the unit (Table 1).

Phenocryst percentages in South Canyon Tuff increase from 2% at the base to 35% at the top. The increase is continuous and gradual up to about 25%, but the increase from 25% to 35%, which is only recognized in the north, occurs rapidly in the upper 20-30m of the unit. Phenocrysts throughout the unit are mostly sanidine and quartz in an approximate 3:2 ratio, with minor amounts of plagioclase and biotite, and trace amounts of opaque minerals, and sphene. Sanidine occurs as blocky euhedral grains (1-3mm), and quartz as blocky subhedral grains (1-3mm) that are usually resorbed. Plagioclase, which rarely composes more than 2% of the tuff, occurs either as individual subhedral grains (<1mm) or in glomeroporphyritic growths (1-3mm) with biotite, sphene, or opaque minerals. Biotite occurs as flakes (0.5-1.0mm), and opaque minerals as rounded grains (<0.5mm). Sphene occurs as euhedral grains which average 0.5mm, but are as large as 1.5mm.

Table 1. Petrographic data from samples of the South Canyon Tuff throughout the study area. Phenocryst percentages are visually estimated from thin sections, and lithic and pumice percentatges are estimated from hand specimens.

Sample no.	Lithics	Pumice	Total phen.	San.	Qtz.	Plg.	Biot.	Opaq.	Sphene
84-168	5	10	35	20	13	1.5	0.5	m	t
83-125	1	12	25	15	9	m	m	m	t
83-152	5	15	23	12	10	-	m	m	t
83-153	5	12	20	9	10	0.5	m	t	t
83-118	t	10	20	12	6	2	m	m	t
83-44	2	?	20	13	6	1	t	t	t
83-45	4	12	19	9	9	1	t	t	t
83-53	4	?	17	9	8	m	m	t	-
83-151	5	15	17	10	6	1	t	t	-
84-167	2	2	15	9	5	0.5	m	t	t
83-104	7	5	15	7	6	2	t	t	t
83-128	2	17	15	10	5	m	t	t	t
83-99	3	15	15	7	7	1	t	t	-
83-181	4	10	12	6	6	-	t	t	t
83-102	2	10	12	6	5	0.5	t	t	t
83-103	3	15	9	4	5	m	m	t	-
83-129	3	10	7	3	3	1	t	t	-
83-145	3	7	6	3	3	m	t	t	-
83-41	2	-	2	1	1	-	-	-	t

m minor (less than 0.5%)
t trace (less than 0.1%)
- not observed

The matrix of the South Canyon Tuff is only partially devitrified, and contains well preserved glass shards. Uncompacted shards (0.1-0.5mm long) are found in poorly welded tuff just below the basal vitrophyre (83-41), but in densely welded and lineated tuff, shards are stretched up to 1.0mm long, and have compaction ratios as high as 20:1.

Pumice fragments in the South Canyon Tuff are vertically zoned with percentages increasing from 0% at the base to 15-18% in the middle to upper part of the unit (Table 1). Pumice in the unit are typically elongated and preferentially oriented, with compaction ratios up to and greater than 20:1 (Fig. 12). Pumice that are elongated and preferentially aligned are usually found only in the lower to middle part of the unit (3%-12% phenocrysts). In the north and northeast elongated and aligned pumice fragments are found throughout the unit. Field azimuth measurements of aligned pumice fragments in the South Canyon Tuff are plotted in Figure 13. Figure 13 shows pumice elongated northwest-souhteast in a 2-3km wide belt adjacent to and parallel to the southeast margin of the Mt. Withington Cauldron. Viewed in thin section, samples of the South Canyon Tuff from this belt contain stringy pumice fragments composed of devitrified glass (Figure 14). Northwest of this belt, aligned pumice azimuths abruptly swing around to an east-west orientation. These pumice, in contrast to the glassy variety, are all completely replaced by vapor phase

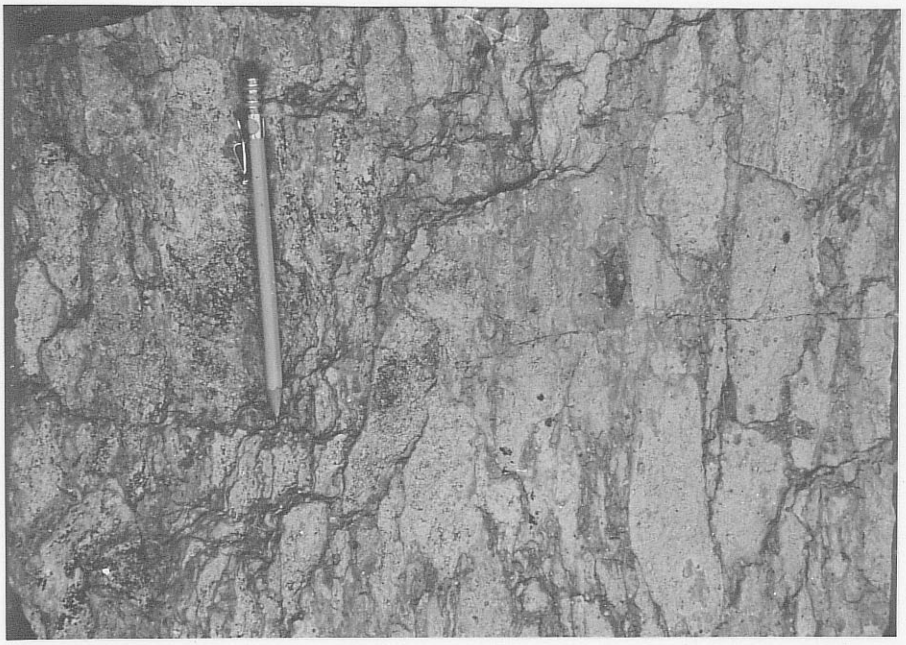

Figure 12. Photograph of lineated pumice in the South Canyon Tuff (sec. 10, T6S, R6W).

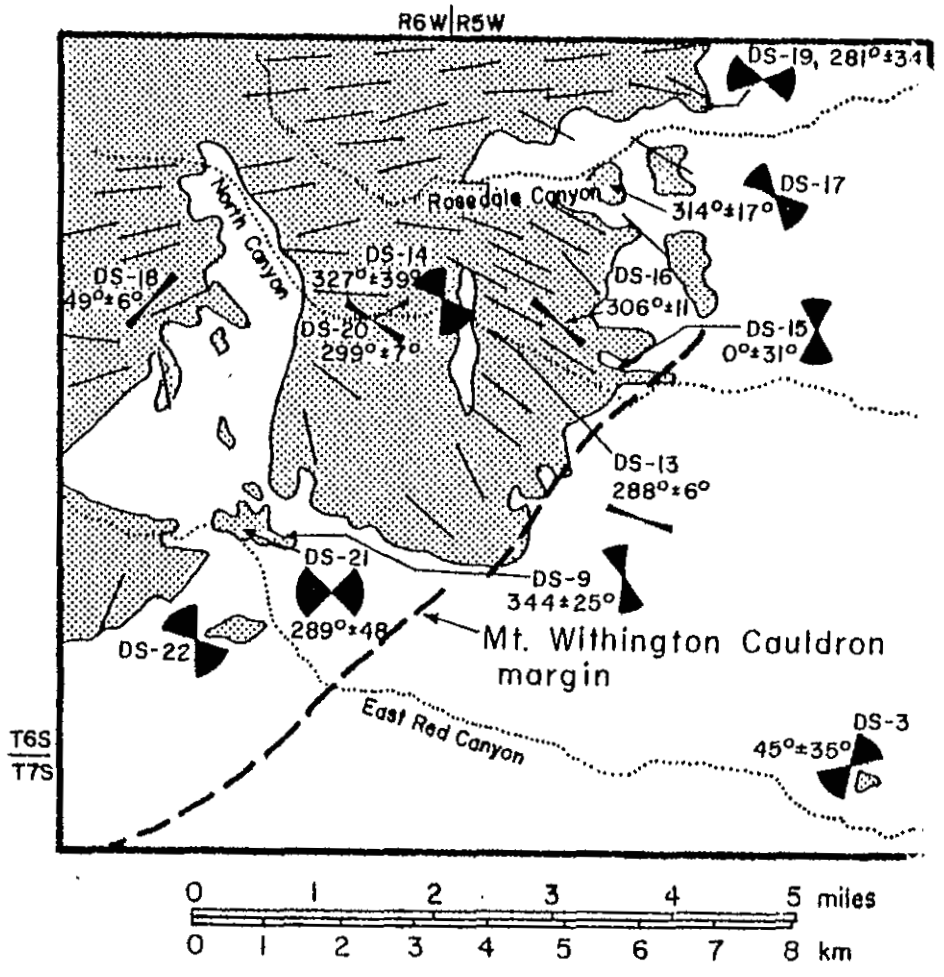

Figure 13. Outcrop map of the South Canyon Tuff showing field measurements of lineated pumice (lines) and magnetic anisotropy of susceptibility azimuth cones of confidence (95% level). Paleomagnetic sample numbers are showr with each anisotropy azimuth. Possible vents for the South Canyon Tuff are also shown. Paleomagnetic data from McIntosh and others (1986).

A

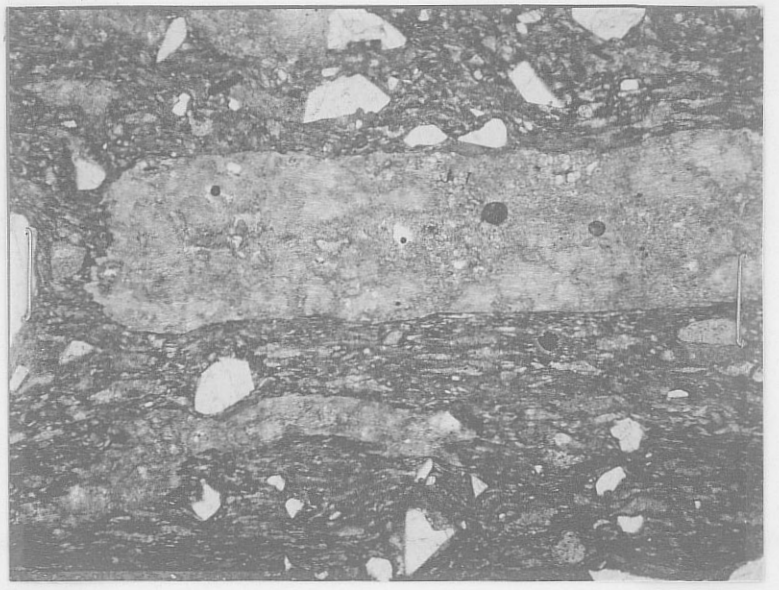

2 mm

B

Figure 14. Photomicrographs of "glassy" devitrified pumice fragments in the South Canyon Tuff (C-83-103). A) plain light, B) crossed polars.

intergrowths of sanidine and quartz (Figure 15).

Hydrothermal alteration

In the north part of the study area, the South Canyon Tuff hosts two abandoned epithermal gold mines (Rosedale Mine, Bell Mine). At these mines, according to Neubert (1983), mineralized veins parallel basin and range faults that trend 340 degrees and dip about 75 degrees to the west. Argillic alteration, associated with the mineralization, occurs parallel to and adjacent to faults throughout the area. The zone of alteration, defined as the area where sanidine phenocrysts are white and chalky, is outlined in Figure 11. The alteration also occurs along the Lemitar-South Canyon contact on the west side of North Canyon. Along this contact, alteration is most advanced in thin poorly welded tuff just below the vitrophyre of the South Canyon Tuff. Alteration extends downward about 30m into the Lemitar Tuff, but upward only about 10m into the South Canyon vitrophyre.

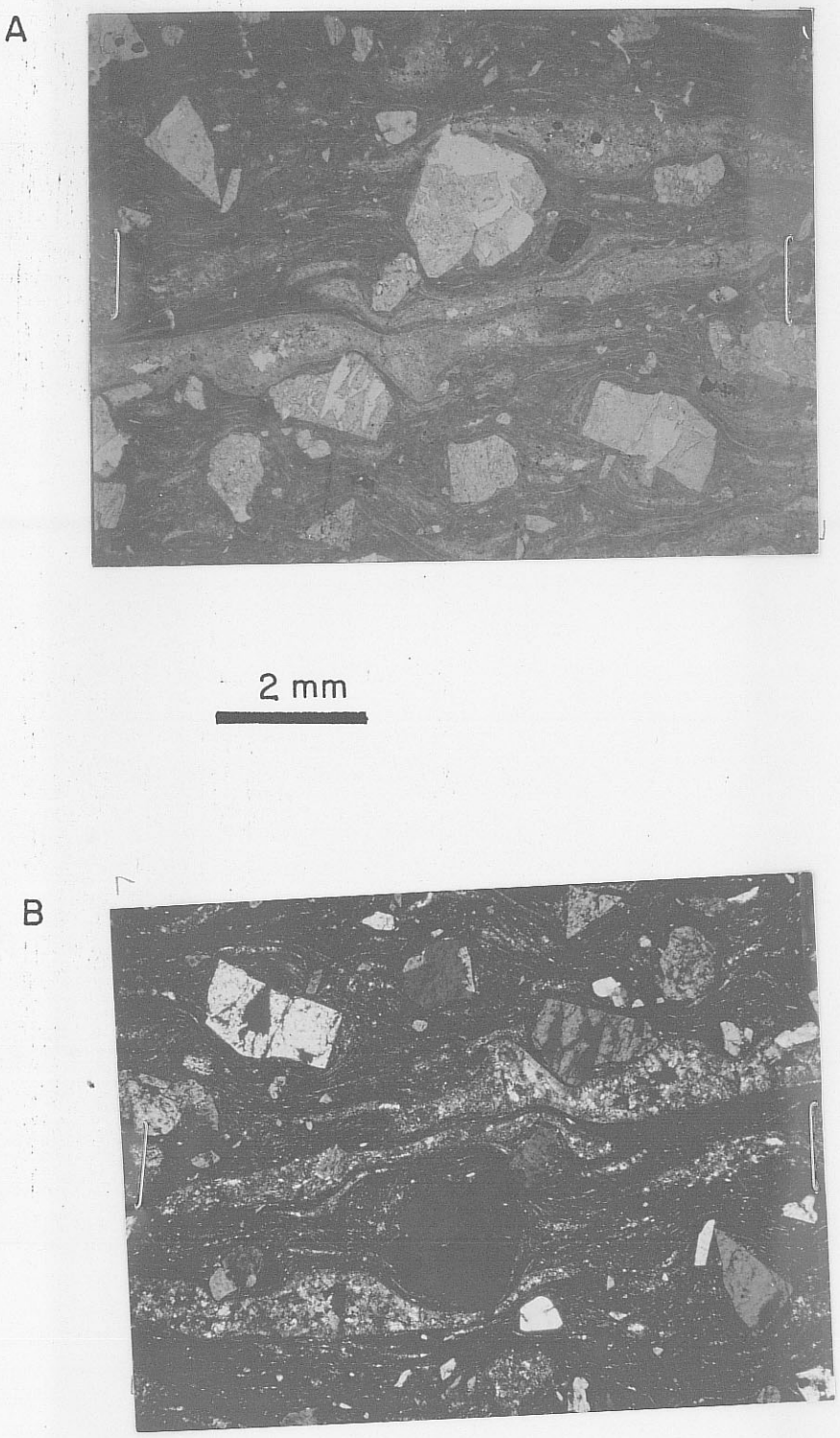

Figure 15. Photomicrographs of vapor phase recrystallized pumice fragments in the South Canyon Tuff (C-83-128). A) plain light, B) crossed polars.

Unit of East Red Canyon

Distribution

The unit of East Red Canyon (new informal name) is a sequence of volcaniclastic and minor pyroclastic rocks interpreted as moat-fill for the Mt. Withington Cauldron. The proposed moat is a northeast trending basin, 5 km wide, that extends across the study area from southwest to northeast (Fig. 16). To the southeast, the unit laps onto the margin of the Mt. Withington Cauldron. At the southern edge of the study area, the unit buries the north face of the 3km wide rhyolite lava dome of Cave Peaks. To the southwest, the unit continues into unmapped terrane. All evidence of the unit's northwestward extent has been removed by erosion. A major east-west trending south-side down fault, just north of East Red Canyon, exposes the lower 10-50m of the unit to the north of the fault. Coarse grained sediments of the unit here are interlayered with thin (<2m) lithic-rich ash-flow tuffs. South of this fault, the unit of East Red Canyon is overlain by the tuff of Turkey Springs, and is at least 200m thick.

In the northern part of the study area, most of the unit of East Red Canyon is eroded away, and its top is not preserved. About 2km north of Wildcat Peak the unit fills a slight depression where it is at least 50m thick. The unit

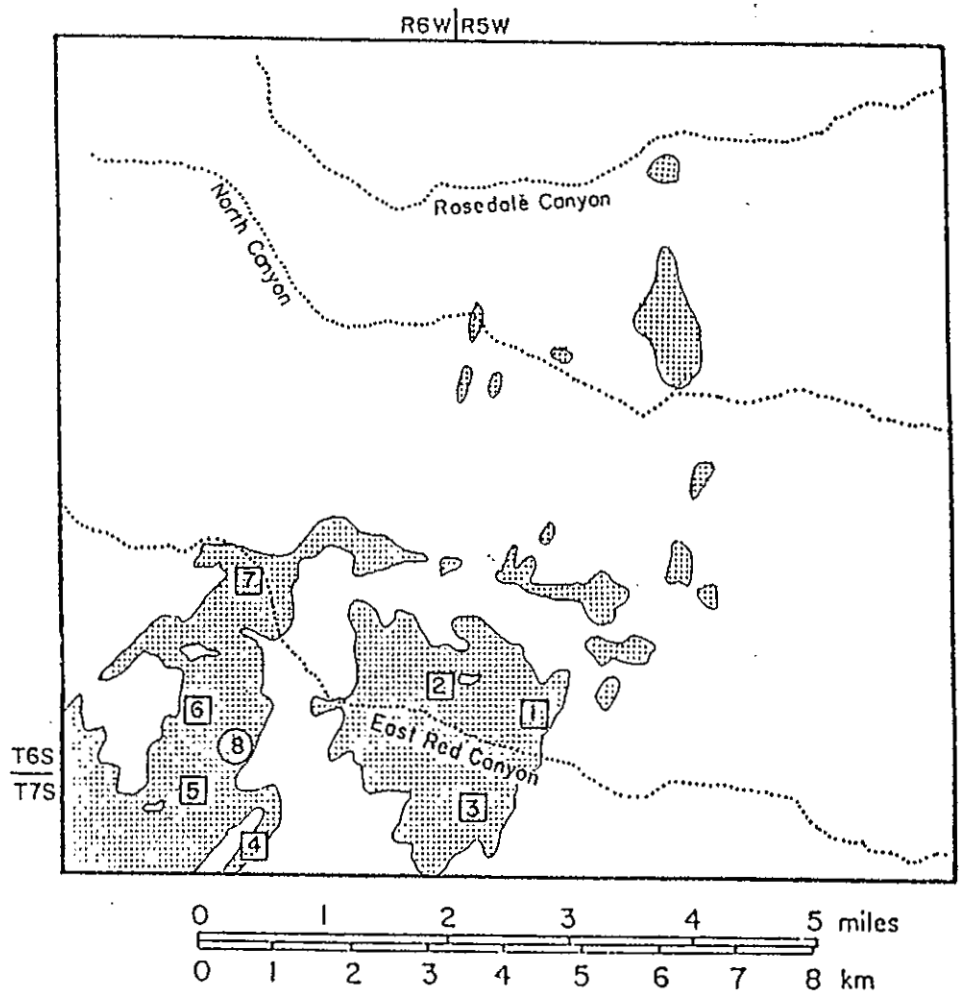

Figure 16. Outcrop map of the unit of East Red Canyon showing the location of the measured sections described in Figure 17a,b.

rests with slight angular unconformity (Plate 1) on South Canyon Tuff throughout this area. The unit here consists mostly of epiclastic rocks (Diamictite, conglomerate, and cross-stratified sandstone), but lithic-rich poorly welded ash-flow tuffs are also present. These pyroclastic rocks are spatially related to the rhyolite dome of Wildcat Peak, and are probably derivatives of it. South and east of Wildcat Peak, the unit of East Red Canyon consists of bedded lithic-rich ash-flow tuffs with minor amounts of epiclastic material. These rocks overlie the rhyolite lavas of Horse Mountain Canyon, and are intruded by the rhyolite of Horse Mountain.

Epiclastic rocks of the unit of East Red Canyon in the northern part of the study area become finer grained towards the northwest. Clasts in all lithologies of the unit are mostly crystal-rich tuff (Lemitar and/or South Canyon), and rhyolite lava. Minor amounts of biotite-rich monzogranite are also present. The northwesternmost exposures of the unit are tan colored cross-stratified sandstone. These rocks, which rest directly on South Canyon Tuff, are interpreted as eolian.

Petrography

Six generalized stratigraphic sections (located in Fig. 16) of the unit of East Red Canyon were measured in the southern part of the study area. One detailed section was described from a sequence of cross-stratified sandstone in the western part of the basin. Lithologies in the stratigraphic sections (Fig. 17a,b) are listed and described below.

CLAST-SUPPORTED DIAMICTITE

Clast-supported diamictite occurs in 0.3 to 3.0m thick beds that have sharp, but usually non erosional, lower contacts. The clasts (<1cm-3.0m), cemented in a medium to fine-grained matrix, are subangular to subrounded. The beds are interpreted as deposits of either clast-rich debris flows (Shultz 1984) or gravel dominated hyperconcentrated flood flows (Smith, 1986, p. 4). They are characterized by an absence of layering or sedimentary structures, except for reverse grading at their base.

MATRIX-SUPPORTED DIAMICTITE

Matrix-supported diamictite, interpreted as deposits of pseudoplastic debris flows (Shultz, 1984), occur in beds (0.5-5.0m thick). They contain 5-20% clasts (0.5-10.0cm) suspended in matrix-supported sandstone (Fig. 18). The base

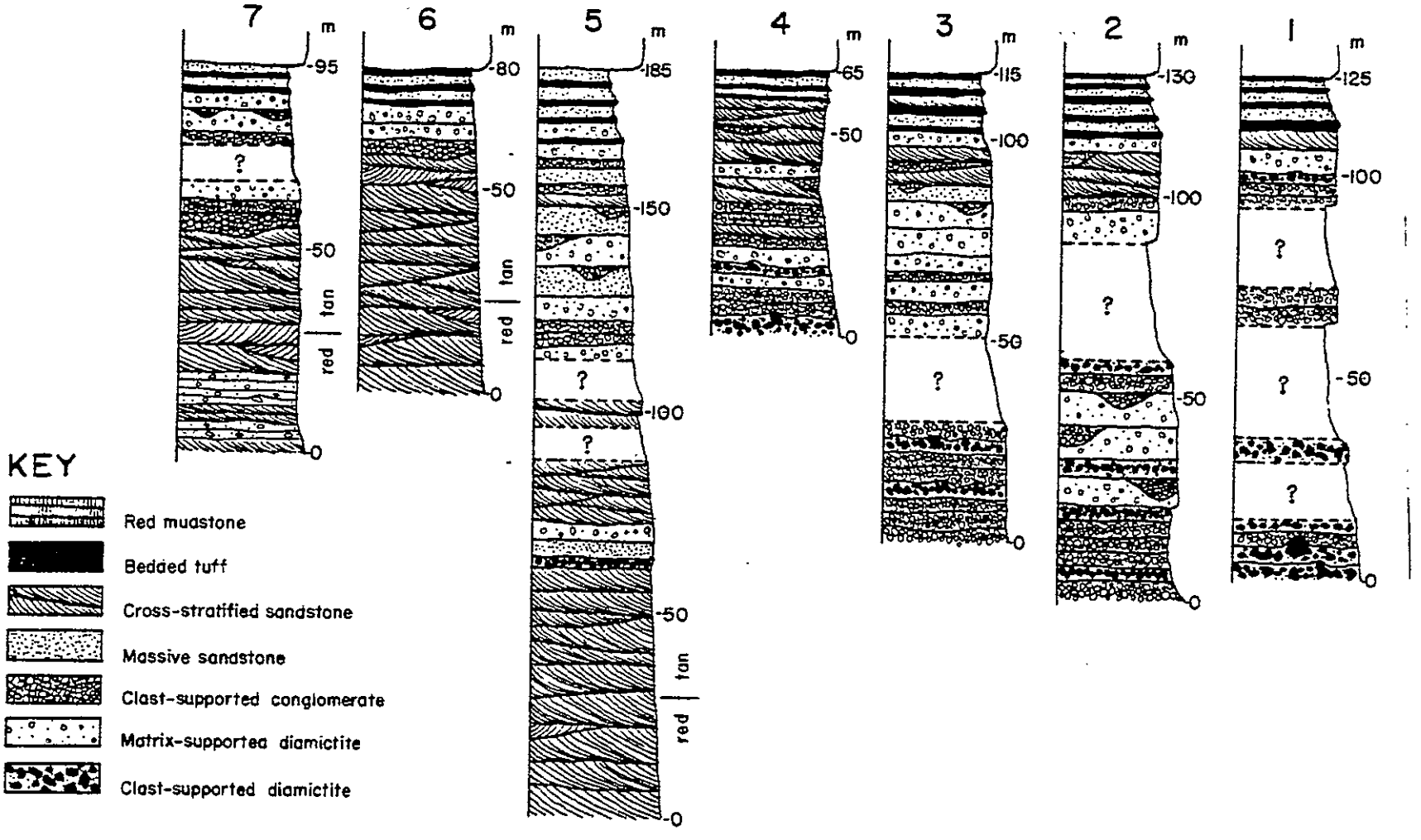

Figure 17(a). Generalized stratigraphic sections of the unit of East Red Canyon.

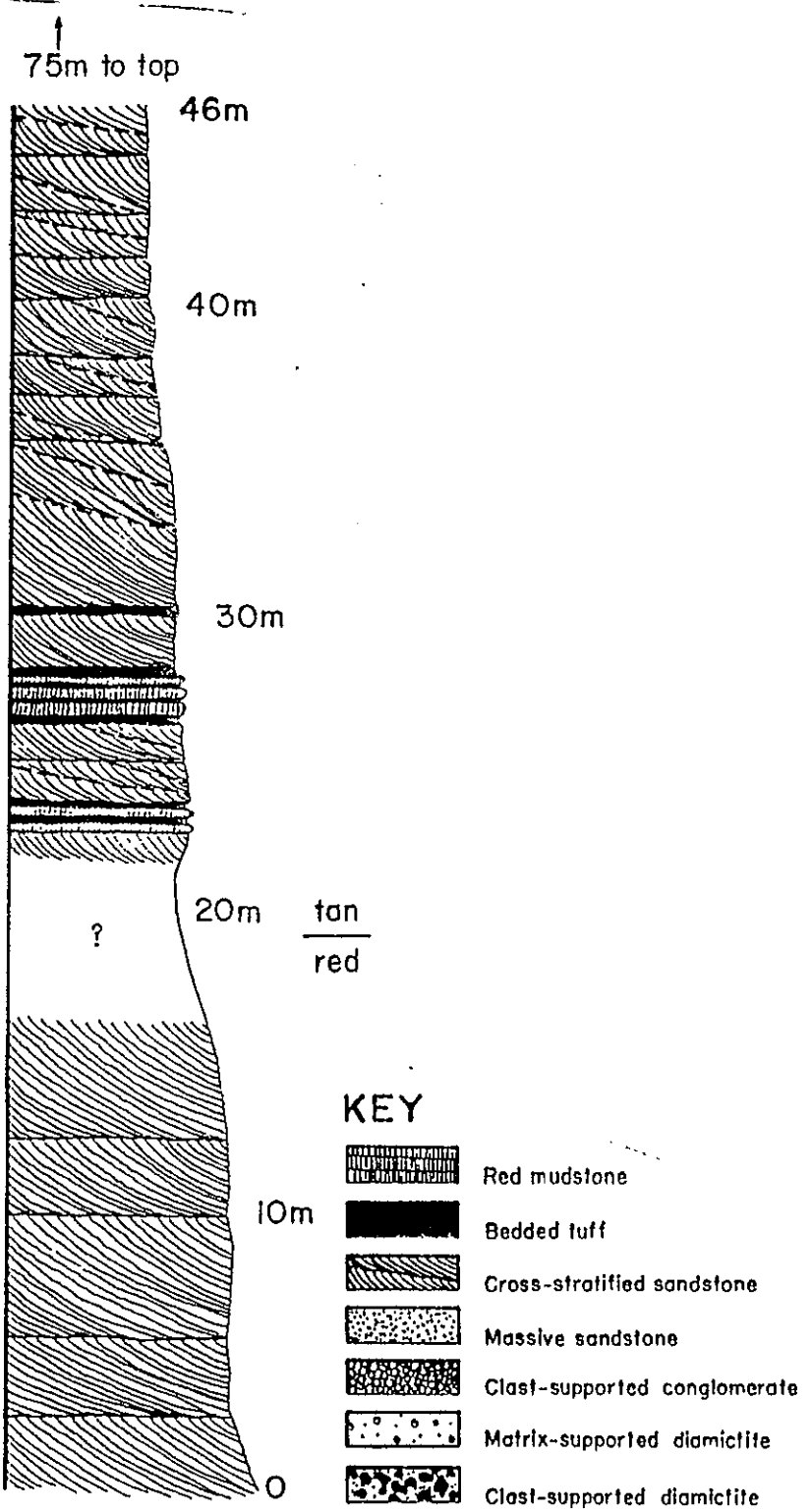

Figure 17(b). Detailed stratigraphic section of an eolian sandstone sequence in the unit of East Red Canyon (sec. 3, T7S, R6W).

Figure 18. Photograph of matrix supported diamictite (sec. 3, T7S, R6W).

of the beds are typically coarser grained, and may be clast-supported.

MASSIVE SANDSTONE

Massive sandstone occurs in beds 0.5-6.0m thick composed of medium to coarse-grained, moderately well to poorly-sorted sandstone. Lower and upper contacts may be sharp or gradational with adjacent units. The sandstone may contain up to 15% pumice fragments that are 5 to 10 times larger than the median grain size. Much of the massive sandstone and the finer grained matrix-supported diamictites are possible sand-dominated hyperconcentrated flood-flow deposits (Smith, 1986, p. 5).

CLAST-SUPPORTED CONGLOMERATE

Clast-supported conglomerates, interpreted as stream-channel or sheetflood deposits, are the most abundant coarse-clastic lithology in the basin. They occur in lenticular to tabular 0.1 to 2.0m thick sets that usually have sharp lower contacts. Clasts (<1cm to 30cm) are sub-rounded to rounded, and are arranged in beds that are usually normally graded.

CROSS-STRATIFIED SANDSTONE

Cross-stratified sandstone occurs in planar tabular to wedge-shaped sets 0.5-7.0m thick. The sand is moderately well-sorted to very-well sorted medium to fine grained, and is deposited in extremely continuous cross-strata that dip from 2 to 35 degrees (Fig. 19). The sandstones are thought to be eolian partly because the thickness of the sets (up to 7.0m thick) is too great to be realistically compared with any non-eolian terrestrial environment. The most diagnostic eolian characteristic of the sandstones, however, is the widespread occurrence in these rocks of the three principle types of eolian stratification; grainfall; grainflow; and wind-ripple laminae (Hunter, 1977; Kocurek and Dott, 1981). Grainfall deposits, the most abundant stratification type observed in this study area, are thin blanket-like laminae that accumulate on the lower lee-slopes of dunes. Grainflow deposits, lenticular bodies of sand that have avalanched down over-steepened dune faces, are usually found on the upper lee slopes of dunes, and therefore are rarely preserved. Grainflow deposits are rare, but do occur in the upper part of the thickest cross-strata sets in this study area. Eolian rippleform laminae commonly form on windward slopes, reactivation surfaces, and the lower lee slopes of dunes. Rippleform laminae from this area are identified as eolian because of their high (>15) ripple indices

Figure 19. Photograph of basal portion of a cross-stratified sandstone set (sec. 26, T6S, R6W).

(wavelength divided by the height), and because they are inversely graded.

An important feature of cross-stratified sandstone in the unit of East Red Canyon is laterally extensive planar erosion surfaces that bound the sets. Brookfield (1977), and Kocurek (1981, 1984) recognize three orders of bounding surfaces in eolian sandstones. Higher (first) order surfaces truncate progressively lower (second and third) order surfaces. First order surfaces represent interdune deflation areas that have been buried by migrating complex dunes or draas. Second order surfaces separate individual dunes that migrate across the complex dunes, and third order surfaces are reactivation surfaces within these dunes. In the detailed stratigraphic section of cross-stratified sandstone (Fig. 17b), first and second order surfaces are delineated with solid and dashed lines, respectively. Third order surfaces are too subtle to be shown here. Figure 20 is a photograph of a cliff of eolian sandstone illustrating typical first order surfaces in this study area. Figure 21 is a schematic block diagram showing migrating eolian bedforms that may account for these bounding surfaces. In Figure 21, the interdune deflation areas, when buried by the next dune system, become first order bounding surfaces.

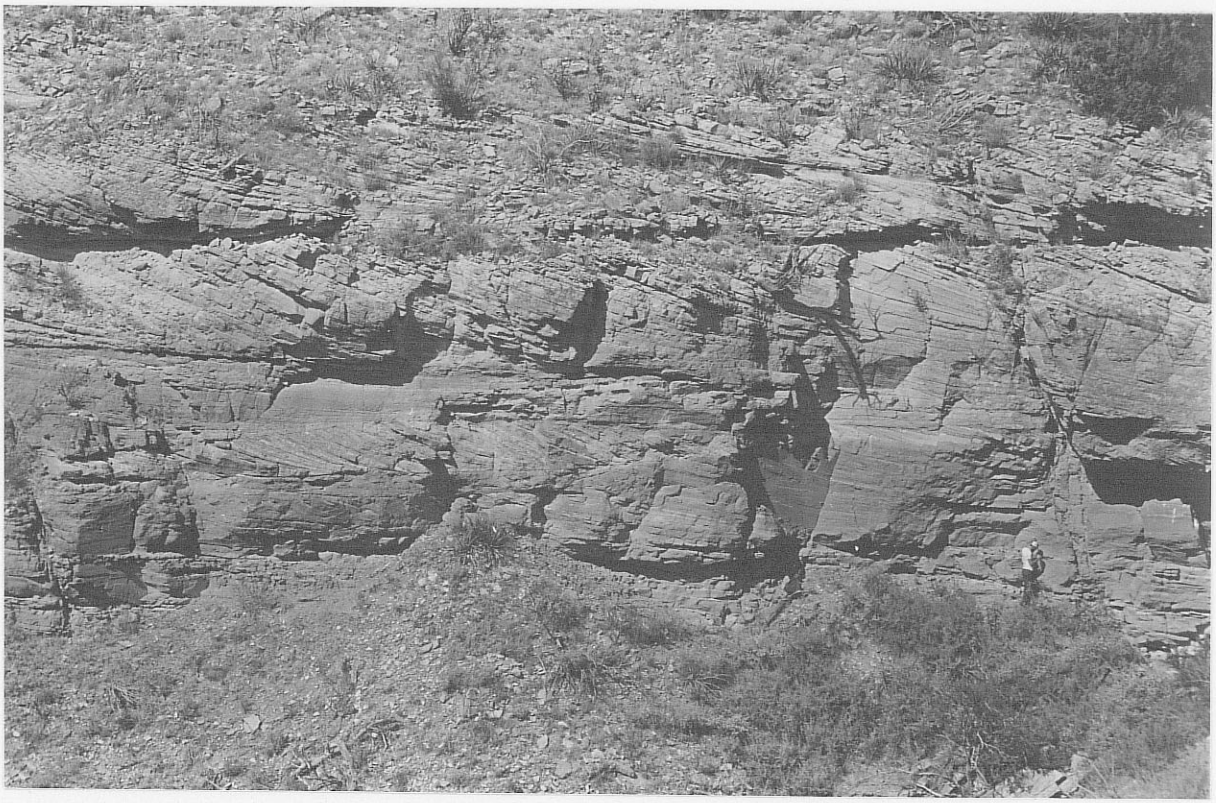

Figure 20. Photograph of cliff of eolian sandstone illustrating typical first order bounding surfaces (sec. 26, T6S, R6W). Geologist Gunarz Berzins is standing at the contact between eolian beds and medium-bedded matrix-supported diamictite.

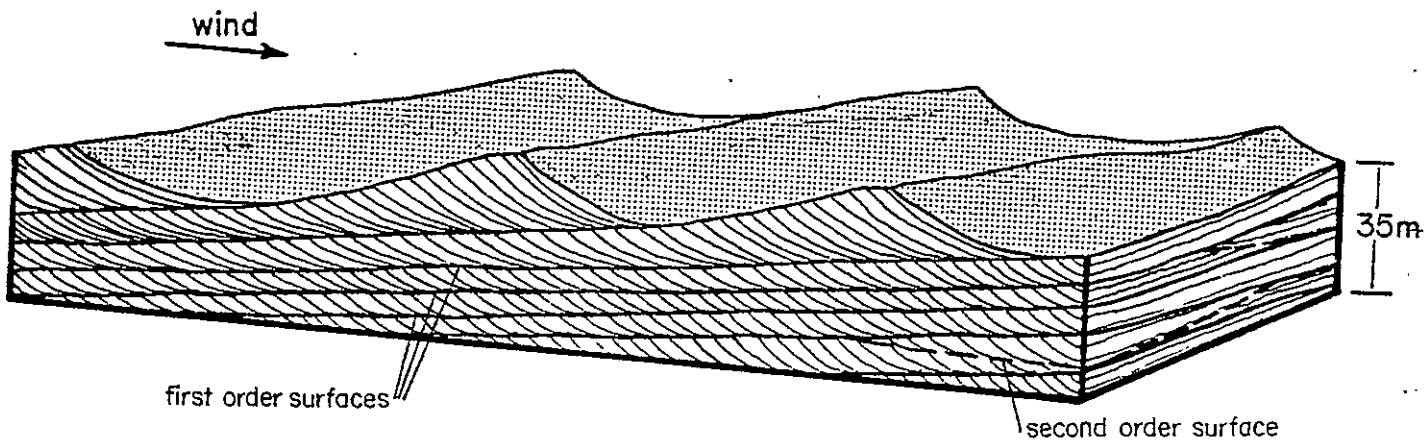

Figure 21. Block diagram showing a possible origin of the first order bounding surfaces observed in the unit of East Red Canyon.

BEDDED TUFF AND RED MUDSTONE

Bedded Tuff occurs in 0.2-2.0m thick beds of crystal-poor unwelded thin-bedded to very thin-bedded ash-fall tuff, ash-flow tuff and possible surge deposits (Fig. 22). Red mudstone ocurs as 2-5cm thick beds of silicified red mudstone which commonly show desiccation cracks (Fig. 23).

Stratigraphic sections

The stratigraphic sections of the unit of East Red Canyon in the study area (Fig. 17a,b) indicate different depositional histories in the east and west parts of the basin. The only consistent part of the unit throughout it's basin is the upper 10-30m, which consists of massive-sandstone or cross-stratified sandstone interlayered with sequences of bedded-tuff.

The eastern part of the basin, interpreted as the proximal region of an alluvial fan complex, consists mostly of clast-supported diamictite and clast-supported conglomerate that grades upward into a sandstone dominated sequence in the upper 20-30m of the unit. Coarse-clastic detrital fragments in the eastern part of the basin consist of 90% rhyolite lava and about 10% moderately crystal-rich ash-flow tuff which is probably South Canyon Tuff. Paleocurrent directions were not measured here because

Figure 22. Photograph of a 1 meter thick sequence of bedded ash-flow tuff (sec. 35, T6S, R6W).

Figure 23. Photograph of desiccation cracks in a mudstone bed (sec. 26, T6S, R6W).

imbrication or cross-stratification was not recognized. However, because of an overall decrease in the average size, and increase in textural maturity of the sedimentary grains from east to west, It is likely that the southeast margin of the basin was a major source of sediment for this fan complex.

The transition from coarse-clastic dominated lithologies in the east to sandstone dominated lithologies in the west is obscured by a north-south trending structural graben that transects the basin. The unit of East Red Canyon west of this graben, in contrast to the fining upward sequence to the east, is a coarsening upward sequence. The lower 100m consists dominately of cross-stratified sandstone (3-7m thick sets), and minor (<1m thick) matrix-supported diamictite interpreted as distal equivelents of debris flow deposits (Fig. 17a). The lower 100m of the unit is distinctively red colored, but above rocks are tan colored (Fig. 17a,b). In Figure 17b, this color change occurs just below a sequence of bedded tuffs and red mudstones. The mudstones probably formed just above a permanent water table in periodically wet interdune deflation areas. Sediment below this paleo water table may have been oxidized and stained red before the upper light colored sand was deposited. The upper tan sequence consists of cross-stratified sandstone (1-5m thick sets) that grade upward into coarse-clastic dominated lithologies (Fig. 17a).

Coarse detrital fragments in the western partof the basin consist of about 60% rhyolite lava, 20% crystal-poor tuff (Vicks Peak) and 20% crystal-rich tuff (South Canyon?).

One thin section (83-300) of the lower red colored sandstone, and two thin sections (83-51,207) of the upper tan colored sandstone were studied and point-counted (Table 2). The sandstones are composed primarily of rhyolitic lithic grains (55-75%), but also contain significant amounts of basaltic lithic grains.

A rose diagram of paleocurrent measurements in eolian sandstones throughout the unit of East Red Canyon is plotted on Figure 24. The northeast transport direction is typical of Cenozoic wind directions in central New Mexico (Wright, 1956; Lambert, 1968, p. 197, 211).

Paleontology

Two kinds of ichnofossils were found in the upper part of the unit of East Red Canyon. A cast of arctiodactyl (split hooved mammal) hoof prints (Fig. 25) was found in a loose slab of bedded-tuff in Allen Spring Canyon. In the same canyon, an inclined burrow, about 6cm in diameter, was found at the top of a cross-stratified sandstone set (Fig. 26). The burrow, filled with ash below and sand above, is overlain by a 0.5m thick set of bedded tuff, which is in turn overlain by a bed of massive sandstone. One possible

Table 2. Percentages (determined by point-count) of grain types in eolian sandstones from the unit of East Red Canyon.

Sample	pore space	felsic volcanic lithics	mafic volcanic lithics	sanidine and quartz	plagioclase	mafic minerals	microcline	points counted
83-301	29	40	19	10	1	0.1	0.1	1638
83-207	10	68	8	9	3	1.2	0.2	1604
83-51	24	61	5	13	2	1.8	0.3	1000

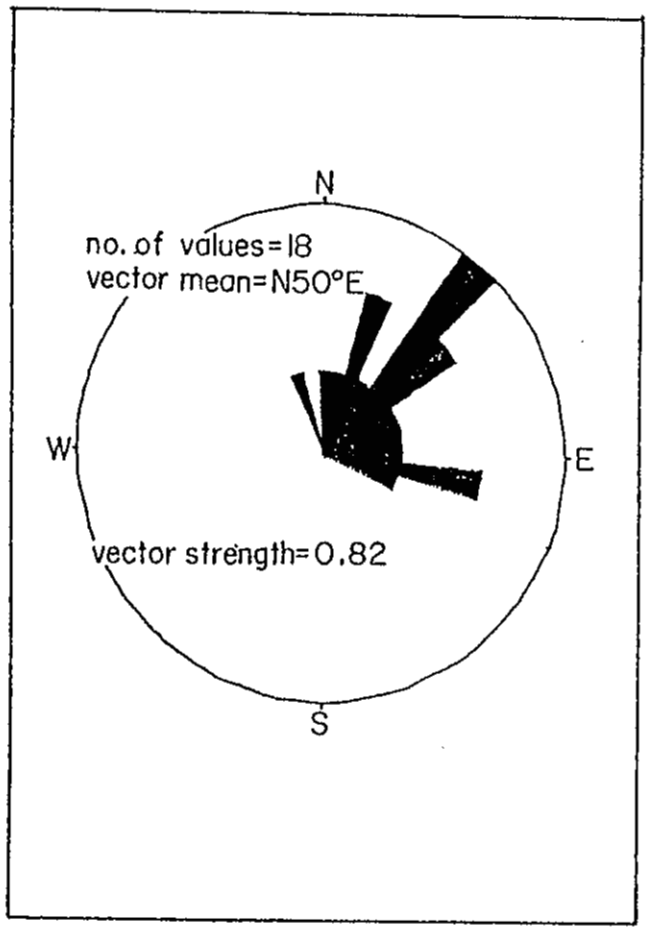

Figure 24. Rose diagram of paleocurrent directions from eolian sandstone in the unit of East Red Canyon.

Figure 25. Photograph of arctiodactyl hoof print molds in a slab of bedded tuff (sec. 35, T6S, R6W). The pencil for scale is about 10cm long.

Figure 26. Photograph of inclined burrow about 6cm in diameter (sec. 35, T6S, R6W), see text for discussion.

interpretation is that, buried by an ash-fall layer, the burrowing animal dug it's way out, and in route to the surface pushed stoped ash to the bottom of the burrow. Eventually, the burrow would have filled with sand from above.

Tuff of Turkey Springs

Distribution

The tuff of Turkey Springs (new informal name) is a crystal-poor to moderately crystal-rich vertically zoned rhyolite ash-flow tuff. The unit overlies the unit of East Red Canyon, and is exposed only in the southwest part of the study area (Fig. 27). The unit is not correlated with the member of Rosedale Canyon of the South Canyon Tuff because their paleomagnetic pole positions are different (Chapter 4). The top of the unit is not preserved anywhere in the study area, and it is at least 150m thick near Turkey Springs in East Red Canyon.

The tuff of Turkey Springs is divided into two members: 1) lower unwelded member; and 2) upper welded member. The lower member is a massive crystal-poor unwelded tuff that is distinguished from tuffs in the upper unit of East Red Canyon because it is not bedded and it is continuous with welded tuff of the upper member. The lower member is thickest (70m) near Turkey Springs, but it thins northward to <5m stepwise across south side down faults which do not effect the overlying welded tuff member.

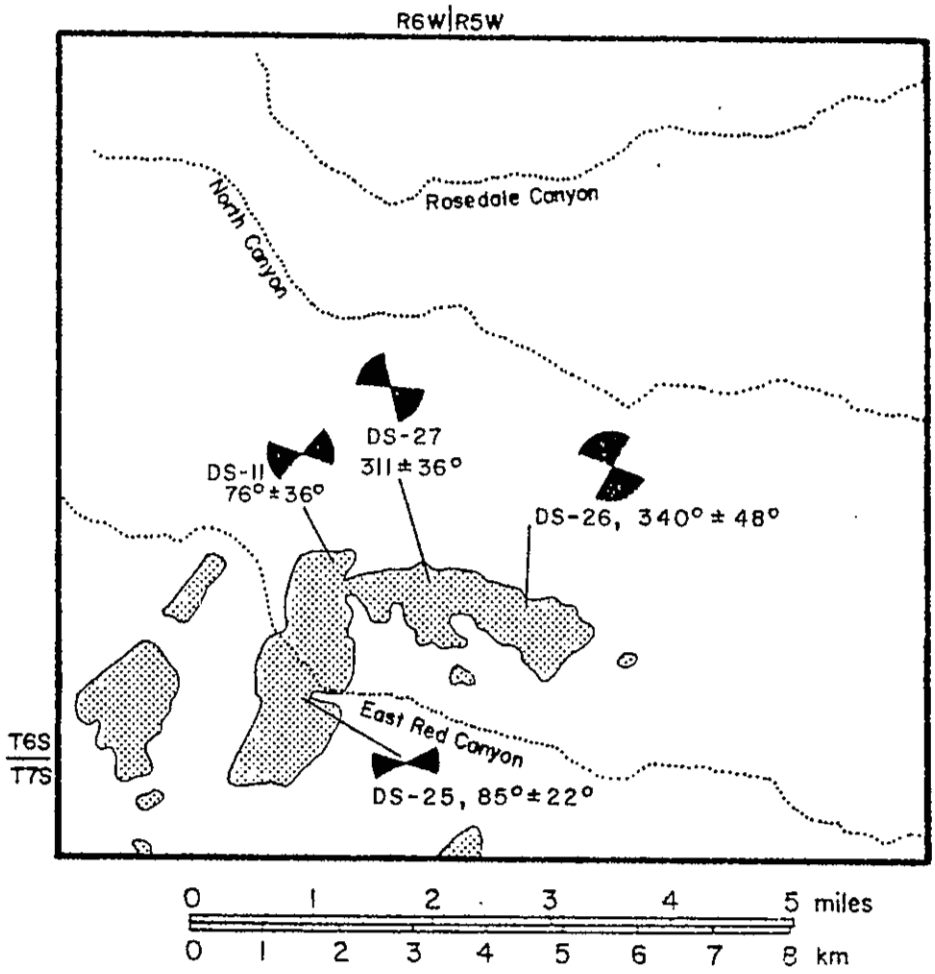

Figure 27. Outcrop map of the tuff of Turkey Springs showing magnetic anisotropy of susceptibility azimuth cones of confidence (95% level). Paleomagnetic sample numbers are shown with each azimuth. Paleomagnetic data from McIntosh and others (1986).

Petrography

A 100m thick vertical section of the tuff of Turkey Springs comprising 7 samples (84-4-1,7), was collected at Turkey Springs (Plate 4) for combined micropetrographic and geochemical studies. Estimates of phenocryst, pumice, and lithic content in samples from this section are presented in Figure 28.

Phenocryst percentages in the tuff of Turkey Springs increase upward from 3% to 20%. Dominant phenocryst types are sanidine and quartz with minor plagioclase and traces of biotite, opaque minerals, and sphene. Sanidine phenocrysts are twice as abundant as quartz in the lower 40m of the unit. Higher in the section quartz and sanidine are present in subequal proportions. Sanidine occurs as blocky subhedral to euhedral grains (1-3mm), and quartz as blocky subhedral grians (1-3mm) that are typically resorbed.

The lowermost tuff of Turkey Springs contains 10-15% lithic fragments (0.2-2.0cm) that are mostly rhyolite lava and basaltic andesite lava. Lithic content decreases upward to less than 1% 50m above the base.

Pumice fragments less than 5mm long compose <1% of the lowermost tuff of Turkey Springs. Pumice gradually increase in size (2-3cm) and in abundance (up to 5%) from 0-50m above the base. From 50-60m pumice content increases rapidly to

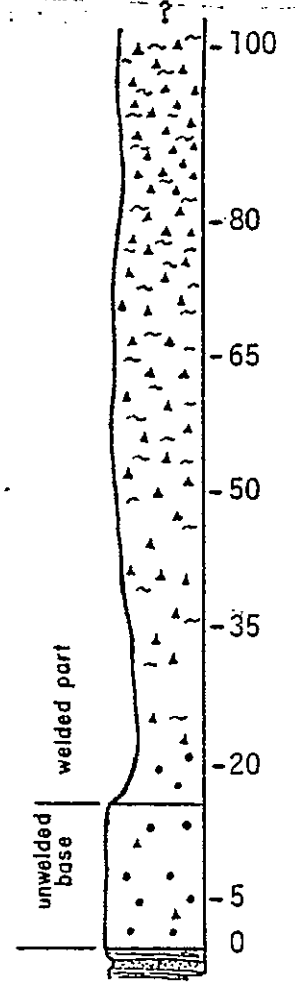

Thickness meters	Sample no.	Color unweathered matrix	Lithics	Pumice	Total phen.	San.	Qtz.	Plg.	Biot.	Opaq.	Sphene
?											
100	84-4-7	light-brownish-gray 5YR 6/1	1-2	12-15	20	12	8	0.5	t	t	t
80	84-4-6	mod-reddish-brown 10R 4/6	1-2	10-12	17	9	8	m	t	t	t
65	84-4-5	pale-red-purple 5RP 6/2	1-2	8-10	17	9	8	m	t	t	t
50	84-4-4	pale-red 5R 6/2	2-4	4-6	10	5	5	m	t	t	0
35	84-4-3	light-gray N 7	4-6	2-4	7	5	2	m	t	t	0
20	84-4-2	white N 9	6-10	1-2	5	4	1	m	0	0	0
5	84-4-1	white N 9	10-12	1-2	3	2	1	m	0	t	t
0											

m-minor(less than 0.5%) t-trace(less than 0.1%) 0-not observed

Figure 28. Stratigraphic section of the tuff of Turkey Springs measured at Turkey Springs (sec. 35, T6S, R6W). Visual estimates of phenocryst percentages are from thin sections. Lithic and pumice percentages are estimated from hand specimens.

10%. Above 60m, the unit contains 12% to 15% pumice fragments that average 5-10cm in length. Most of the pumice fragments in the tuff of Turkey Springs are completely replaced by vapor-phase intergrowths of sanidine and quartz. In the center of some of the largest fragments there is an intersitial growth (<0.2mm) of a highly birefringent mineral. This mineral, which appears to be the last phase to crystallize in the pumice, may be an incompatible-element-enriched mineral such as allanite.

The tuff of Turkey Springs contains two oval shaped phreatic pipes within the welded upper member (about 20m across) in the Turkey Springs area (Plate 1). The pipes consist of unwelded bedded tuffs in the center, some of which may be water-laid, and massive unwelded tuff around the edges. The contact with the welded tuff is sharp, and characterized by veins of agate (<1cm thick) that invade fractures in the welded tuff. Both pipes are located adjacent to, and on the downthrown side of, a pair of graben faults in the sedimentary basin of the unit of East Red Canyon. The pipes are interpreted as syn-depositional phreatic explosion tubes that punched through the ash-flow tuff as it cooled. The source of water was possibly from springs or standing water along the buried fault traces.

Rhyolite intrusives and lavas

Introduction

There are 12 occurences of crystal-poor rhyolite intrusive and/or lava in the study area. From field evidence (intrusive or depositional contacts) at least four temporally defined generations of rhyolite can be recognized. First generation (Tr1) rhyolites are older than Lemitar Tuff, second generation (Tr2) rhyolites are older than South Canyon Tuff, third generation (Tr3) rhyolites are older than the unit of East Red Canyon, and fourth generation rhyolites (Tr4) are younger than the unit of East Red Canyon. Several of the rhyolite's ages are poorly constrained and are mapped simply as Tertiary rhyolite unconstrained (Tru) on Plate 1. Each occurence of rhyolite is given an informal name, and located on Plate 1. The absolute age constraints of each occurence is also given on Plate 1.

Most of the intrusive rhyolites occur in a north-south trending belt in the east-central part of the study area. The plugs and dikes are elongated in a north-south direction, and are bisected by a series of south-side down faults which expose successively deeper stratigraphic levels to the north. In the north, ryholite is exposed as

north-trending anastomosing dikes, but to the south it occurs as elongate plugs. Farther south, at higher stratigraphic levels, the plugs are more cylindrical in shape.

The rhyolite intrusions in the study area are typically strongly flow-banded, and foliation is usually near vertical. In some of the larger plugs, cooling joints up to 0.5m in diameter occur oriented perpendicular to the dominant plane of flow-banding, and to intrusive contacts.

First generation rhyolites

DISTRIBUTION

There are two rhyolites in the study area that are known to be older than the Lemitar Tuff. Both rhyolites (rhyolite lava of Drift Fence Canyon, and rhyolite of Exter Canyon) occur in the southwest part of the study area. These rhyolites are temporally related to the formation of the Nogal Canyon Cauldron (eruption of Vicks Peak Tuff) in the southern San Mateo Mountains.

The rhyolite lava of Drift Fence Canyon consists of at least one plug, a series of north-northwest trending dikes, and at least two lava flows. The plug intrudes the Vicks Peak Tuff and the lava flows are overlain by two small outcrops of Lemitar Tuff that fill a paleocanyon. The

plug(s) and dikes are the source of at least two flows, with a composite thickness of at least 70m, that extend about 1.6 km to the north and south of East Red Canyon (Plate 1).

Eruptive centers for the Drift Fence Canyon lavas form a linear array that trends about N20E, but the orientation of individual feeder dikes trends about N30W (Fig. 11). The phenomenon of en-echelon feeder dikes along linear arrays of silicic domes has been discussed by Fink (1984) for the Inyo Volcanic Chain, Long Valley Caldera, California. Fink proposes that at depth, magma propagates along established joints and fractures, but near the surface (intruding younger rocks) it propagates along dikes whose trends reflect regional stress patterns. The dikes of the rhyolite lava of Drift Fence Canyon fit this pattern. The aligned eruptive sites for the Drift Fence Canyon rhyolites parallel local Basin and Range faults, whereas the individual feeder dikes trend northwest, perpendicular to the regional least principle stress direction (Fig. 11).

Almost all of the rhyolite lava of Drift Fence Canyon lava, to the north and east of the vent area, was eroded by the end of pre-Lemitar time. The remaining outcrops of lava near the vent area formed a divide between two north-northeast trending paleocanyons that were subsequently filled with the Lemitar Tuff (Fig. 9). Younger deposits to the west bury evidence of the unit's westward extent, and

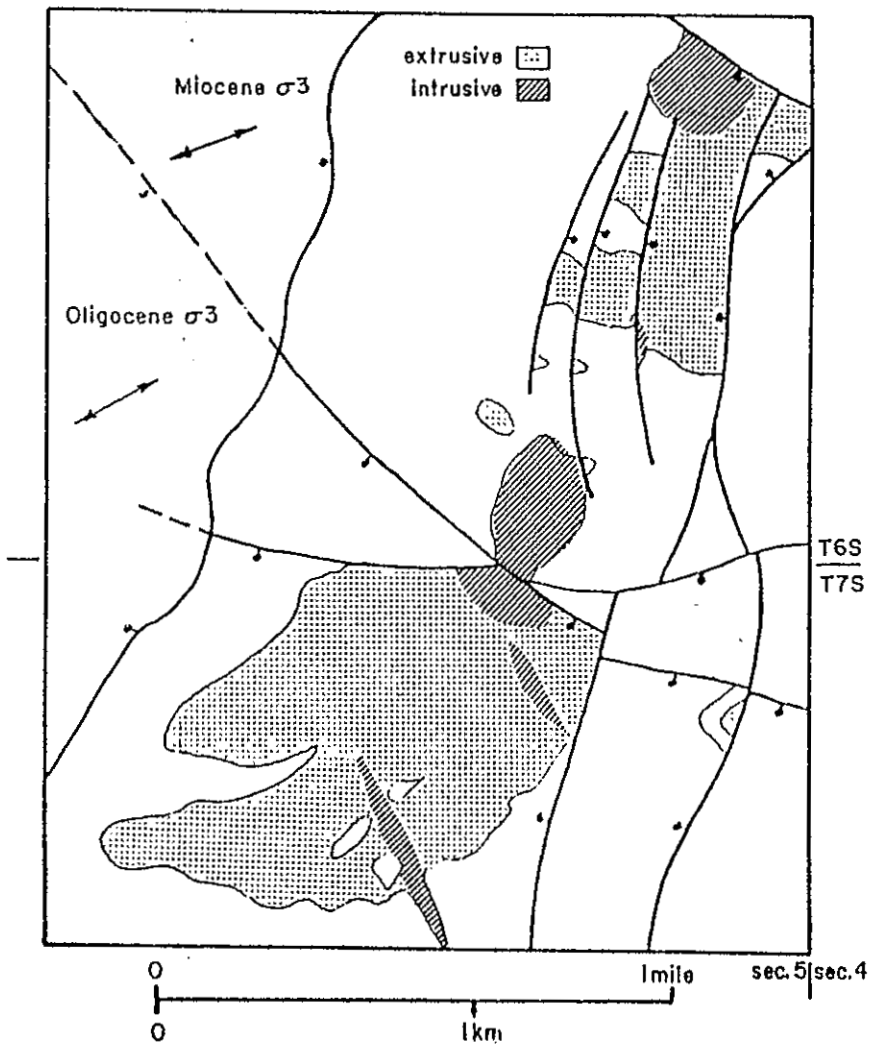

Figure 29. Outcrop map of the rhyolite lava of Drift Fence Canyon, see text for discussion. The Miocene σ 3 is from Zoback and others (1981), and the Oligocene σ 3 is from this study (see Table 5).

only a small remnant of the unit is preserved to the east (NE 1/4 sec. 33, T6S, R5W).

The rhyolite of Exter Canyon is exposed along the west-central edge of the study area where it is overlain by Lemitar Tuff. The ryholite's lower age is unconstrained, but it is also thought to be younger than the Vicks Peak Tuff. The rhyolite's outcrop pattern between East Red Canyon and Exter Canyon suggests that it is an eroded intrusive plug.

PETROGRAPHY

The rhyolite lava of Drift Fence Canyon (sample 85-7) contains 5-10% phenocrysts of euhedral blocky sanidine (1mm), and subhedral blocky plagioclase (1mm) in subequal proportions. Subhedral resorbed quartz (1mm), biotite (0.5mm), and opaque minerals (0.3mm) occur in trace amounts.

In thin section, the rhyolite of Exter Canyon (sample 84-159) contains 10% phenocrysts of euhedral blocky sanidine (1-2mm), and euhedral blocky plagioclase (1-2mm) in subequal proportions. Both feldspars are almost completely altered to clay minerals. Plagioclase was distinguished from Sanidine by remnant twinning structures. Biotite, which occurs in trace amounts, is altered to opaque minerals and a highly birefringent material that is probably a mixture of epidote and zoisite.

Second generation rhyolites

DISTRIBUTION

There are two occurences of intrusive rhyolite in the study area that are thought to be younger than the Lemitar Tuff, and known to be older than the South Canyon Tuff. These are the rhyolite intrusions of North Canyon, and the rhyolite just west of Wildcat Peak. These rhyolites are overlain by South Canyon Tuff in an area which became an important post-South Canyon Tuff silicic eruptive center (Wildcat Peak).

PETROGRAPHY

In hand specimen, the second stage rhyolites are light-gray to light-brownish-gray, and contain 3-10% phenocrysts of feldspar and quartz. The quartz to feldspar ratio in these rhyolites, estimated in the field, is about 1:1.

Third Generation Rhyolites

DISTRIBUTION

There are two occurrences of third generation rhyolites in the study area. These are the rhyolite of Cave Peaks, and the rhyolite intrusion of Wildcat Peak/rhyolite lavas of

Horse Mountain Canyon. They intrude the southern structural margin of the Mt. Withington cauldron, and are thought to seal possible vents for the South Canyon Tuff.

The rhyolite of Wildcat Peak is named for a resistant plug (it's principle source) that intrudes the South Canyon Tuff at the intersection of Exter Canyon and North Canyon in the east central part of the study area. The rhyolite is also found to the north as a series of east-northeast trending dikes (Plate 1). The eastern edge of the rhyolite of Wildcat Peak, just south of North Canyon, appears to intrude the lowermost pyroclastic deposits of the unit of East Red Canyon. To the south, the rhyolite lavas of Horse Mountain Canyon, which are continous with the rhyolite of Wildcat Peak, are overlain by epiclastic deposits of the unit of East Red Canyon. This indicates that the unit of East Red Canyon was being deposited before, during, and after the eruption of these rhyolites.

The rhyolite of Cave Peaks is an eroded lava dome partially buried by the unit of East Red Canyon at the southern edge of the study area. The rhyolite of Cave Peak's lower age constraint is the Lemitar Tuff, which it overlies in Hidden Spring Canyon. South Canyon Tuff is believed to absent in this part of the study area.

PETROGRAPHY

In thin section the rhyolite of Wildcat Peak (sample 85-7) contains phenocrysts of sanidine (3%), and plagioclase (3%), and trace amounts of biotite, sphene, amphibole, and opaque minerals. Sanidine and plagioclase occur as blocky euhedral crystals (2mm). Quartz is present only as a vapor phase mineral in lithophysae cavities.

Fourth generation rhyolite

The rhyolite intrusion of Horse Mountain is the only rhyolite in the study area that is known to be younger than the unit of East Red Canyon. This rhyolite intrudes pyroclastic rocks of the unit of East Red Canyon which in turn overlie the rhyolite lavas of Horse Mountain Canyon (Tr3).

In thin section, the rhyolite of Horse Mountain (83-32), contains 6% phenocrysts of blocky euhedral sanidine (1-2mm), blocky subhedral quartz (1-2mm), and blocky subhedral plagioclase (1mm) in an approximate 2:2:1 ratio. Quartz is slightly resorbed, and plagioclase is commonly glomeroporphyritic. Biotite (0.3mm), opaque minerals (0.2mm), and euhedral sphene (0.3mm) occur in trace amounts.

Unconstrained rhyolite intrusives

There are five rhyolite intrusives in the eastern part of the study area whose ages are poorly constriained. These are: 1) the rhyolite intrusion of little Black Mountain; 2) the rhyolite dikes of North Canyon; 3) the rhyolite intrusion of little Horse Mountain; 4) the rhyolite intrusion of Tigner Ranch; and 5) the rhyolite intrusion of Wilson Hill. These intrusives bodies are elongated in a north-south direction, and are probably eastern equivelents of the second, third or fourth generation rhyolites. They are crystal-poor (<10% phenocrysts) and contain subequal amounts of feldspar and quartz.

CHAPTER 3

CHEMISTRY

Introduction

Major element analyses of 3 ash-flow tuffs and 7 shallow intrusives, were done by the X-ray fluorescence method in order to chemically characterize the rocks in the study area. Analyses of the ash-flow tuffs are presented in Table 3, and of the intrusive rhyolites in Table 4. The coefficients of variation for each major element, calculated from 3 separate analyses of one ash-flow tuff sample (84-5-3), are presented in Table 3. Ion selective electrode analyses for fluorine and chlorine in the intrusive rocks are presented in Table 4.

All of the rocks analyzed (located on Plate 4) are rhyolites, and almost all of them contain >75% SiO_2. The rhyolites average about 5% K_2O, placing this study area outside of a high-K_2O anomaly (characterized in rhyolites by K_2O contents as high as 10.4%, and Na_2O contents as low as 0.2%) that affects Oligocene to Miocene rocks throughout the Socorro area (D'andrea-Dinkelman and others, 1983).

Table 3. Major element chemical data of the tuff of Turkey Springs(84-4-2,3,4,5,6,7), the South Canyon Tuff (84-5-3,4,5), and the Lemitar Tuff (84-5-1,2) from this study area. Also shown are the coefficients of variation for each element (determined from 3 analyses of sample 84-5-3).

Sample	SiO_2	TiO_2	Al_2O_3	Fe_2O_3*	MnO	MgO	CaO	Na_2O	K_2O	P_2O_5	LOI	Total
84-4-7	77.45	0.14	12.27	0.86	0.04	0.02	0.40	3.41	5.00	0.02	0.46	100.07
84-4-6	78.20	0.12	11.93	0.82	0.04	0.01	0.35	3.35	4.86	0.02	0.37	100.71
84-4-5†	77.54	0.12	12.00	0.78	0.04	0.07	0.37	3.34	4.85	0.02	0.61	99.74
84-4-4	77.61	0.10	12.13	0.70	0.04	0.09	0.35	3.87	4.66	0.02	0.70	99.82
84-4-3	76.74	0.10	12.41	0.60	0.04	0.11	0.38	3.77	4.81	0.02	0.82	99.78
84-4-2	76.78	0.09	12.77	0.69	0.06	0.16	0.35	3.52	4.86	0.02	1.10	100.41
84-5-5	72.33	0.35	14.52	1.84	0.05	0.17	0.30	2.52	6.98	0.03	1.07	100.14
84-5-4	73.60	0.27	14.08	1.42	0.02	0.11	0.55	3.58	5.54	0.04	0.64	99.85
84-5-3°	75.67	0.18	12.98	1.09	0.05	0.08	0.36	3.44	5.58	0.02	0.51	99.51
C.O.V. (%)	0.4	3.4	0.6	2.8	5.5	2.5	0.8	2.5	0.7	8.7		
84-5-2	78.02	0.16	11.83	0.92	0.07	0.03	0.29	3.20	5.13	0.02	0.34	100.01
84-5-1	77.86	0.16	11.86	0.92	0.08	0.07	0.30	3.30	5.10	0.03	0.37	100.03

†average of two analyses
°average of three analyses
*total Fe
C.O.V.=coefficient of variation

Table 4. Major element chemical data of rhyolite intrusives in the study area.

Sample no.	SiO_2	TiO_2	Al_2O_3	Fe_2O_3*	MnO	MgO	CaO	Na_2O	K_2O	P_2O_5	F	Cl	LOI	Total
84-6	77.34	0.10	12.44	0.79	0.04	0.06	0.43	3.21	5.15	0.02	0.03	0.003	0.64	100.22
84-7	77.00	0.12	12.37	0.85	0.05	0.09	0.43	3.40	5.27	0.02	0.02	0.005	0.67	100.28
84-8	79.60	0.10	10.96	0.75	0.05	-	0.30	2.95	4.69	0.02	0.02	0.01	0.71	100.11
84-9†	77.02	0.11	12.51	0.79	0.07	0.01	0.29	3.52	5.07	0.02	0.03	0.002	0.51	99.88
84-10	77.20	0.11	12.39	0.81	0.06	0.02	0.39	3.53	4.84	0.02	0.03	0.003	0.57	99.94
84-11	77.38	0.11	12.61	0.79	0.04	-	0.27	3.37	4.93	0.02	0.03	0.003	0.43	99.95
84-12	77.15	0.12	12.57	0.83	0.06	0.03	0.32	3.31	5.06	0.02	0.03	0.002	0.65	100.11
84-13	77.74	0.12	12.30	0.88	0.07	0.03	0.29	3.55	4.95	0.02	0.06	0.002	0.41	100.36
84-27	77.01	0.18	12.43	0.97	0.05	-	0.17	3.61	4.79	0.004	na	na	0.46	99.61
84-159	70.94	0.38	14.19	1,93	0.05	0.28	0.41	3.16	7.42	0.06	na	na	0.41	99.37

†average of two analyses
*total Fe
na=no analysis

-not detected

Ash-flow tuffs

Samples from vertical sections of the South Canyon Tuff (84-5-1,2,3), the Lemitar Tuff (84-5-4,5), and the tuff of Turkey Springs (84-4-2,3,4,5,6,7) were analyzed for major elements (Table 3). The Tuff of The Park, and the South Canyon Tuff are both high silica rhyolites (>75% SiO_2), and show very little vertical variation. The South Canyon Tuff shows a slight upward increase in TiO_2 (0.09%-0.19%), and a signficant upward decrease in MgO (0.16%-0.02%). The Lemitar Tuff is less silicic than the other tuffs (72-73% SiO_2). The upper sample of the Lemitar (84-5-5) appears to be altered, being enriched in K_2O (7.0%), and depleted in Na_2O (2.5%) and CaO (0.3%) compared to the lower sample (84-5-4)(K_2O, 5.5%; Na_2O, 3.6%; CaO, 0.5%).

Intrusives

All of the intrusive rocks analyzed in the study area are high-K_2O (5%), high-SiO_2 rhyolites (>77%; Table 4). Of the first stage rhyolites, two samples of the rhyolite of Drift Fence Canyon (84-8,9), and one of the rhyolite of Exter Canyon (84-159), which is pervasively altered, were analyzed. Two samples of the rhyolite of Cave Peaks (84-12,13), and one each of the rhyolite of Horse Mountain (84-10), rhyolite of Wilson Hill (84-11), and rhyolite of little Black Mountain (84-27) were analyzed. Two analyses

of the rhyolite of Wildcat Peak (84-8,9), a third generation intrusive, were analyzed. Sample (84-8) is higher in SiO_2 (79.6%), and lower in Al_2O_3 (11.0%) than all the other rhyolites in the study area, and is probably altered.

CHAPTER 4

PALEOMAGNETISM

Introduction

Paleomagnetic data presented in this paper is part of a larger study being done by Bill McIntosh at the New Mexico Institute of Mining and Technology. More detailed descriptions of laboratory procedures and the quality of the data will be presented in his forthcoming Ph.D. dissertation. Preliminary results of his study are published in McIntosh, 1983; and McIntosh and others, 1986.

Regional ash-flow tuffs (La Jencia, Vicks Peak, Lemitar, and South Canyon Tuffs) were analyzed for paleomagnetic polarity and anisotropy of susceptibility data. All of the sample sites are located on Plate 4. One local ash-flow tuff (tuff of Turkey Springs) and two intrusive rhyolites (rhyolite of Drift Fence Canyon, and rhyolite of Cave Peaks) were also analyzed. Both of the intrusive rhyolites have reversed polarities.

Polarity

Polarity data for the ash-flow tuffs is presented in Figures 30,31 along with the average paleopole positions for each regional unit outside this study area. The average paleopole position for the tuff of Turkey Springs, excluding

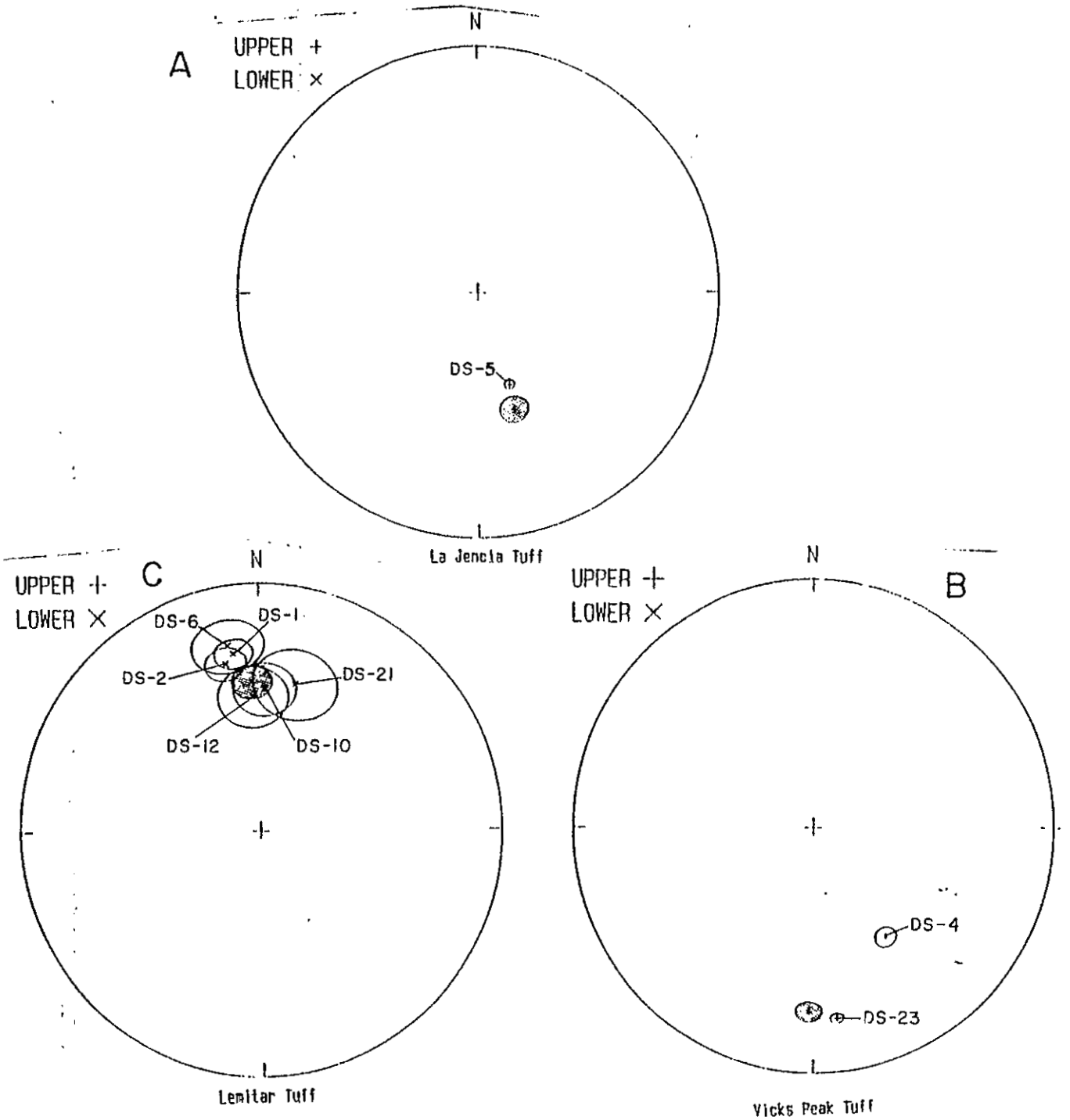

Figure 30. Paleomagnetic pole positions for samples of the La Jencia Tuff (A), Vicks Peak Tuff (B), and the Lemitar Tuff (C) from this study area. Average pole positions for samples outside this study area are shown with stippled patterns. Paleomagnetic data from McIntosh and others (1986).

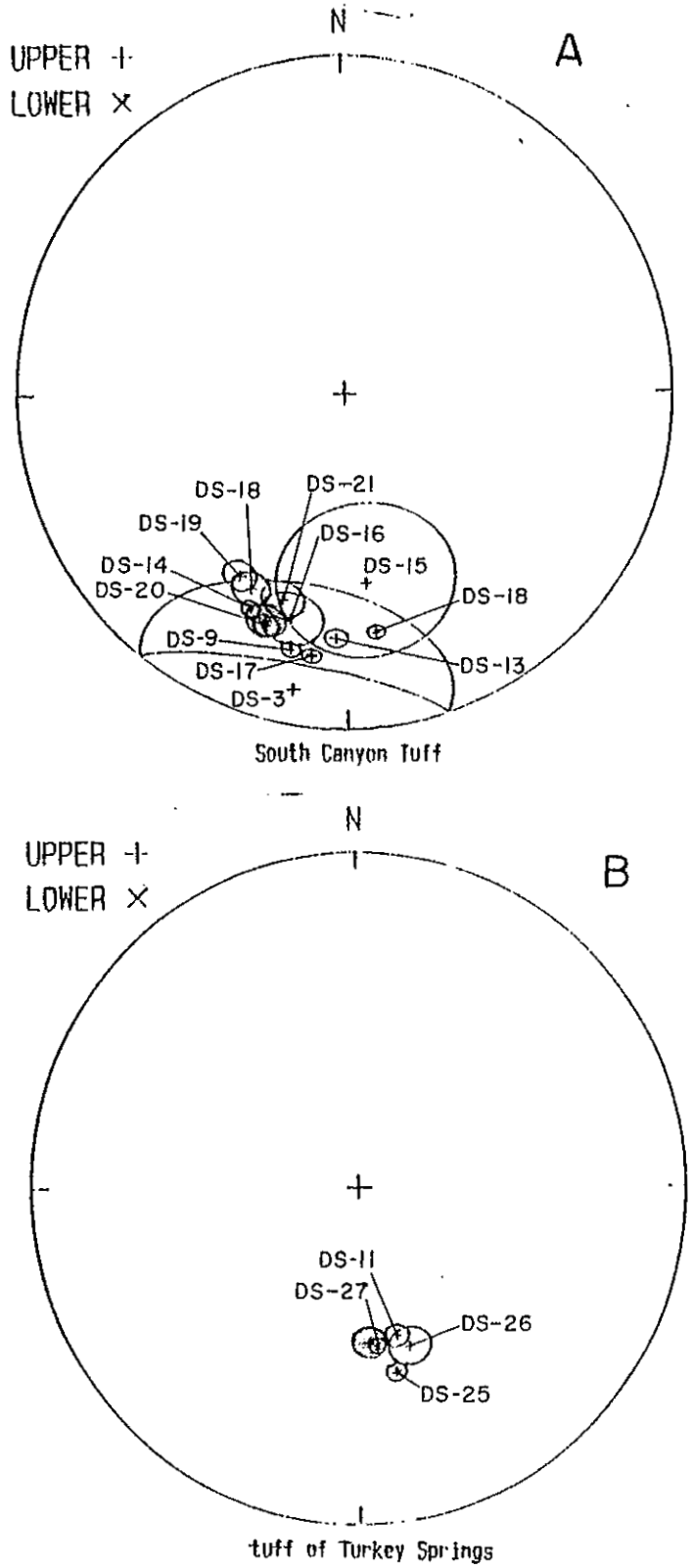

Figure 31. Paleomagnetic pole positions for samples of the South Canyon Tuff (A), and the tuff of Turkey Springs (B) from this study area. The average pole positions for samples from outside this study area is shown with a stippled pattern. Paleomagnetic data from McIntosh and others (1986).

samples from this study area, is given in Fig. 31 All of the ash-flow tuffs in the study area are reverse polarized, except for the Lemitar Tuff.

Anisotropy of susceptibilty

Magnetic anisotropy of susceptibilty is a measurement of the orientation of elongated magnetic mineral grains. Anisotropy of susceptibilty data is plotted as azimuths with cones of confidence (95% level) along with field measurements of aligned pumice fragments in Figures 5,7,9,11, and 27. The cones of confidence are narrowest for samples that are in strongly lineated tuff. The magnetic azimuths agree remarkably well with nearby field measurements of lineated pumice.

CHAPTER 5

STRATIGRAPHY

Introduction

Figure 32 illustrates the stratigraphic sequence for this study area, and compares it with the regional stratigraphy for the northeast Datil-Mogollon volcanic field (Osburn and Chapin, 1983). Figure 32 also includes high precision $^{40}Ar/^{39}Ar$ dates of 5 regional ash-flow tuffs (McIntosh and others, 1986). All rocks exposed in the study area are Oligocene silicic volcanic and volcaniclastic rocks. The oldest regional unit is the Oligocene La Jencia Tuff (28.8 Ma), and the youngest is the South Canyor Tuff (27.4 Ma). The youngest volcanic unit in the study area, the tuff of Turkey Springs, is nearly Miocene in age (McIntosh, personal communication).

The stratigraphic sequence is not exposed continuously anywhere in the study area. The lower part of the sequence consists of outflow sheets of regional ash-flow tuffs that are exposed mostly in the southeast part of the study area. To the west, these outflow sheets are downfaulted and buried by younger rocks. These younger rocks consist of a >600m thick sequence of the South Canyon Tuff which is intruded and overlain by rhyolite intrusions/lavas and volcaniclastic

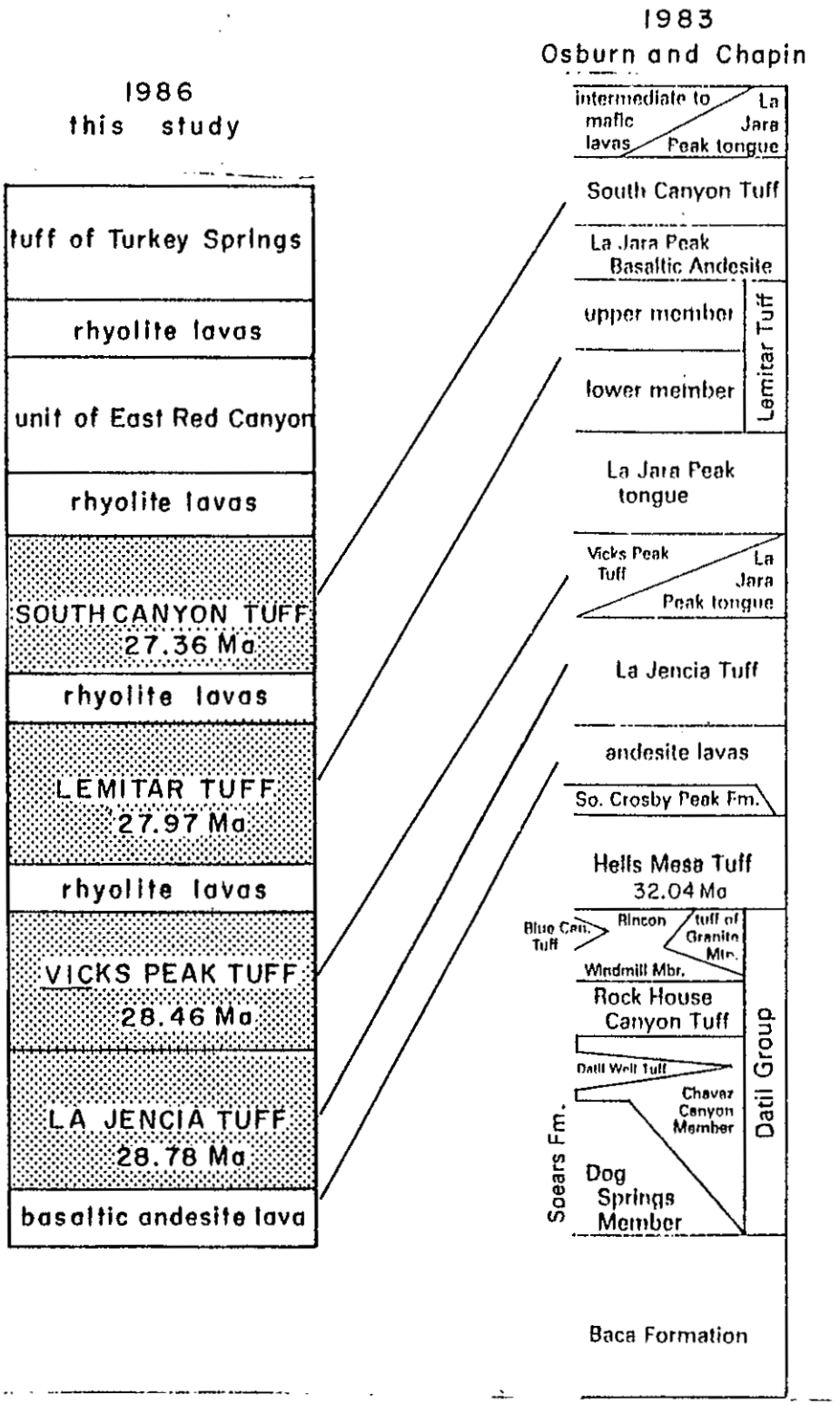

Figure 32. Stratigraphic sequence from this study compared with the regional sratigraphy of Osburn and Chapin (1983). Also shown are high precision $^{40}Ar/^{39}Ar$ dates ($\pm$ 0.15 m.y.) of the regional ash-flow tuff units (McIntosh and others, 1986). The regional ash-flow tuffs are shown with a stippled pattern.

sedimentary rocks.

Correlation with previous work

Figure 33 correlates the stratigraphic sequence from this study area with stratigraphic sequences for adjacent areas described by Deal (1973), Donze (1980), and Atwood (1982).

Correlation with Deal (1973)

Comparing Deal's (1973) stratigraphy with this study's detailed stratigraphy (Fig. 33) reveals that two of his tuff units were miscorrelated, and that one lumped together several regional tuff units. The tuff mapped by Deal (1973) as the Hells Mesa Tuff, within this study area, was reinterpreted as the Lemitar Tuff for three reasons: 1) it's stratigraphic position below the South Canyon Tuff; 2) it's distinctive mineralogic zonation (quartz-poor interval); and 3) it's normal paleomagnetic polarization (Hells Mesa Tuff is reverse polarized; McIntosh, 1983). In the northern part of the study area, Deal's (1973) A-L Peak Tuff was reinterpreted as the South Canyon Tuff, because it overlies the Lemitar Tuff, and it contains subequal amounts of quartz and sanidine phenocrysts. In the southern part of this study area, Deal's (1973) A-L Peak Tuff was mapped as the La Jenica Tuff, because it underlies the Lemitar Tuff,

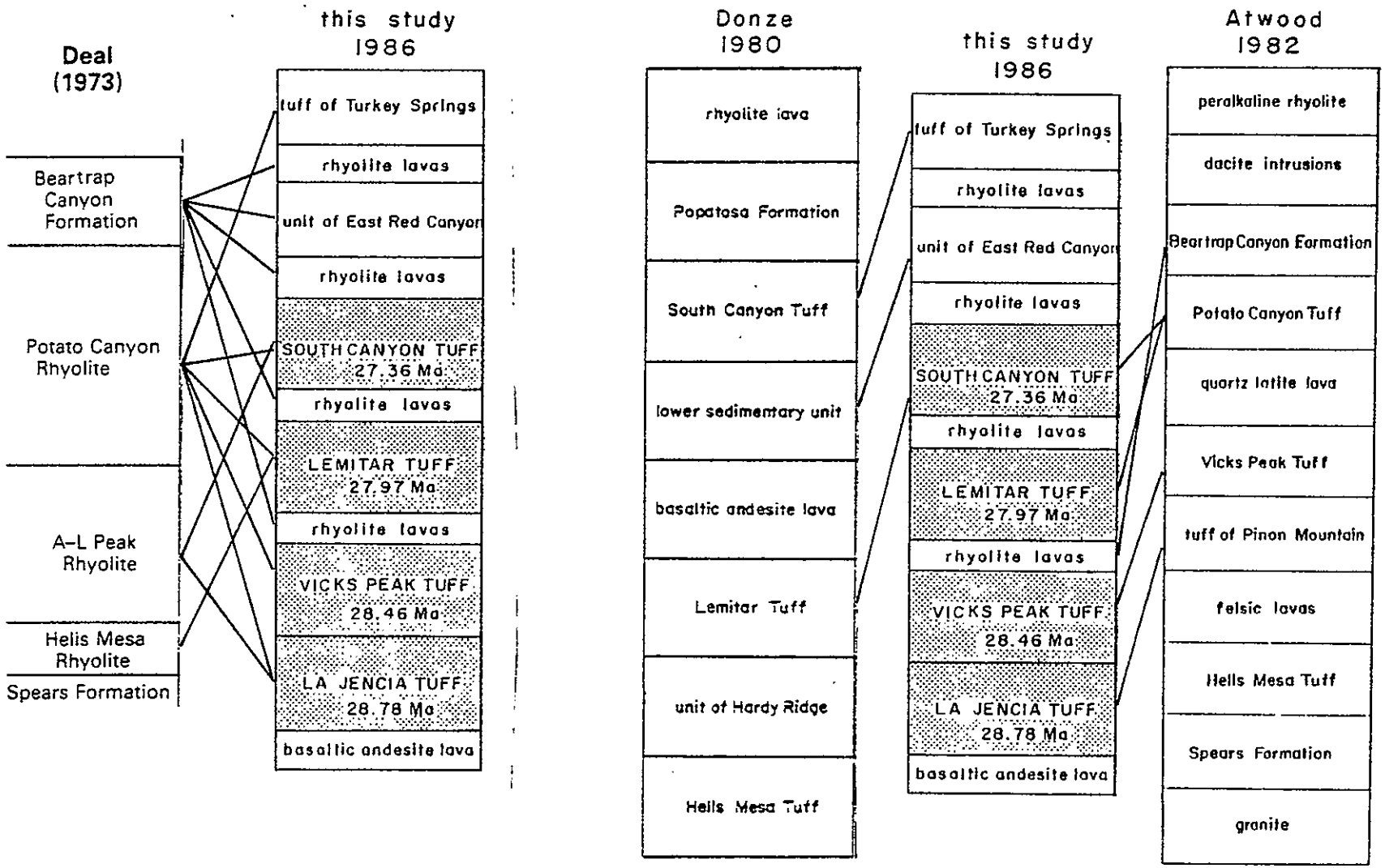

Figure 33. Stratigraphic sequence from this study (regional ash-flow units shown with a stippled pattern) compared with the stratigraphic sequences of previous workers in adjacent areas (see Fig. 1).

and contains only sanidine phenocrysts. Note that the A-L Peak Tuff has been renamed the La Jencia Tuff (Osburn and Chapin, 1983). The Potato Canyon Tuff, mapped by Deal (1973), was correlated with the South Canyon Tuff in the northern part of this study area. In the southern part of the study area, the Potato Canyon Tuff was correlated with 4 regional ash-flow tuff sheets. These outflow sheets (La Jencia, Vicks Peak, Lemitar, and South Canyon Tuffs) are seperated by major cooling breaks, and are distinguished by individually distinct petrographic and paleomagnetic properties. Deal's (1973) Beartrap Canyon Formation consists of all felsic intrusions/lavas and sedimentary rocks in the study area, regardless of their age. This study recognizes 4 generations of felsic lavas, and 1 sequence of sedimentary rocks. Deal's (1973) mapping approximately located the southern margin of the Mt. Withington Cauldron in this study area. However, the use of an oversimplified stratigraphy prevented him from recognizing the complexity or age of the stucture.

Correlation with Atwood (1982)

The lower part of Atwood's (1982) stratigraphic sequence (below the Vicks Peak Tuff) correlates well with the stratigraphy established in this study area (Fig. 33). Overlying the Vicks Peak Tuff, to the south of this study area, is a 300m thick sequence of felsic lavas, tuffs, and

volcaniclastic sediments which were grouped by Atwood (1982) into the Beartrap Canyon Formation. These rocks overlie the Vicks Peak Tuff to the west of a major west-side down fault in the western part of Atwood's area. Atwood placed the Beartrap Canyon Formation stratigraphically above the Potato Canyon Tuff, even though he has no direct evidence for this relationship. Atwood also combined all major ash-flow tuffs younger than the Vicks Peak Tuff together as the Potato Canyon Tuff (Osburn, personal communication). This lumping makes it difficult to correlate Atwood's stratigraphy (particularly in the northern part of his area) with the stratigraphy in this study area.

Correlation with Donze (1980)

Donze's (1980) stratigraphic sequence was named before the regional stratigraphy of Osburn and Chapin (1983) was established. Otherwise, these rocks correlate well with the upper part of the stratigraphic sequence in this study area (Fig. 33). In the eastern part of Donze's (1980) map area, the thick cauldron-filling tuff mapped as the Lemitar Tuff is actually the South Canyon Tuff (Osburn and Chapin, 1983). The tuff Donze mapped as South Canyon Tuff is a younger local ash-flow tuff that correlates with the tuff of Turkey Springs of this study (Fig. 33). Donze (1980) mapped a sequence of volcaniclastic sediments between these two tuff units that is correlated with the unit of East Red Canyon in

this study area.

Summary

The miscorrelated A-L Peak Tuff, and the Potatc Canyon Tuff (combined unit) have been abandoned by Osburn and Chapin (1983) in favor of more specific unit names. The Beartrap Canyon Formation has been used for sedimentary rocks, and associated "moat deposits" related to at least two different cauldrons in the San Mateo Mountains (Deal, 1973; Deal and Rhodes, 1976; Atwood, 1982). Therefore, to avoid confusion in this study area, all local intrusions/lavas, tuffs, and sedimentary rocks are given individual informal names until stratigraphic relations are better understood.

Stratigraphy of this study area

Introduction

Each stratigraphic unit in this study area is described in detail in Chapter 2. This section summarizes the important stratigraphic relationships. The Lemitar Tuff is a useful marker horizon with which to compare lateral changes in stratigraphy. The Lemitar Tuff is chosen because it is the only unit that is exposed throughout the study area.

Units older than the Lemitar Tuff

LA JENCIA TUFF

The La Jencia Tuff, at least 270m thick in this study area, is a crystal-poor sanidine-bearing rhyolite ash-flow tuff. It is strongly flow-banded with a consistent east-west lineation (Fig. 5). The base is exposed only in the eastern part of North Canyon where it overlies at least 60m of basaltic andesite lava (Plate 1).

VICKS PEAK TUFF

The Vicks Peak Tuff is a crystal-poor sanidine-bearing rhyolite ash-flow tuff that is flow-banded and lineated only in the southern part of the study area. Pumice fragments here are consistently oriented northwest-southeast. The unit, which conformably overlies the La Jencia Tuff, thickens from <100m to >300m to the southwest (Fig. 7) where it's base is not exposed.

FIRST GENERATION RHYOLITES

There are two occurences of pre-Lemitar rhyolite intrusive or lava in the study area. The rhyolite of Drift Fence Canyon intrudes Vicks Peak Tuff and is overlain by Lemitar Tuff in the extreme south central part of the study area. In the western part of the study area, the La Jencia

and Vicks Peak Tuffs are not exposed below the Lemitar Tuff. Instead, the Lemitar Tuff overlies the rhyolite of Exter Canyon. The rhyolite of Exter Canyon is thought to be younger than the Vicks Peak Tuff even though there is no established age relationship between the two. This interpretation is compatible with mapping by Atwood (1982) to the south of here, which shows Vicks Peak Tuff buried by local tuffs and lavas (Beartrap Canyon Formation) tc the west of a major west-side down fault. The local tuffs and lavas in Atwood's area (exposed only to the west of the fault) are correlated in a general sense with pre-Lemitar intrusive rhyolites in this study area (Fig. 33).

Lemitar Tuff

The Lemitar Tuff is a crystal-poor to crystal-rich quartz, sanidine, plagioclase-bearing rhyolite ash-flow tuff. It is only 5-15m thick in the southwest part of the study area. From here, it thickens to 80m to the north, and about 240m to the east. In the eastern half of the study area, the Lemitar Tuff fills north and northeast trending paleocanyons, cut into the Vicks Peak Tuff. The lateral variations in thickness, and the trend of paleocanycn walls (Fig. 9) suggest that the southwest corner of the study area was a highland before deposition of the Lemitar Tuff.

South Canyon Tuff

The South Canyon Tuff is a crystal-poor to crystal-rich quartz, sanidine bearing rhyolite ash-flow tuff. It fills a structural basin (Mt. Withington Cauldron) in the north-central part of the study area where it is at least 600m thick. Where it is thickest, South Canyon Tuff is invaded by epithermal gold veins and associated zones of argillic alteration in the Rosedale Mining District. Mineralization occurs along Basin and Range faults which trend about N30E.

In the northern part of the study area, parts of the South Canyon Tuff are strongly flow-banded with lineations oriented about N80E. To the south, towards the southern margin of the Mt. Withington Cauldron, lineations swing around to N50W (perpendicular to the margin) and the tuff thins to <150m (Fig. 11). Southeast of this margin, it is not known how thick the South Canyon Tuff is, or even if it was ever deposited. In the Cave Peaks area, South Canyon Tuff is absent from the section. A few thin exposures of unwelded tuff are tentatively correlated with the base of the South Canyon Tuff in the southeast part of the study area (Plate 1; Fig. 11).

Along the Mt. Withington Cauldron's southern structural margin, lenses of clast-supported lithic breccia are distributed vertically and laterally throughout the South

Canyon Tuff (Plate 1). The average size of lithic fragments in the breccias (Fig. 11) decreases from 170cm to 70cm away from the margin. The breccias are interpreted to be co-ignimbrite lag-fall deposits (defined by Wright and Walker (1977) as accumulations of lithic fragments too large to be carried away from the impact area of a collapsing eruption column). The breccias in this area are thought to have been deposited by a collapsing eruption column from a nearby vent or vents.

Unit of East Red Canyon

The unit of East Red Canyon is a sequence of volcaniclastic conglomerates, sandstones, and minor pyroclastic rocks. The unit fills a northeast-southwest trending basin where it is 200m thick. The basin occupies a moat-like depression just inside the southern margin of the Mt. Withington Cauldron. The minimum volume of material in the basin, including a partially buried rhyolite dome, is about $5km^3$. The eastern part of the basin consists of a west-fining alluvial fan complex derived chiefly from erosion of rhyolite dome material along the basin's eastern margin. Alluvial fan deposits grade westward into a sequence of eolian sandstone derived from deflation of volcaniclastic sediment to the southwest. Eolian sandstone in the western part of the basin is overlain by coarse-grained fluvially deposited rocks that had a probable

western or southern source area.

The unit of East Red Canyon also consists of bedded unwelded lithic-rich ash-flow tuffs in the Wildcat Peak/Horse Mountain area. These rocks were probably deposited by pyroclastic eruptions from the numerous rhyolite domes in the area.

The unit of East Red Canyon can be traced to the southwest over the divide of the San Mateo Mountains, and down West Red Canyon (Deal, 1973; Ferguson, unpublished mapping). To the northwest, the unit of East Red Canyon correlates with 100m to 200m of volcaniclastic rocks exposed between the South Canyon Tuff and the tuff of Turkey Springs (Donze, 1980; Osburn and Chapin,1983). These exposures, together with exposures in East Red Canyon, define a northeast-southwest trending belt which could be interpreted as a moat for the Mt. Withington Cauldron. However, caution is advised about accepting this interpretation. This is because only rocks older than the unit of East Red Canyon are exposed on either side of this belt. Therefore, the original shape of the unit's basin is difficult to reconstruct. The unit of East Red Canyon could have been a blanket-like deposit which overlapped the southern margin of the Mt. Withington Cauldron. The westward-fining alluvial fan facies relationships exposed in East Red Canyon do not have to be interpreted as evidence for a west-facing

cauldron margin. Instead, these relationships could indicate the presence of a ridge-like rhyolite dome inselberg within a larger Basin and Range basin.

Tuff of Turkey Springs

The youngest unit in the study area is a crystal-poor to moderately crystal-rich sanidine-quartz bearing rhyolite ash-flow tuff informally named the tuff of Turkey Springs. This tuff is preserved above the unit of East Red Canyon in the southwest part of the study area. The unit, which is petrographically similar to the South Canyon Tuff, was previously confused with the South Canyon in the eastern San Mateo Mountians (Donze, 1980; Ferguson, 1985). Tuff of Turkey Springs is distinguished from the South Canyon Tuff by stratigraphic position and a different paleomagnetic pole position (McIntosh and others, 1986; Ferguson, 1985; this report).

Rhyolite intrusions/lavas

There are 7 separate occurences of rhyolite intrusions/lavas that intrude rocks younger than and including the Lemitar Tuff. These occur in a north-south belt in the east central part of the study area. This belt includes rhyolites that pre-date and post-date the formation of the Mt. Withington Cauldron. In particular, the Wildcat

Peak area appears to have been a major silicic eruptive center before, during, and after the formation of the cauldron.

The post-Mt. Withington Cauldron rhyolite domes (rhyolite intrusion of Wildcat Peak/rhyolite lavas of Horse Mountain, and rhyolite of Cave Peaks) served as a major sediment source area for the basin of the unit of East Red Canyon.

Summary

The stratigraphic nomenclature used by Deal (1973) for the northern San Mateo Mountains was found to be inadequate for the detailed mapping in this study area. Stratigraphic nomenclature described by Osburn and Chapin (1983) for the Socorro region was used for regional units exposed in this study area.

The oldest units in the study area consist principally of outflow sheets of the La Jencia, Vicks Peak, and Lemitar Tuffs which crop out in the southeast corner. To the west, the La Jencia Tuff and Vicks Peak Tuff are not exposed. Instead, a large intrusive (extrusive?) rhyolite complex is exposed below the Lemitar Tuff. In post-Vicks Peak Tuff time the southwest part of the study area was a highland dissected by north and northeast directed canyons which were subsequently filled with Lemitar Tuff. Uplift may have been

due to either regional resurgence, or large scale accumulation of rhyolite lava.

Outflow sheets of the La Jencia, Vicks Peak, and Lemitar Tuffs in the southeast part of the study area are largely truncated to the west by the downsagged structural margin of the Mt. Withington Cauldron. The South Canyon Tuff thickens from <200m along the cauldron's structral margin to >600m in the northern part of the study area. Possible vents for the South Canyon Tuff, intruded by younger rhyolite domes, are located along the hinge of the downsagged cauldron margin. After eruption of the South Canyon Tuff, a moat-like depression probably formed just inside the Mt. Withington cauldron margin. The eastern topographic margin of the depression was a ridge of post-cauldron rhyolite domes. The depression filled with a west-fining alluvial fan complex and southwesterly derived eolian sandstone (unit of East Red Canyon). The youngest rock in the study area is a local rhyolite ash-flow tuff (tuff of Turkey Springs).

CHAPTER 6

STRUCTURE

Introduction

The oldest structures in the study area are related to eruptions of the Vicks Peak Tuff, and the South Canyon Tuff. These syn-volcanic structures are cut by north-south (west side down) faults throughout the study area, and east-west (south side down) faults in the southern half of the study area. The younger faults are the result of Basin and Range extension (Chapin, 1979), which has tilted fault blocks to the east throughout the study area. Dips increase gradually from 5-15 degrees in the south to 30-50 degrees in the north.

Volcanic Structures

Structures related to the Vicks Peak Tuff

The only Vicks Peak Tuff aged structure exposed in this study area is an apparent syn-volcanic south-side down fault in the southeast part of the study area. The structure, described on page 16, may be related to the formation of the source cauldron for the Vicks Peak Tuff. The Nogal Canyon Cauldron, located in the extreme southeast corner of the San

Mateo Mountains, is currently accepted as the source of the Vicks Peak Tuff (Fig. 1). However, 12km (7.5mi) to the north of its northern edge, is another volcano-tectonic depression that is filled with Vicks Peak Tuff. Within this depression, Vicks Peak Tuff has no exposed base, and is overlain by 300m of local volcanic units. The depression, which is located just south of this study area, is bounded to the east by a north-northeast trending west-side down fault (Atwood, 1982). Because of cover by younger rocks, there is no evidence for the northward continuation of this basin into the southern part of this study area. The terrane directly south and west of Atwood's (1982) study area is unmapped, and the extent of this depression is largely unknown. Reconnaisance mapping shows that the area west of Atwood's (1982) study area (Milligan Peak/Blue Mountain) consists mostly of crystal-poor rhyolite intrusive/lava which appears to overlie Vicks Peak Tuff.

Mt. Withington Cauldron

In the northern part of the study area, the South Canyon Tuff (at least 600m thick) occupies a structural depression (Fig. 11,13). This depression is the south end of the redefined Mt. Withington Cauldron (Deal, 1973; Osburn and Ferguson, 1986). The southern margin of the cauldron, best exposed near Wildcat Peak, is a northeast-trending monoclinal structural zone that is at least 2km wide. The

structural zone consists of northwest tilted pre-South Canyon strata (25-60 degrees). These strata are repeated by closely spaced east-side down faults which dip normal to the truncated strata (Plates 1,2,3). On the east edge of the zone, the transition from untilted to tilted strata occurs abruptly across a narrow (<20m wide) fault zone. The western edge of the structure is concealed by welded South Canyon Tuff which is undeformed by the east-side down faults. The youngest rocks affected by these faults are bedded tuffs at the unwelded base of the South Canyon Tuff. The age of the faulting is therefore constrained between the time of accumulation of the bedded tuffs at the base of the South Canyon Tuff and the welding of the South Canyon Tuff. The intrusive rhyolite of Wildcat Peak (Plate 1) is undeformed by faults related to the structure, and is thought to seal a vent for the South Canyon Tuff. A series of rhyolite dikes, trending about N55E, intrude the South Canyon Tuff to the north of the margin (Plate 1). This suggests that, during intrusion of the dikes, a localized least principle stress field was oriented about N35W.

A balanced cross-section model for the development of the southern structural margin of the Mt. Withington Cauldron is illustrated in Figure 34. The model depicts a flat topped magma chamber, at a depth of about 2-3km, feeding dikes along it's southeast margin. A major pyroclastic eruption follows using these dikes as

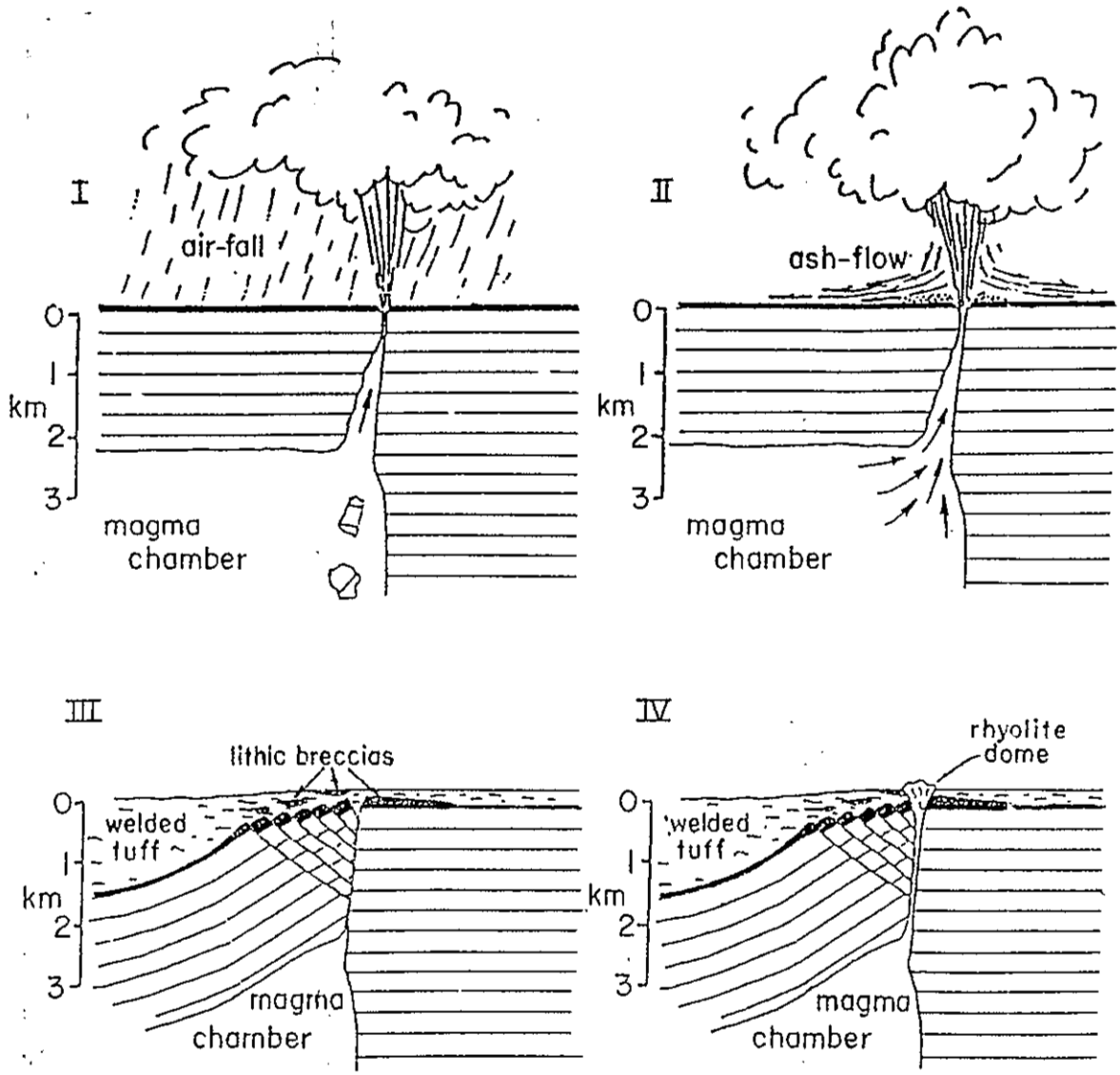

Figure 34. Four stage model for the formation of the southeast structural margin of the Mt. Withington Cauldron, see text for discussion.

conduits. Subsequent magma evacuation causes collapse of the cauldron block, and downsagging along the margin. After the eruption, devolitalized magma (rhyolite intrusion of Wildcat Peak) seals the pyroclastic vent(s).

To the southwest, the margin of the Mt. Withington Cauldron is buried by younger rocks (unit of East Red Canyon). Abrupt thickening of the South Canyon Tuff from the Cave Peaks area northwest to where East Red Canyon enters the study area (0 to >350m) suggests that the cauldron margin is buried underneath the unit of East Red Canyon (Plate 2,3).

Basin and Range structures

Fault patterns and the least principle stress field

Rocks in the study area were broken into both north-south trending and east-west trending fault blocks. These strain patterns are a result of Basin and Range extension which was initiated about 32-27 Ma (Chapin, 1979). From south to north, faults change from an orthogonal north-south and east-west pattern to a northwest-southeast parallel pattern (Fig. 35). The change in fault patterns is thought to reflect the control of different basement structures on a late Oligocene to Miocene N63E to N70E regional least principle stress field. The late Oligocene

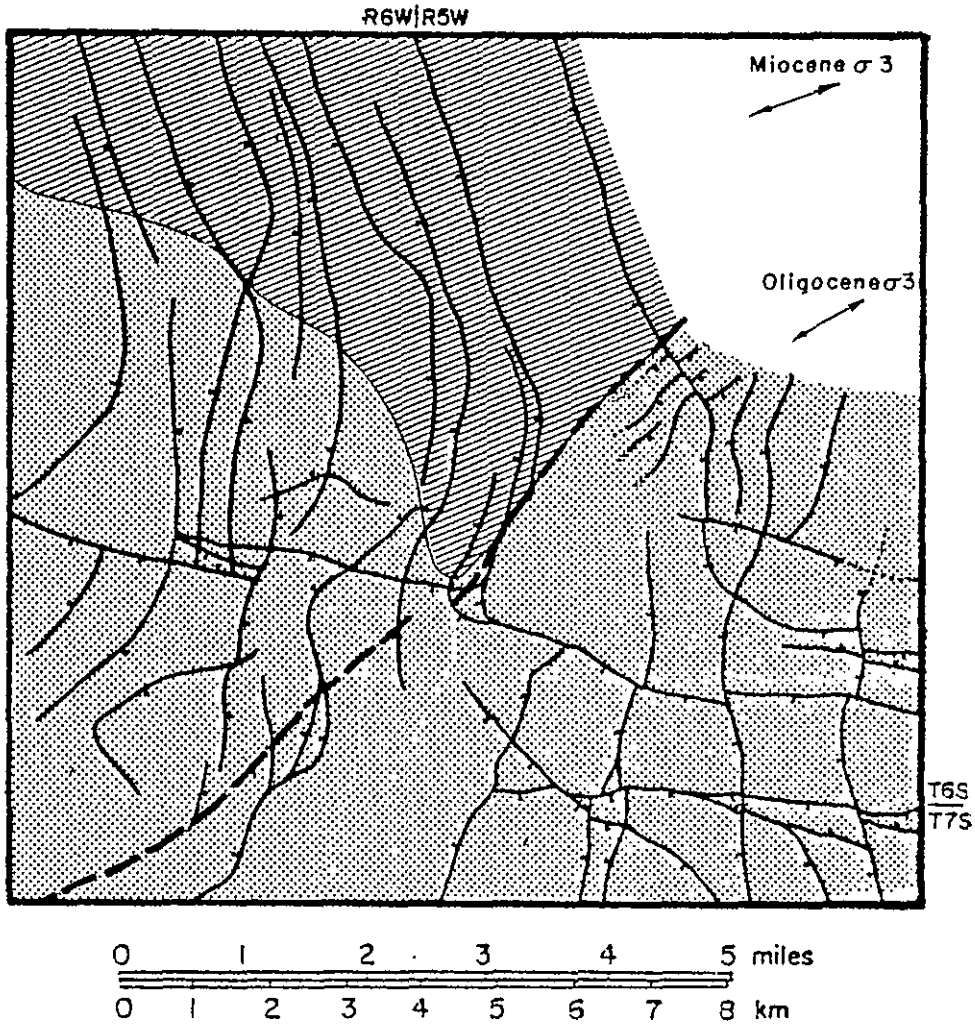

Figure 35. Structural map of the study area showing the moderately extended domain (lined pattern), and the weakly extended domain (stippled). Also shown is the Mt. Withington Cauldron margin (dashed heavy line). The Miocene σ 3 is from Zoback and others (1981), and the Oligocene σ 3 is from this study (see Table 5).

regional least principle stress direction (N63E) was determined from the trends of rhyolite dikes in this study area (Table 5). The Miocene direction (N70E) is an average of two directions from a compilation by Zoback and others (1981, p. 423). The resultant vector of Basin and Range extension for any part of the study area, regardless of how different the fault patterns are, is generally parallel to this least principle stress field (Fig. 35).

In the south, the orthogonal fault pattern is probably controlled by pre-Tertiary basement fractures. As faults cross the Mt. Withington Cauldron margin, from south to north, they curve sharply to the northwest. Within the cauldron, fault patterns appear to be controlled only by the least principle stress field. The author suggests that a shallow pluton beneath the Mt. Withington Cauldron negated the effect of older basement fractures on fault patterns in the cauldron.

Magnitude of tilting and the age of Basin and Range extension

Apart from a northeast trending zone of west-tilted rocks along the southern margin of the Mt. Withington Cauldron, all rocks in the study area are tilted to the east between 5 and 50 degrees. The tilting increases gradually from 5-15 degrees in the south to 30-50 degrees in the northern part of the study area.

Table 5. The location and age constraints of dikes in the study area whose trends are thought to have been determined by a regional stress field.

trend of dike	least principle stress direction	location	name of intrusive	age constraints
N30W	N60E	N1/2 sec. 28, T6S, R5W	rhyolite of Horse Mountain	post-Lemitar (28.0 Ma)
N26W	N64E	S1/2 sec. 28, T6S, R5W		pre-?
N24W	N66E	N1/2 sec. 5, T7S, R5W	rhyolite of Drift Fence Canyon	post-Vicks Peak (28.5 Ma)
N27W	N63E	W1/2 sec. 5, T7S, R5W		pre-Lemitar (28.0 Ma)

In a study of Tertiary tectonics of the Socorro region, Chamberlin and Osburn (1984) relate the degree of tilting to the amount of Basin and Range extension that has occurred. They define domains of weak (0-30%), moderate (30-100%), and severe (100-200%) extension by low (1-20 degrees), intermediate (20-50 degrees) and steep (50-70 degrees) dips, respectively, of Oligocene strata. This study area is divided into the weakly extended domain in the south, and the moderately extended domain in the north, with the boundary coinciding approximately with the margin of the Mt. Withington Cauldron (Fig. 35). In the northwest part of the study area, there is an abrupt decrease in the magnitude of extension from west to east across North Canyon (Fig. 35). Cross-sections (Plate 1; A, B) constructed across this transition are not balanced unless rocks to the east had a component of original dip (20 degrees east). A way to do this is to have the intracauldron South Canyon Tuff deform soon after deposition while it was still hot and pastic. There is little evidence, however, of plastic deformation in the South Canyon Tuff in this area.

Before deposition of the unit of East Red Canyon, in the northern part of the study area, older rocks (South Canyon Tuff) had been tilted east about 10 degrees. Deal (1973) interpreted this tilting as evidence for resurgence of the Mt. Withington cauldron. However, it is also possible that the unit of East Red Canyon was deposited

after Basin and Range extension had tilted older units 10 degrees to the east. Basin and Range extension was probably initiated by at least the time of the eruption of the South Canyon Tuff (27.4 Ma). The duration of extension is constrained only by Quaternary pediment gravels which are undeformed by faults. From stratigraphic and geomorphic evidence in the Socorro area, Chamberlin and Osburn (1984) suggest that the weakly extended domain was stretched from 31 Ma to 20 Ma, and the moderately extended domain from 31 Ma to 10 Ma. These ages may also be applicable to extensional deformation in this study area.

Summary

Rocks in the study area were deformed first by syn-volcanic forces, and then by Basin and Range extensional forces. The syn-volcanic structures, related to the Vicks Peak and South Canyon Tuffs, are the oldest tectonic structures in the study area. A volcano-tectonic depression filled by the Vicks Peak Tuff occurs just south of the study area. Crossing the study area, northeast to southwest, is the southern margin of the Mt. Withington Cauldron. The margin is a west-side down monoclinal sag that was activated during the eruption of the South Canyon Tuff. This cauldron margin segment, along with a segment mapped by G. R. Osburn in the northern San Mateo Mountains, and a segment in the western Magdalena Mountains helps redefine the shape of the

Mt. Withington Cauldron (Fig. 36).

Basin and Range extension developed in a late Oligocene least principle stress field oriented about N63E to N70E. Basin and Range fault patterns were controlled by pre-Tertiary basement fractures in the southeast, and an Oligocene sub-volcanic pluton in the north. The Oligocene volcanic strata has undergone extension which increases from about 20% to almost 100% from south to north in the study area.

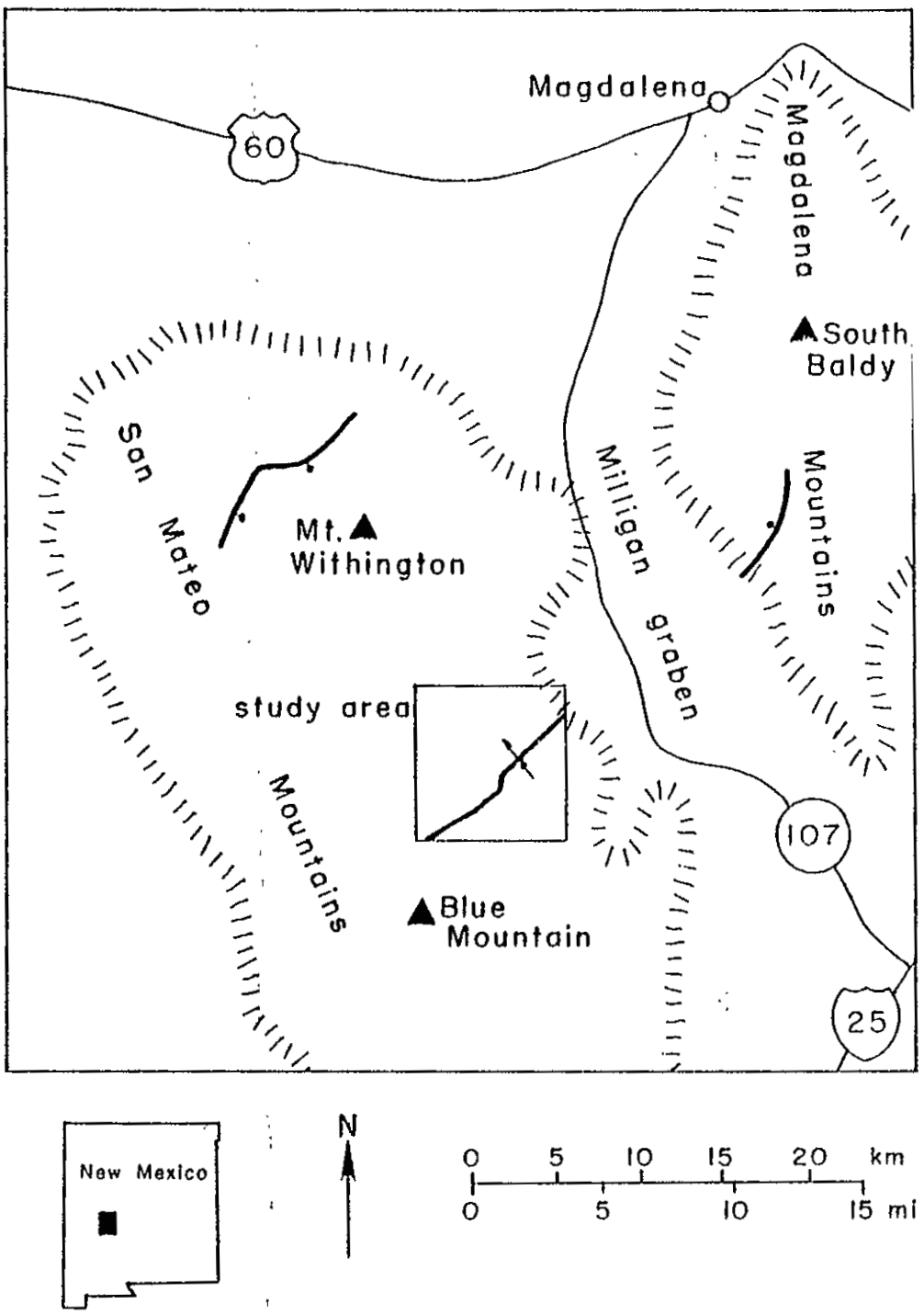

Figure 36. Map of the northern San Mateo Mountains and Magdalena Mountains showing margin segments (from detailed mapping) of the redefined Mt. Withington Cauldron. Cauldron margin segments in the northern San Mateo Mountains and western Magdalena Mountains are form unpublished mapping by G. R. Osburn.

CHAPTER 7

CONCLUSIONS

The major conclusions of this report are listed below.

(1) Directly south of the study area, the Vicks Peak Tuff occupies a structural depression where it is buried by local volcanic units. Subsidence in this area is thought to be related to collapse of the Vicks Peak Tuff's source cauldron somewhere in the south-central San Mateo Mountains.

(2) The southwest part of the study area was uplifted and eroded before deposition of the Lemitar Tuff. This uplift may be due to resurgence of the Vicks Peak Tuff's cauldron or to the massive accumulation of rhyolite lava to the southwest of the study area (Milligan Peak/Blue Mountain area).

(3) The Lemitar Tuff and older rocks in the study area are truncated to the west by a structural sag which formed during the eruption of the South Canyon Tuff. This sag is the southern margin of the redefined Mt. Withington Cauldron.

(4) Vents for the South Canyon Tuff are located along the southern downsagged margin of the Mt. Withington Cauldron (Wildcat Peak and Cave Peaks rhyolite domes).

(5) A sedimentary basin developed along the inside edge of the Mt. Withington Cauldron after the eruption of the South

Canyon Tuff. The basin filled with coarse sediment shed off rhyolite domes along the cauldron margin, and with eolian sand that was transported by prevailing southwest winds. (6) Late Oligocene volcanic rocks, erupted from vents in this study area, are all high-K_2O (5%), high SiO_2 rhyolites. (7) Most of the rocks in this study area were not affected by the K_2O metasomatic enrichment event that altered Oligocene to Miocene rocks throughout the Socorro area. (8) Rocks in the study area were deformed by late Oligocene to Miocene Basin and Range extensional stresses oriented about N63E. Extension, which tilted blocks to the east from 5-50 degrees, increases from about 20% in the south to about 100% in the north.

REFERENCES

Atwood, G. W., 1982, Geology and geochemistry of the San Juan Peak area, San Mateo Mountains, New Mexico: with special reference to the geochemistry, mineralogy, and petrogenesis of an occurence of riebeckite-bearing rhyolite: M. S. thesis, University of New Mexico, 156 pp.

Bobrow, D. J., 1984, Geochemistry and petrology of Miocene silicic lavas in the Socorro-Magdalena area of New Mexico: M. S. thesis, New Mexico Institute of Mining and Technology, 145 pp.

Brookfield, M. E., 1977, The origin of bounding surfaces in ancient aeolian sandstones: Sedimentology, v. 24, p. 303-332.

Brown, D. M., 1972, Geology of the southern Bear Mountains, Socorro County, New Mexico: M. S. thesis, New Mexico Institute of Mining and Technology, 110 pp.; New Mexico Bureau of Mines and Mineral Resources, Open-file Report 42, 110 pp.

Chamberlin, R. M., and Osburn, G. R., 1984, Character and evolution of extensional domains in the Socorro area of the Rio Grande Rift, central New Mexico (abs): Geologic Society of America, Abstracts with programs, v. 16, no. 6, p. 467.

Chapin, C. E., 1979, Evolution of the Rio Grande Rift - a summary: in Riecker, R. E., Rio Grande Rift: tectonics and magmatism: American Geophysical Union, p. 1-5.

Deal, E. G., 1973, Geology of the northern part of the San Mateo Mountains, Socorro County, New Mexico - a study of a rhyolite ash-flow tuff cauldron and the role of laminar flow in ash-flow tuffs: Ph. D. dissertation, University of New Mexico, 136 pp.

Deal, E. G., and Rhodes, R. C., 1976, Volcano-tectonic structures in the San Mateo Mountains, Socorro County, New Mexico: in Elston, W. E., and Northrop, S. A. (eds.), Cenozoic volcanism in southwestern New Mexico: New Mexico Geological Society, special publication 5, p. 51-56.

Deer, W. A., Howie, R. A., and Zussman, J., 1966, An introduction to the rock forming minerals: Longman, 528 pp.

D'andrea-Dinkelman, J. F., Lindely, J. I., Chapin. C. E., and Osburn, G. R., 1983, The Socorro K_2O anonaly: A fossil geothermal system in the Rio Grandé Rift: in Chapin, C. E., and Callender, J. F., (eds.), New Mexico Geologic Society, Guidebook to 34th field conference, p. 76-77.

Donze, M. A., 1980, Geology of the Squaw Peak area, Magdalena Mountains, Socorro County, New Mexico: M. S. thesis, New Mexico Institute of Mining and Technology, 120 pp., New Mexico Bureau of Mines and Mineral Resources, Open-file Report 123, 131 pp.

Ferguson, C. A., 1985, Geology of the east-central San Mateo Mountains, Socorro County, New Mexico: Unpublished M. S. thesis, New Mexico Institute of Mining and Technology, Socorro, 118 pp.

Fink, J. H., 1984, Spatial variations in the volume, texture, and structure of silicic domes fed by dikes (abs): Geologic Society of America, Abstracts with programs, v. 16, no. 6, p. 509.

Furlow, J. W., 1965, Geology of the San Mateo Peak area, Socorro County, New Mexico: M. S. thesis, University of New Mexico, 83 pp.

Hunter, R. E., 1977, Basic types of stratification in small eolian dunes: Sedimentology, v. 24, p. 361-387.

Jahns, R. H., 1944, Beryllium and tungsten deposits of the Iron Mountain District, Sierra and Socorro Counties, New Mexico: U. S. Geologic Survey Bulletin 945-C, 79 pp.

Kocurek, G., 1981, Significance of interdune deposits ard bounding surfaces in aeolian dune sands: Sedimentology, v. 28, p. 753-780.

Kocurek, G., 1984, Origin of first order bounding surfaces in aeolian sandstone: Sedimentology, v. 31, p. 125-127.

Kocurek, G., and Dott, R. H., 1981, Distinctions and uses of stratification types in the interpretation of eoliar sand: Journal of Sedimentary Petrology, v. 51, p. 579-595.

Lambert, P. W., 1968, Quaternary stratigraphy of the Albuquerque area, New Mexico: Ph.D. dissertation, University of New Mexico, 329 pp.

McIntosh, W. C., 1983, Preliminary results from a paleo- and rock magnetic study of Oligocene ash-flow tuffs in Socorro County, New Mexico: in Chapin, C. E., and Callender, J. F. (eds.), New Mexico Geologic Society, Guidebook to 34th field conference, p. 205-210.

McIntosh, W. C., Sutter, J. F., and Chapin, C. E., Osburn, G. R., and Ratte, J. C., 1986, A stratigraphic framework for the eastern Mogollon-Datil volcanic field based on paleomagnetism and high-precision $^{40}Ar/^{39}Ar$ dating of ignimbrites - a progress report: New Mexico Geological Society, Guidebook to 37th Field Conference, p. 183-196.

Neubert, J. T., 1983, Mineral investigations in the Apache Kid and Withington wilderness areas, Socorro County, New Mexico: U. S. Bureau of Mines open file report MLA 72-83, 35 pp.

Osburn, G. R., 1978, Geology of the eastern Magdalena Mountains, Water Canyon to Pound Ranch, Socorro County, New Mexico: M. S. thesis, New Mexico Insitute of Mining and Technology, 150 pp.; New Mexico Bureau of Mines and Mineral Resources Open-file report 113, 160 pp.

Osburn, G. R., 1982, Gallery of Geology: New Mexico Geology, v. 4, no. 3, p. 38.

Osburn, G. R., and Chapin, C. E., 1983, Nomenclature for Cenozoic rocks of northeast Mogollon-Datil volcanic field, New Mexico: New Mexico Bureau of Mines and Mineral Resources, Stratigraphic Chart 1, 7 pp., 2 sheets.

Osburn, G. R., and Ferguson, C. A., 1986, Redefinition of the Mt. Withington Cauldron (abs.): New Mexico Geology, v. 8, no. 4.

Shultz, A. W., 1984, Subaerial debris-flow deposition ir the upper Paleozoic Cutler Formation, western Colorado: Journal of Sedimentary Petrology, v. 54, p. 759-772.

Smith, G. A., 1986, Coarse-grained nonmarine volcaniclastic sediment: Terminology and depostional process: Geological Society of America Bulletin, v. 97, p. 1-10.

Sparks, R. S. J., 1976, Grain size variations in ignimbrites and implications for the transport of pyroclastic flows: Sedimentology, v. 23, p. 147-188.

Tonking, W. H., 1957, Geology of Puertecito quadrangle, Socorro County, New Mexico: New Mexico Bureau of Mines and Mineral Resources, Bulletin 41, 67 pp.

Wright, H. E., 1956, Origin of the Chuska Sandstone, Arizona-New Mexico: a structural and petrographic study of a Tertiary eolian sediment, Geological Society of America Bulletin, v. 67, p. 413-434.

Wright, J. V., and Walker, G. P., 1977, The ignimbrite source problem: Significance of a co-ignimbrite lag-fall deposit: Geology, v. 5, p. 729-732.

Zoback, M. L., Anderson, R. E., and Thompson, G. A., 1981, Cainozoic evolution of the state of stress and style of tectonism of the Basin and Range Province of the western United States: Philosophical Transactions of the Royal Society of London, v. 300, p. 407-434.

APPENDIX A

PETROGRAPHIC PROCEDURES

Observations of 50 standard thin sections of ash-flow tuffs (43), rhyolite intrusives and lavas (4), and sandstones (3) are presented in this paper. Thin sections were studied on Nikon type 102 and type 104 binocular petrographic microscopes. The Geologic Society of America rock color chart was used to standardize color names.

So that sanidine could be easily distinguished from quartz, volcanic thin sections were stained with sodium cobaltinitrate, following procedures described by Deer and others (1966, p. 311). Crystal-poor one feldspar tuffs required longer etching times (60-90 seconds) than the quartz-feldspar bearing tuffs (20-40 seconds). Phenocryst abundances of volcanic rocks were visually estimated from thin sections, and pumice and lithic abundances from hand specimens. Three sandstone thin sections were point counted on a Swift automatic point counter.

APPENDIX B

GEOCHEMICAL PROCEDURES

Twenty samples of silicic ash-flow tuffs (11), and lavas (9) were analyzed for major elements by x-ray fluorescence on a Rigaku 3064 spectrometer at New Mexico Bureau of Mines and Mineral Resources. Rocks were selected by checking the feldspars and biotite for obvious signs of alteration; all samples with >5% lithics were rejected. Samples were trimmed of weathered material in the field to make specimens weighing at least 1kg. These were later reduced to pieces <4cm using a hammer and a steel plate. A steel jaw crusher and steel rolls were then used to reduce the sample to pieces <5mm. A portion of each sample was then ground in a Tema mill to produce an approximate 200-mesh powder.

Procedures used for preparation of the powdered samples for major element analysis are described by Bobrow (1984, p. 137). One sample (S-37) was analyzed for iron and trace elements by instrumental neutron activation. Procedures for this sample are described by Bobrow (1984, p. 138).

Chlorine and fluorine analyses were done at the New Mexico Bureau of Mines and Mineral Resources by ion selective electrode.

APPENDIX C

PALEOMAGNETIC PROCEDURES

Twenty four outcrops of ash-flow tuff and intrusive rhyolite were sampled for paleomagnetism in the study area (Plate 4). Structural attitudes of eutaxitic foliation in ash-flow tuff samples were measured with a magnetic compass at each outcrop site. Regional attitudes were used for structural correction of intrusive rhyolite samples (DS-7,8), and for two flow-banded and contorted ash-flow tuff samples (DS-11,23) Eight 2.5cm diameter cores, 5 to 10cm in length, were drilled from each outcrop site using a gasoline-powered, water-cooled, diamond-bit drill produced by Roc Drill Systems. Cores were oriented with magnetic compass and suncompass and later sliced into 2.2cm lengths.

Paleomagnetic measurements were performed on a Schonstedt SSM-1 spinner magnetometer interfaced with a Northstar microcomputer. After initial measurements of natural remanent magnetization, samples were subjected to stepwise alternating field demagnetization in peak fields of up to 40 milliteslas using a non-commercial single-axis alternating field demagnetization device. The remanence directions of samples were remeasured after each demagnetization step and average directions and statistics were calculated for the eight samples from each site. Data

from the demagnetization step which produced the smallest within-site dispersion was used to characterize the remanence direction at each site. The anisotropy of susceptibility of the ash-flow tuff samples was determined using a Sapphire Instuments SI-2 susceptibility bridge interfaced with an Apple II computer.

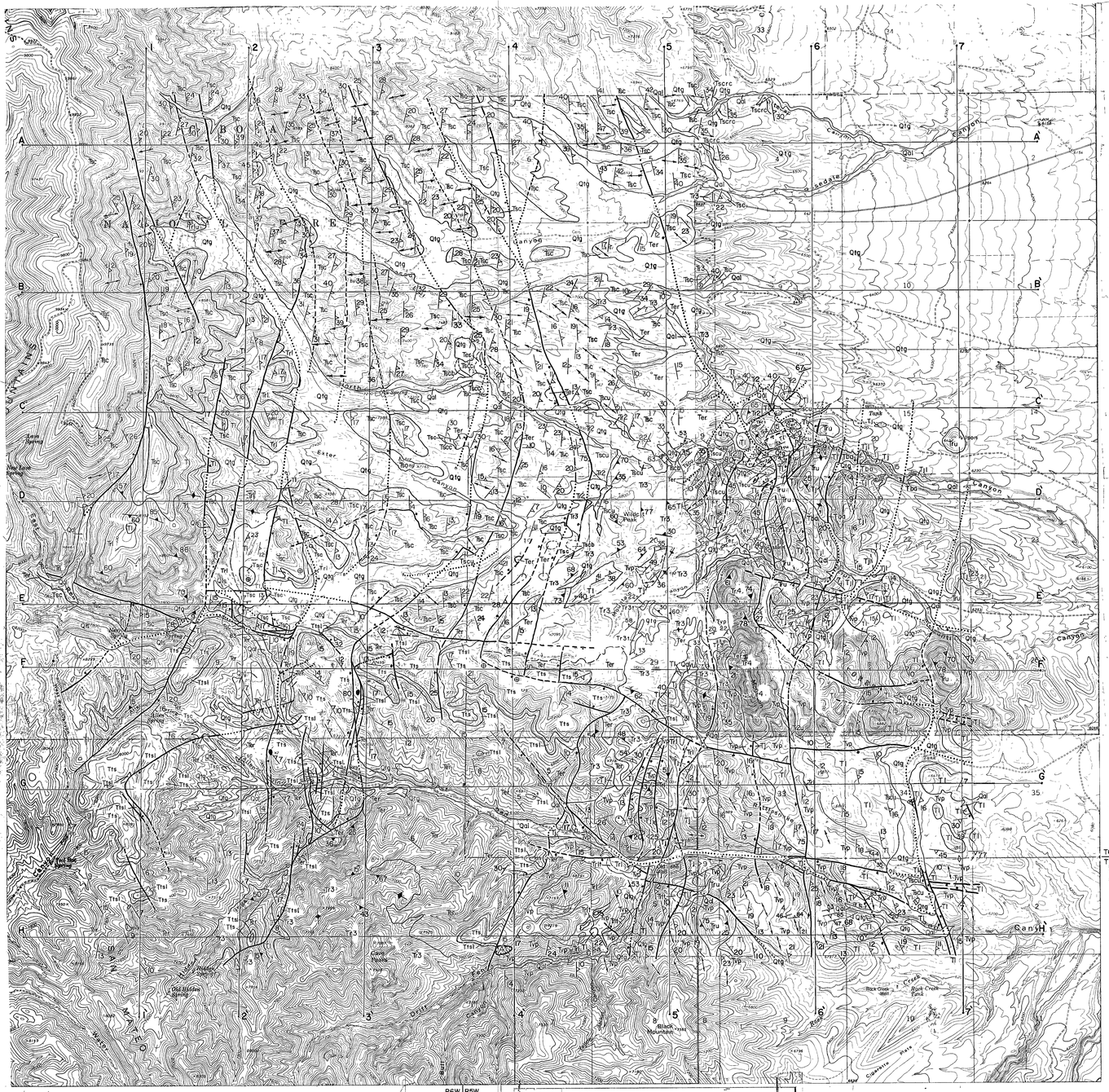

GEOLOGIC MAP OF THE EAST CENTRAL SAN MATEO MOUNTAINS, SOCORRO COUNTY, NEW MEXICO

1985
by
Charles A. Ferguson

EXPLANATION

Quaternary

- **Qal** Unconsolidated alluvium
- **Qls** Unconsolidated landslide deposits
- **Qtg** Poorly consolidated pediment and terrace gravels

Tertiary

Oligocene

- **Tts** Tuff of Turkey Springs: welded rhyolite ash-flow tuff. >100m (>330')
- **Ttsl** Unwelded base of the tuff of Turkey Springs 0-70m (0-230')
- **Tr4** Rhyolite intrusion younger than the unit of East Red Canyon
  (A)rhyolite intrusion of Horse Mountain.
- **Ter** Unit of East Red Canyon: Bedded lithic-rich unwelded tuffs near Horse Mountain and Wildcat Peak. Elsewhere the unit consists of volcaniclastic fanglomerates that grade northwestward into eolian cross-stratified feldspathic litharenites. The sandstones are moderate-red in the lower 50-100m of the unit, and pale-yellowish-orange above. 0-190m (0-625')
- **Tr3t** Bedded poorly welded to welded ash-flow tuffs between rhyolite lava flows of Horse Mountain Canyon. 0-12m (0-36')
- **Tr3** Rhyolite intrusions and lavas younger than the South Canyon Tuff
  (B)rhyolite intrusion of Wildcat Peak/rhyolite lavas of Horse Mountain Canyon.
  (C)rhyolite dome of Cave Peaks.
- **Tscrc** Member of Rosedale Canyon of the South Canyon Tuff: Welded rhyolite ash-flow tuff >50m (>165')
- **Tscc** Crystal-rich top of the South Canyon Tuff. Mapped separately only where it overlies Tscb 0-20m (0-65')
- **Tscb** Clast-supported (>50% lithics) mega-breccias within the South Canyon Tuff. Occurs in lenses that are gradational with less lithic-rich tuff. 0-100m (0-33')
- **Tsc** South Canyon Tuff: Welded rhyolite ash-flow tuff. 130-600m (425-1970')
- **Tscu** Bedded lithic-rich unweided tuff at the base of the South Canyon Tuff. 0-100m (0-330')
- **Tr2** Rhyolite intrusions older than the South Canyon Tuff.
  (D)rhyolite intrusions of North Canyon
  (E)rhyolite just west of Wildcat Peak
- **Tru** Rhyolite intrusions whose ages are poorly constrained (see age correlation chart for age constraints).
  (F)rhyolite intrusion of little Black Mountain*
  (G)rhyolite dikes of North Canyon
  (H)rhyolite intrusion of little Horse Mountain*
  (I)rhyolite intrusion of Tigner Ranch
  (J)rhyolite intrusion of Wilson Hill
- **Tl** Lemitar Tuff. Welded rhyolite ash-flow tuff. 40-200m (130-660')
- **Trl** Rhyolite intrusives and lava flows older than the Lemitar Tuff.
  (K)rhyolite intrusion of Drift Fence Canyon (one dome, a series of dikes and two flows with composite thickness of at least 70m (230').
  (L)rhyolite intrusion of Exter Canyon
- **Trlt** Unwelded bedded ash-flow tuffs underlying both Drift Fence Canyon lava flows 0-50m (0-165')
- **Tvp** Vicks Peak Tuff: Welded rhyolite ash-flow tuff. 0-215m (0-705')
- **Tj** La Jencia Tuff (upper member): Flow-banded welded rhyolite ash-flow tuff. 200m (660')
- **Tjl** La Jencia Tuff (lower member): Massive welded rhyolite ash-flow tuff. 70m (231')
- **Tbo** Basaltic andesite: massive to blocky grayish-red-purple lava flow. >60m (197')

*Informal place names used by the author to locate these two rhyolite intrusions. Both are smaller hills near mountain of same name.

Petrographic data from measured sections of the major ash-flow tuffs in this map area. Color names are from the U. S. G. S. rock color chart.

Tuff of Turkey Springs, Tts-Ttsl

Thickness meters	Color unweathered matrix	Lithics	Pumice	Total phen	San.	Qtz.	Plg.	Biot.	Opaq.	Sphene
100	light-brownish-gray 5YR 6/1	1-2	12-15	20	12	8	0.5	t	t	t
80	mod-reddish-brown 10R 4/6	1-2	10-12	17	9	8	m	t	t	t
65	pale-red-purple 5RP 6/2	1-2	8-10	17	9	8	m	t	t	t
40	pale-red 5R 6/2	2-4	4-6	10	5	5	m	t	t	0
35	light-gray N 7	4-6	2-4	7	5	2	m	t	t	0
20	[illegible] N 9	6-10	1-2	5	4	1	m	0	0	0
5	white N 9	10-12	1-2	3	2	1	m	0	t	t

South Canyon Tuff, Tsc

A section of the South Canyon Tuff was not measured in this map area. The South Canyon Tuff is petrographically similar to the tuff of Turkey Springs. Petrographic data for the South Canyon Tuff is available in the text accompanying this report.

Lemitar Tuff, Tl

Thickness meters	Color unweathered matrix	Lithics	Pumice	Total phen	San.	Qtz.	Plg.	Biot	Opaq	Sphene	Cpx
72	pale-red 5R 6/2	1	8-10	40	25	10	5	0.5	t	t	t
55	reddish-pink 10R 7/2	1	8-10	35	14	7	14	0.5	t	t	0
45	reddish-orange 10R 6/4	1-2	6-8	27	15	2	10	1	t	t	0
35	pale-red 10R 6/2	1-2	3-6	17	9	3	5	0.5	t	t	0
20	pale-red 10R 6/2	1-2	3-6	12	6	5	1	t	t	t	0
10	grayish-orange-pink 10R 8/2	1-2	1-3	5	3	2	t	t	t	0	0

Vicks Peak Tuff, Tvp

Thickness meters	Color unweathered matrix	Lithics	Pumice	Total phen	San.	Qtz.	Plg.	Biot	Opaq	Cpx
175	brownish-gray 5YR 4/1	t	12-20	12	12	0	0	0	t	m
120	medium-gray N 6	t	4-8	9	9	0	0	t	t	t
80	light-brownish-gray 5YR 6/1	t	4-8	2	2	0	0	t	t	t
25	light-gray N 7	t	4-8	1	1	t	t	t	0	0

La Jencia Tuff, Tj-Tjl

Thickness meters	Color unweathered matrix	Lithics	Pumice	Total phen	San.	Qtz	Plg	Biot	Opaq	Sphene
265	pale-grysh-red 10R 5/2	5-7	2-5	4	4	m	m	t	t	0
190	pale-red 5R 6/2	1	20-30	4	4	m	m	t	t	0
28	pale-red 10R 6/2	1	4-8	7	7	m	t	t	t	t

MAP SYMBOLS

- Contact dashed where approximately located; number indicates dip of contact (if known)
- Normal Fault dashed where approximately located; ball on downthrown side; dip of fault plane shown (if known)
- Fault trace buried by Quaternary deposits
- Fault trace buried by Tertiary deposits; *points to downthrown side
- Strike and dip of eutaxitic foliation (ash-flow tuffs)
- Strike and dip of pilotaxitic foliation (lavas)
- Vertical foliation
- Strike and dip of sedimentary layering
- Flow lineations in ash-flow tuffs; azimuth corrected for hitting
- Line of cross-section
- Slump block
- Flat lying foliation
- Phreatic tuff pipe

LOCATOR MAP FOR RHYOLITE INTRUSIONS / LAVAS

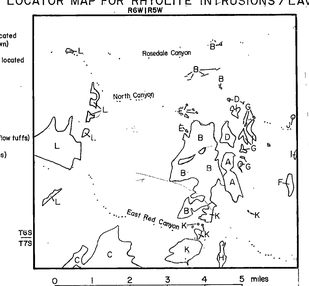

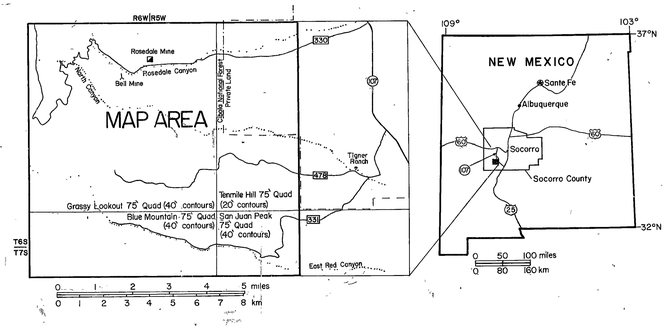

Relative age correlation chart

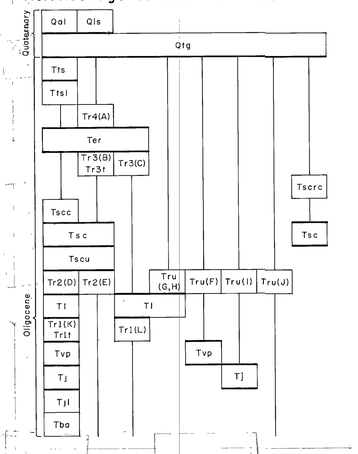

Each horizontal line on this chart describes the age relationship between vertically adjacent rock units. Rock units that occupy the same horizontal position are thought to be the same age.

Age relationship not conclusively determined.

Age relationship conclusively determined by intrusive or depositional contacts

New Mexico Bureau of Mines and Mineral Resources Open-File Report 252

WEST-EAST CROSS SECTIONS

Vertical scale in thousands of feet

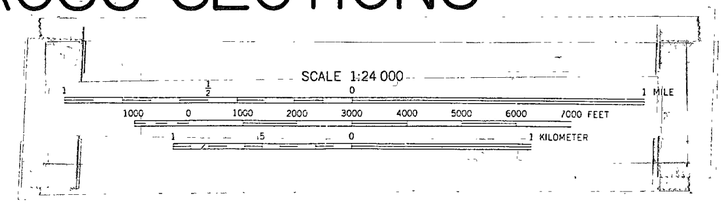

Eutaxitic foliation not parallel to depostional contacts

Fault, arrows showing movement. o denotes arrow coming out of paper, i=into paper

~~10~~ 10% phenocryst horizon in the South Canyon Tuff (Tsc) shown only where it's lower contact is unconstrained

B4 Intersection of two cross sections

All other symbols explained on plate 1

Note. the upper and lower members of the La Jencia Tuff are combined on cross sections

PLATE 2 (of 4)

New Mexico Bureau of Mines and Mineral Resources Open-File Report 252

NORTH-SOUTH CROSS SECTIONS

PLATE 3

(of 4)

Vertical scale in thousands of feet

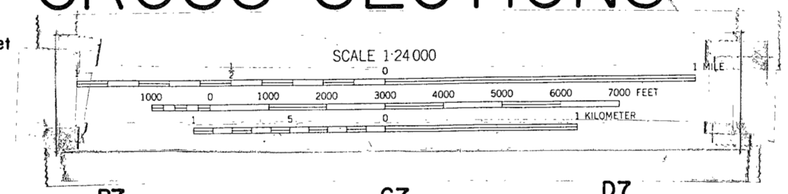

For explanation of symbols see plate 2

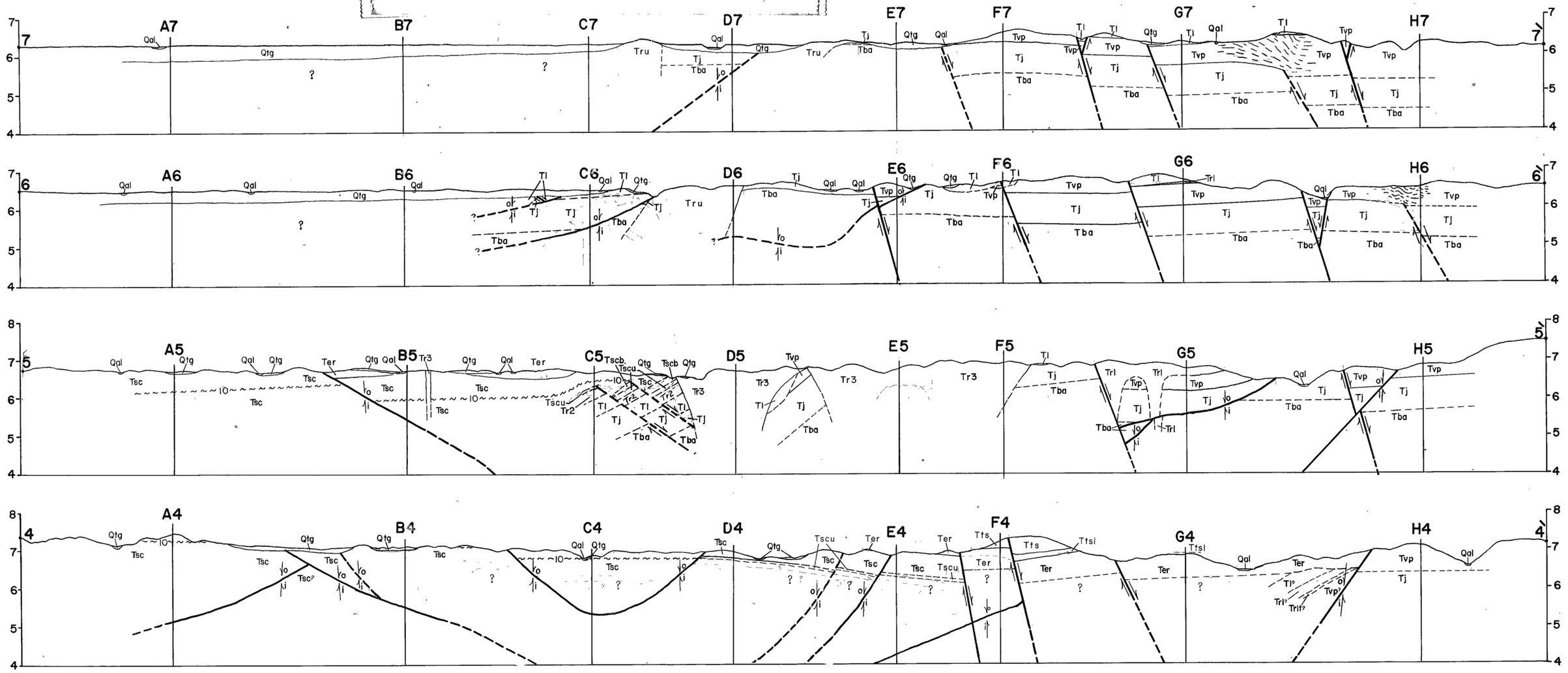

PLATE 4

(of 4)

SAMPLE LOCATION MAP (with cross section lines)

0 2 miles

0 2 km

New Mexico Bureau of Mines and Mineral Resources Open-File Report 252